12-22-2016

Janus Dendritic Ligands for Nanoparticle Assemblies

Katherine Elbert
University of Pennsylvania, kelbert@sas.upenn.edu

Christopher B. Murray
University of Pennsylvania, cbmurray@sas.upenn.edu

Janus Dendritic Ligands for Nanoparticle Assemblies

Abstract
This project was conducted in the laboratory of Professor Christopher B. Murray at the University of Pennsylvania. The project described herein includes the synthesis of a Janus dendrimer as well as complimentary dendrimers of hydrophobic and hydrophilic nature to study the self-assembly and organizational properties of these molecules on gold surfaces. A complete synthesis and characterization of these molecules is described, as well as grafting the molecules onto both gold nanoparticle and thin film surfaces. How the different dendritic molecules guide self-assembly of the nanoparticles and how the Janus molecule assembles itself on a gold surface was studied. To characterize these systems, TEM and solid state UV-vis were employed, and general trends are described herein.

Disciplines
Chemistry | Inorganic Chemistry | Materials Chemistry | Organic Chemistry

AN ABSTRACT OF THE CAPSTONE REPORT OF

Katherine Clausen Elbert for the degree of Master of Chemical Sciences

Title: Janus Dendritic Ligands for Nanoparticle Assemblies

Project conducted at: *University of Pennsylvania, 231 S. 34th Street, Philadelphia, PA 19104-6323*
Supervisor: *Christopher B. Murray, Richard Perry University Professor of Chemistry and Materials Science and Engineering*
Dates of Project: May 15, 2016 to December 15, 2016
Abstract approved: *Professor Christopher B. Murray,* Academic Advisor

This project was conducted in the laboratory of Professor Christopher B. Murray at the University of Pennsylvania. The project described herein includes the synthesis of a Janus dendrimer as well as complimentary dendrimers of hydrophobic and hydrophilic nature to study the self-assembly and organizational properties of these molecules on gold surfaces. A complete synthesis and characterization of these molecules is described, as well as grafting the molecules onto both gold nanoparticle and thin film surfaces. How the different dendritic molecules guide self-assembly of the nanoparticles and how the Janus molecule assembles itself on a gold surface was studied. To characterize these systems, TEM and solid state UV-vis were employed, and general trends are described herein.

Janus Dendritic Ligands for Nanoparticle Assemblies

by

Katherine C. Elbert

A CAPSTONE REPORT

submitted to the

University of Pennsylvania

in partial fulfillment of

the requirements for

the degree of

Masters of Chemical Sciences

Presented *November 15, 2016*

Commencement *December 2016*

Master of Chemical Sciences Capstone Report of *Katherine C. Elbert* presented on *November 15, 2016*.

APPROVED:

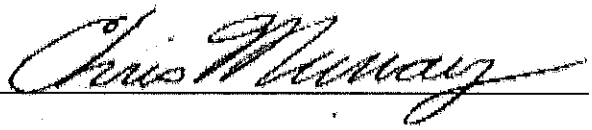

Christopher B. Murray, representing *Materials Chemistry*

I understand that my Capstone Report will become part of the permanent collection of the University of Pennsylvania Master of Chemical Sciences Program. My signature below authorizes release of my final report to any reader upon request.

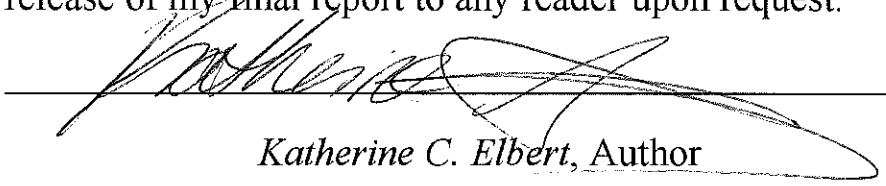

Katherine C. Elbert, Author

Acknowledgements

I deeply acknowledge the invaluable mentorship I have received from my research advisor, Professor Christopher B. Murray. I acknowledge my mentor Davit Jishkariani, who has taught me a tremendous amount in the past year and has poured an incredible number of hours into this project. I would also like to thank my lab mates: Yoating Wu for synthesizing the gold nanoparticles, Jennifer D. Lee for performing SAXS measurements, and the rest of the Murray group for valuable discussions regarding the project. I would also like to thank Professor Donald Berry for being my secondary reader for my Masters Capstone Project, and Ana-Rita Mayol-Cabassa for her continued support throughout this process.

Table of Contents

List of Figures, Schemes, and Tables

List of Appendices

Introduction

The study of coordination and self-assembly behavior of ligands on nanoparticle (NP) surfaces are of critical importance to nanotechnology as it provides the key to understanding and engineering various properties such as solubility,[1,2] electronic conduction,[3] optical properties,[4,5] and catalytic activity.[6] Typically, NPs are synthesized with commercially available ligands for solubility in either organic or aqueous media. Ligands used for the synthesis of particles synthesized in organic media usually consist commercially available alkyl containing molecules that have either acid, amine, phosphonate, or thiol surface binding groups.[7,8] On the other hand, aqueous synthesis of nanoparticles involves polar ligands such CTAB, ascorbic acid, citric acid, or polyethylene glycol derived molecules.[9,10] In both cases, synthesis utilizing commercially available ligands have produced NPs with good control of size and shape.

One way ligands are placed on the surface of NPs is post-synthesis surface modification through ligand exchange. To this end many different types of ligands such as polymeric,[11–13] dendritic,[14–17] liquid crystalline[18–20] and small molecules[21] have been grafted to surfaces to introduce certain solubility, steric, optical, magnetic and electronic properties.[22] In most cases, the nature of ligands is limited to being either hydrophilic or hydrophobic, introducing aqueous compatibility or dispersibility properties in organic solvents, respectively.

Amongst all surface modification methods, of particular importance are the directions that allow the formation of particles with multiple surface functionalities. These can be achieved by creating islands of certain functionalities on particle surfaces. Particles with only two anisotropic surface domains, with close to a 50:50 ratio, are generally referred to as Janus particles after the two-faced Roman god Janus,[23] while particles with a larger number of domains are called patchy particles.[24] The interest in formation of such domains is their similarity to anisotropy found in nature such as in heme[25] and pollens,[26] as well as their potential application in electronics,[27] photonic crystals,[28] and drug delivery.[29,30]

Literature methods for preparation of patchy particles are achieved by liquid phase deposition (LPD) and vapor phase deposition methods (VPD), and generally involve the functionalization of one part of the particle while masking another by using a template,[31] particle assembly,[32] glancing angle deposition,[33] lithography[34,35] or physical forces such as surface tension.[31] However, most of these methods are applied to micron or submicron sized particles, can only guarantee the formation of particles with only a few large patches (1-5), and have limited production volume.[24] To the best of my knowledge there is no literature method capable of creating highly precise 2-3nm size consistent patches over an entire surface. The goal of this project is to create a patchy surface using dendritic ligands. The size range of interest is much smaller than the resolution of common fabrication techniques and requires the development of bottom-up synthetic protocols.

Herein a conceptually different method for preparation of patchy particles that only involves a simple solution phase ligand exchange step and produces highly uniform coverage with less than 3 nm surface anisotropy domains is presented. To achieve such precise control, a dendritic ligand with Janus character will be engineered equipped with

surface binding disulfide groups and therefore can be used for ligand exchange. Hydrophobic and hydrophilic moieties will be mounted by covalent linkage on different branches of the same building motif and therefore are inseparable by means of self-segregation. These moieties are located on the periphery of the dendron, to allow for interaction between the different groups as well as the surrounding environment, which will influence self-assembly and organization of the molecule. To achieve this, a stepwise introduction of each of the different groups will be utilized, which allows for flexibility in ligand design. To characterize the dendritic system, NMR and MALDI-TOFF will be employed to confirm the structure and purity of the compounds. The hydrophobic or hydrophilic branches of neighboring dendritic ligands should self-assemble to form well defined patches of either hydrophobic or hydrophilic nature about 2 nm in size.

Moreover, this strategy also solves problems associated with production difficulty of common patchy particle fabrication techniques as it only involves a single solution phase ligand exchange and therefore can be scaled up without limitations. Complimentary ligands of only hydrophobic or hydrophilic nature will be also synthesized, to highlight the unique property of the Janus molecule. How this set of ligands play a role in the self-assembly of NPs will also be presented, to show the complete set of properties of the ligands. To gain further insights into the self-assembly properties of the ligands, NPs with different ligands on their surfaces will be combined, and their self-assembly properties will be studied. To characterize all self-assemblies, TEM will be used to visualize the NPs and estimate the interparticle spacing. Confirmation of the long-range crystallinity and trends in interparticle spacing will be achieved with solid state UV-vis. To elucidate the patchy surface that the Janus dendron creates on a surface, a thin film of Au will be employed. This is due to Au being electron rich, which appears very dark when visualizing with TEM, and a very thin film of Au will be lighter than an Au NP. The contrast of the Au surface is important for this study, because stains will be employed to visualize the different moieties of the Janus dendron, where a stain will bind to the oxygen rich, hydrophilic group of the molecule. The results of these studies are described herein.

Materials and Methods

Materials

Potassium Iodide (99 %), p-toluenesulfonyl chloride (≥ 98 %), and triethylene glycol monomethyl ether (≥ 97 %) and were purchased from Sigma-Aldrich and used without further purification. Methyl 3,4,5-trihydroxybenzoate (98 %), 1-bromodecane (97 %), 4-dimethylaminopyridine (≥ 99 %), and lithium aluminum hydride (95 %) were purchased from Aldrich and used without further purification. 3,5-dihydroxybenzoate (97 %), 2,6-ditertbutyl 4-methyl pyridine (98 %), and oxalyl chloride (98 %) were purchased from Acros Organics. All chemicals were used as received. Thionyl chloride (> 98 %) was purchased from TCI and used without further purification. Uranyl acetate was purchased from Spi Chem and was used without further purification. Potassium carbonate (reagent grade), sodium sulfate (anhydrous, reagent grade), silica gel (230-400 mesh, grade 60), triethyl amine (reagent grade), dimethylfomamide, tetrahydrofuran, methanol, hexanes, and ethyl acetate were purchased from Fisher Scientific and used without further purification. All solvents were ACS grade or higher. Dichloromethane was purchased

from Fisher Scientific and was dried with activated molecular sieves (3A, 4 to 8 mesh, purchased from Acros Organics) before use.

Techniques

NMR. ^{1}H NMR (500 MHz) and ^{13}C NMR (126 MHz) spectra were recorded on Bruker UNI500 or BIODRX500 NMR spectrometer. ^{1}H and ^{13}C chemical shifts (δ) are reported in ppm while coupling constants (J) are reported in Hertz (Hz). The multiplicity of signals in ^{1}H NMR spectra is described as "s" (singlet), "d" (doublet), "t" (triplet), "q" (quartet), "p" (pentet), "dd" (doublet of doublets) and "m" (multiplet). All spectra were referenced using solvent residual signals ($CDCl_3$: ^{1}H, δ 7.27 ppm; ^{13}C, δ 77.2 ppm).[36] Heteronuclear single quantum coherence (^{1}H-^{13}C HSQC) and heteronuclear multiple bond coherence (HMBC) experiments were used to confirm NMR peak assignments.

Mass Spectroscopy. Matrix-assisted laser desorption/ionization time of flight (MALDI-TOF) mass spectrometry was performed on Bruker Ultraflex III (Maldi-Tof-Tof) mass spectrometer using dithranol as matrix.

X-ray scattering. Small-angle transmission X-ray scattering was performed using a Multi-angle X-ray scattering instrument equipped with a Bruker Nonius FR591 40 kV rotating anode generator operated at 85 mA, Osmic Max-Flux optics, 2D Hi-Star Wire detector, and pinhole collimation, with an evacuated beam path. Measurements were performed on thin glass coverslips (0.1 mm) and collected for roughly 2 hours. Samples were prepared by dropcasting colloidal solutions which were allowed to dry slowly in a partially enclosed chamber. The same samples were used for solid-state UV-Vis experiments.

Optical Extinction Spectra. Optical extinction spectra were collected using a Cary 5000 UV-VIS-NIR, for solid films. Spectral band-pass was set to 2 nm and integration time to 0.25 seconds. Solution-phase measurements were collected on an Analytical Spectral Devices QSP 350-2000 UV-VIS-NIR spectrometer.

Electron Microscopy. TEM micrographs were collected using a JEOL 1400 microscope operated at 120 kV. The TEM was calibrated using a MAG*I*CAL® TEM calibration standard.

Ligand Exchange with Dendrimers. Ligand exchange of oleylamine-capped Au NPs was performed using 0.25 mL of Au NPs in hexanes at 80 mg/mL added to 20 mg of the replacement ligand disulfide dissolved in 3 mL of chloroform. Each reaction was stirred for 1 hour at room temperature, then the reaction was stopped by precipitation of the NPs with methanol. After centrifugation, the solid pellet of NPs was redispersed in hexanes and precipitated a second time with a mixture of isopropanol and ethanol. For the hydrophilic ligands, after ligand exchange the NPs were redispersed in methanol and precipitated with toluene.

Self Assembly of NCs. NC self-assembly was performed using previously-described methods.[37] A solution containing the NCs was made with hexanes at a defined stoichiometry and concentration (5-10 mg/mL). This solution was cast onto a diethylene glycol surface formed by loading 1.7 mL diethylene glocol into 1.5 cm^2 x 1.0 cm deep well machined from Teflon. The evaporating droplet was covered immediately with a glass slide to slow evaporation, which was allowed to occur over 12 hours. Once dry, the floating film was transferred to TEM grids by scooping up sections from below. Residual diethylene glycol was removed under vacuum before imaging.

Synthetic procedures and details

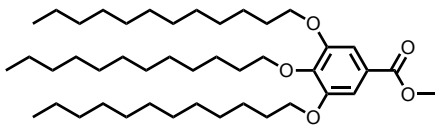

Methyl 3,4,5-tris(dodecyloxy)benzoate 2.[ref]. To a stirred solution of methyl 3,4,5-trihydroxybenzoate **1** (5g, 27.17 mmol) and 1-bromododecane (27g, 108.4 mmol) in DMF (45 mL) was added potassium carbonate (18.7g, 135.5 mmol) and the resulting mixture was stirred at 90 °C for 12 hours. The reaction was cooled to room temperature, diluted with $CHCl_3$ (XX mL) and then washed with H_2O (3 x 100 mL) and 1 M HCl (3 x 100 mL). The organic layer was dried over anhydrous Na_2SO_4, filtered, and the filtrate was concentrated under reduced pressure. The product was purified by dissolving in small amount of $CHCl_3$ and precipitated out by adding excess MeOH affording pure methyl 3,4,5-tris(dodecyloxy)benzoate **2** as a white solid (16.5 g, 88%). ^{1}H NMR ($CDCl_3$) δ 7.25 (s, 2H), 4.01 (td, J = 6.5, 4.1 Hz, 6H), 3.88 (s, 3H), 1.86 – 1.78 (m, 4H), 1.78 – 1.70 (m, 2H), 1.50 – 1.44 (m, 6H), 1.37 – 1.25 (m, 48H), 0.88 (t, J = 6.9 Hz, 9H); ^{13}C NMR ($CDCl_3$) δ 167.16, 153.05, 142.64, 124.87, 108.26, 73.71, 69.42, 52.30, 32.17, 32.16, 30.56, 29.98, 29.96, 29.95, 29.92, 29.89, 29.86, 29.79, 29.62, 29.59, 29.54, 26.31, 26.29, 22.92, 14.33.

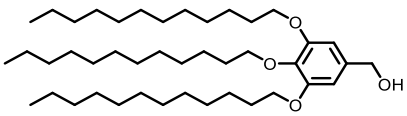

(3,4,5-Tris(octadecyloxy)phenyl)methanol 3. To a stirred solution of $LiAlH_4$ (2.48g, 65.35 mmol) in THF (100 mL) at 0 ^{o}C was added methyl 3,4,5-tris(dodecyloxy)benzoate **2** (14.7g, 21.78 mmol) portionwise over a period of 10 minutes and the resulting mixture was stirred at 0 ^{o}C for 30 minutes under nitrogen atmosphere. The reaction mixture was then allowed to warm up to room temperature for 30 minutes after which it was stirred at 60 ^{o}C for an additional 3 hours. Then it was cooled to 0 ^{o}C and quenched slowly by adding small portions of cold water while monitoring the evolution of hydrogen bubbles. The mixture was then concentrated under reduced pressure, dissolved in $CHCl_3$ (200 mL) and washed with 1 M HCl (2 x 50 mL), dried over anhydrous Na_2SO_4, filtered, and the filtrate was concentrated under reduced pressure. The residue was redissolved in the smallest possible amount of warm $CHCl_3$ and mixed with MeOH to induce precipitation. The precipitate was collected by filtration and dried to obtain pure (3,4,5-tris(dodecyloxy)phenyl)methanol **3** as a white solid (13.38g, 93 %). ^{1}H NMR ($CDCl_3$) δ 6.54 (s, 2H), 4.57 (s, 2H), 3.94 (dt, J = 13.5, 6.5 Hz, 6H), 1.81 – 1.73 (m, 6H), 1.46 (td, J = 9.7, 8.9, 5.2 Hz, 6H), 1.37 – 1.24 (m, 48H), 0.88 (t, J = 6.9 Hz, 9H); ^{13}C NMR ($CDCl_3$) δ 153.52, 137.88, 136.23, 105.63, 73.66, 69.36, 65.91, 32.17, 32.15, 30.56, 29.98, 29.96, 29.93, 29.89, 29.87, 29.85, 29.66, 29.65, 29.62, 29.59, 26.37, 26.33, 22.92, 14.33.

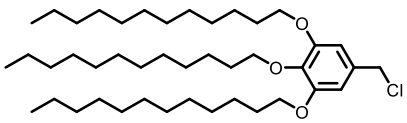

5-(Chloromethyl)-1,2,3-tris(octadecyloxy)benzene 4. To a stirred solution of (3,4,5-tris(octadecyloxy)phenyl)methanol **3** (5g, 7.56 mmol) in CH_2Cl_2 (100 mL) was added DMF (0.05 mL), and thionyl chloride (3.09g, 25.99 mmol, 1.89 mL), and the resulting mixture was stirred for 3 hours at room temperature under nitrogen atmosphere. The reaction mixture was then concentrated under reduced pressure and the residue was redissolved in the smallest possible amount of warm $CHCl_3$ and mixed with MeOH to induce precipitation. The precipitate was collected by filtration and dried to obtain pure 5-(chloromethyl)-1,2,3-tris(octadecyloxy)benzene **4** as a white solid (5.03g, 98%). ^{1}H NMR ($CDCl_3$) δ 6.57 (s, 2H), 4.51 (s, 2H), 3.96 (dt, J = 13.9, 6.5 Hz, 6H), 1.77 (dt, J = 31.0, 7.4 Hz, 6H), 1.47 (t, J = 7.6 Hz, 6H), 1.36 – 1.25 (m, 48H), 0.88 (t, J = 6.8 Hz, 9H); ^{13}C NMR ($CDCl_3$) δ 153.29, 138.42, 132.45, 107.14, 77.43, 73.44, 69.17, 46.89, 32.08, 32.07, 30.49, 29.90, 29.88, 29.85, 29.81, 29.78, 29.74, 29.55, 29.54, 29.51, 26.28, 26.24, 22.81, 14.18.

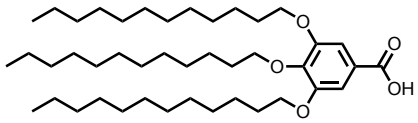

Methyl 3,4,5-tris(dodecyloxy)benzoate 5. To a stirred solution of methyl 3,4,5-tris(dodecyloxy)benzoate **2** (5g, 7.26 mmol) in THF (10 mL) was added potassium hydroxide (1.22g, 21.77 mmol), H_2O (2 mL), and MeOH (2 mL). The reaction mixture was stirred at 80 ^{o}C for 4 hours. The solvents were evaporated under reduced pressure, and the resulting product was acidified with 1 M HCl before being extracted with chloroform (3 x 75 mL). The organic layer was dried over anhydrous Na_2SO_4, filtered, and the filtrate was concentrated under reduced pressure to yield 3,4,5-tris(dodecyloxy)benzoic acid **5** as a pure white solid (4.85g, 99 %). ^{1}H NMR ($CDCl_3$) δ 7.31 (s, 2H), 4.09 – 3.95 (m, 6H), 1.81 (p, 4H), 1.78 – 1.70 (m, 2H), 1.52 – 1.42 (m, 6H), 1.39 – 1.22 (m, 48H), 0.88 (t, J = 6.8 Hz, 9H); ^{13}C NMR ($CDCl_3$) δ 171.82, 153.03, 143.20, 124.33, 108.74, 73.75, 69.40, 32.17, 32.16, 30.57, 29.98, 29.96, 29.93, 29.93, 29.89, 29.87, 29.80, 29.64, 29.62, 29.60, 29.54, 26.33, 26.28, 22.92, 14.32; MALDI-TOF (m/z): $[M+Na]^+$ calcd. for $C_{43}H_{78}O_5Na$, 697.57; found 702.354.

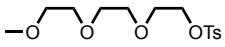

2-(2-(2-methoxyethoxy)ethoxy)ethyl 4-methylbenzenesulfonate 6. A stirred solution of triethylene glycol monomethyl ether (20 g, 121.95 mmol) and 4-toluenesulfonyl chloride (22.08 g, 115.90 mmol) in dichloromethane (75 mL) was cooled to 0 ^{o}C under a nitrogen atmosphere before the addition of triethylamine (14.78 g, 20.25 mL, 146.34 mmol). The resulting reaction mixture was allowed to warm up to room temperature and was stirred for 12 hours. The mixture was then washed with 1 M HCl (2 x 50 mL) and 1 M Na_2O_3 (2 x 50 mL), and the organic layer was dried over anhydrous Na_2SO_4, filtered, and the filtrate was concentrated under reduced pressure to give pure 2-(2-(2-methoxyethoxy)ethoxy)ethyl 4-methylbenzenesulfonate as a colorless oil (33.37 g, 86 %). ^{1}H NMR (500 MHz, Chloroform-*d*) δ 7.46 (d, J = 8.3 Hz, 2H), 7.05 (d, J = 8.1 Hz,

2H), 3.83 (t, 2H), 3.33 (t, 2H), 3.26 – 3.23 (m, 2H), 3.22 (s, 4H), 3.18 – 3.13 (m, 2H), 2.99 (s, 3H), 2.10 (s, 3H); ^{13}C NMR (126 MHz, $CDCl_3$) δ 144.06, 132.36, 129.16, 127.04, 77.42, 71.03, 69.69, 69.58, 69.56, 68.80, 67.71, 57.84, 20.59.

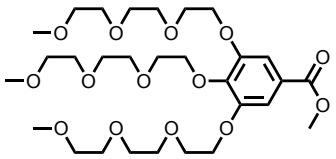

Methyl 3,4,5-tris(2-(2-(2-methoxyethoxy)ethoxy)ethoxy)benzoate 7.[ref] . To a stirred solution of methyl 3,4,5-trihydroxybenzoate **1** (2.17g, 11.78 mmol) and 2-(2-(2-methoxyethoxy)ethoxy)ethyl 4-methylbenzenesulfonate (15g, 47.11 mmol) in DMF (30 mL) was added potassium carbonate (8.13g, 58.89 mmol) and potassium iodide (200 mg, catalyst) and the resulting mixture was stirred at 80 ^{o}C for 12 hours. The reaction was cooled to room temperature, then washed with H_2O (3 x 75 mL) and 1 M HCl (3 x 50 mL). The organic layer was dried over anhydrous Na_2SO_4, filtered, and the filtrate was concentrated under reduced pressure. The crude product was purified with column chromatography (hexanes → 5% MeOH:EtOAc) to afford pure Methyl 3,4,5-tris(2-(2-(2-methoxyethoxy)ethoxy)ethoxy)benzoate **7** as a pale yellow oil (5.2 g, 74%). ^{1}H NMR ($CDCl_3$) δ 7.10 (s, 2H), 4.04 (t, 2H), 4.01 (t, J = 4.9 Hz, 4H), 3.68 (s, 3H), 3.67 (t, J = 4.5 Hz, 4H), 3.61 (t, 2H), 3.55 – 3.51 (m, 6H), 3.48 – 3.42 (m, 12H), 3.35 – 3.31 (m, 6H), 3.16 (s, 9H); ^{13}C NMR ($CDCl_3$) δ 166.03, 151.94, 142.27, 124.51, 108.65, 72.03, 71.55, 70.43, 70.30, 70.22, 70.15, 70.11, 69.25, 68.55, 58.53, 51.69; MALDI-TOF (m/z): $[M+Na]^+$ calcd. for $C_{29}H_{50}O_{14}Na$, 645.31; found 646.342.

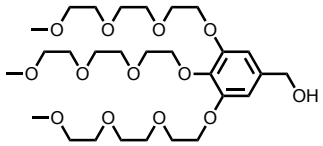

(3,4,5-Tris(2-(2-(2-methoxyethoxy)ethoxy)ethoxy)phenyl)methanol 8. To a stirred solution of $LiAlH_4$ (1.34g, 35.33 mmol) in THF (50 mL) at 0 ^{o}C was added Methyl 3,4,5-tris(2-(2-(2-methoxyethoxy)ethoxy)ethoxy)benzoate **7** (5.5g, 8.83 mmol) portionwise over a period of 10 minutes and the resulting mixture was stirred at 0 ^{o}C for 30 minutes under nitrogen atmosphere. The reaction mixture was then allowed to warm up to room temperature for 30 minutes after which it was stirred at 60 ^{o}C for an additional 3 hours. Then it was cooled to 0 ^{o}C and quenched slowly by adding small portions of cold water while monitoring the evolution of hydrogen bubbles. The mixture was then concentrated under reduced pressure, dissolved in $CHCl_3$ (200 mL) and washed with H_2O (2 x 50 mL), dried over anhydrous Na_2SO_4, filtered, and the filtrate was concentrated under reduced pressure to give pure (3,4,5-tris(2-(2-(2-methoxyethoxy)ethoxy)ethoxy)phenyl)methanol **8** as a pale yellow oil. (4.58g, 87 %). ^{1}H NMR ($CDCl_3$) δ 6.63 (s, 2H), 4.57 (d, J = 5.9 Hz, 2H), 4.17 (t, 4H), 4.13 (t, 2H), 3.83 (t, 4H), 3.78 (t, 2H), 3.73 – 3.70 (m, 6H), 3.64 (ddd, J = 13.1, 6.0, 3.5 Hz, 12H), 3.55 – 3.53 (m, 6H), 3.37 (d, J = 1.4 Hz, 9H); ^{13}C NMR ($CDCl_3$) δ 152.93, 138.09, 136.84, 106.89, 72.48, 72.17, 72.15, 71.00, 70.94, 70.92,

70.76, 70.73, 70.72, 70.04, 69.10, 65.49, 59.22, 0.20; MALDI-TOF (m/z): $[M+Na]^+$ calcd. for $C_{28}H_{50}O_{13}Na$, 617.31; found 618.411.

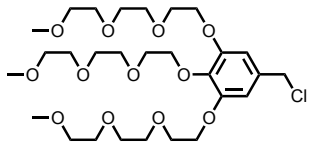

5-(Chloromethyl)-1,2,3-tris(2-(2-(2-methoxyethoxy)ethoxy)ethoxy)benzene 9. To a stirred solution of (3,4,5-tris(2-(2-(2-methoxyethoxy)ethoxy)ethoxy)phenyl)methanol **8** (4.58g, 7.70 mmol) in CH_2Cl_2 (75 mL) was added DMF (0.05 mL), and thionyl chloride (2.75g, 23.10 mmol, 1.68 mL), and the resulting mixture was stirred for 3 hours at room temperature under nitrogen atmosphere. The reaction mixture was then concentrated under reduced pressure to obtain pure 5-(chloromethyl)-1,2,3-tris(2-(2-(2-methoxyethoxy)ethoxy)ethoxy)benzene **9** as a yellow oil (4.72g, 100 %). ^{1}H NMR ($CDCl_3$) δ 6.36 (s, 2H), 4.23 (s, 2H), 3.92 – 3.81 (m, 6H), 3.56 (t, 5H), 3.50 (t, 2H), 3.47 – 3.41 (m, 6H), 3.38 – 3.33 (m, 12H), 3.27 – 3.22 (m, 6H), 3.07 (d, J = 1.9 Hz, 9H); ^{13}C NMR ($CDCl_3$) δ 151.97, 137.76, 132.19, 107.54, 77.43, 71.66, 71.26, 71.24, 70.09, 69.97, 69.90, 69.80, 69.78, 69.04, 68.27, 58.20, 45.93; MALDI-TOF (m/z): $[M+Na]^+$ calcd. for $C_{28}H_{49}O_{12}Na$, 635.28; found 636.112.

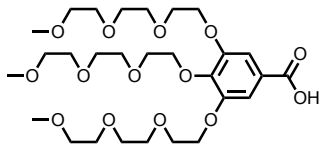

3,4,5-Tris(2-(2-(2-methoxyethoxy)ethoxy)ethoxy)benzoic acid 10. To a stirred solution of Methyl 3,4,5-tris(2-(2-(2-methoxyethoxy)ethoxy)ethoxy)benzoate **7** (2g, 3.21 mmol) in THF (10 mL) was added potassium hydroxide (0.54g, 9.64 mmol), H_2O (2 mL), and MeOH (2 mL). The reaction mixture was stirred at 80 ^{o}C for 4 hours. The solvents were evaporated under reduced pressure, and the resulting product was acidified with 1 M HCl before being extracted with chloroform (3 x 75 mL). The organic layer was dried over anhydrous Na_2SO_4, filtered, and the filtrate was concentrated under reduced pressure to yield 3,4,5-Tris(2-(2-(2-methoxyethoxy)ethoxy)ethoxy)benzoic acid **10** as a yellow oil (1.75g, 89.6 %). ^{1}H NMR ($CDCl_3$) δ 7.33 (s, 2H), 4.22 (t, 2H), 4.18 (t, J = 5.0 Hz, 4H), 3.85 (t, 4H), 3.79 (t, 2H), 3.73 – 3.69 (m, 6H), 3.66 – 3.61 (m, 12H), 3.55 – 3.51 (m, 6H), 3.35 (d, J = 1.7 Hz, 9H); ^{13}C NMR ($CDCl_3$) δ 170.68, 152.61, 143.52, 124.49, 109.91, 72.74, 72.23, 71.13, 70.99, 70.97, 70.89, 70.85, 70.81, 69.95, 69.20, 59.29; MALDI-TOF (m/z): $[M+Na]^+$ calcd. for $C_{28}H_{48}O_{12}Na$, 631.29; found 632.244.

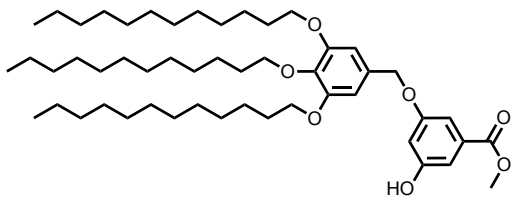

Methyl 3-hydroxy-5-((3,4,5-tris(dodecyloxy)benzyl)oxy)benzoate 12. To a stirred solution of methyl 3,5-trihydroxybenzoate **11** (4.45g, 26.49 mmol) and 5-(chloromethyl)-1,2,3-tris(dodecyloxy)benzene **4** (6g, 8.83 mmol) in DMF (100 mL) was added potassium carbonate (3.66g, 26.49 mmol) and potassium iodide (0.20g, 1.20 mmol) and the resulting mixture was stirred at 85 ^{o}C for 12 hours. The reaction was cooled to room temperature, then washed with H_2O (3 x 50 mL) and 1 M HCl (3 x 50 mL). The organic layer was dried over anhydrous Na_2SO_4, filtered, and the filtrate was concentrated under reduced pressure. The product was purified using column chromatography (hexanes → 30:5 hexanes:ethyl acetate) to afford pure methyl 3-hydroxy-5-((3,4,5-tris(dodecyloxy)benzyl)oxy)benzoate **12** as a white solid (3.77 g, 53%). ^{1}H NMR ($CDCl_3$) δ 7.25 (dd, J = 2.3, 1.3 Hz, 1H), 7.14 (dd, J = 2.3, 1.2 Hz, 1H), 6.66 (t, J = 2.3 Hz, 1H), 6.61 (s, 2H), 4.94 (s, 2H), 4.02 – 3.95 (m, 6H), 3.90 (s, 3H), 1.78 (dq, J = 14.2, 7.5, 7.1 Hz, 6H), 1.50 – 1.44 (m, 6H), 1.32 – 1.23 (m, 48H), 0.90 – 0.86 (m, 9H); ^{13}C NMR ($CDCl_3$) δ 167.26, 160.03, 157.39, 153.37, 137.78, 131.99, 131.79, 109.81, 108.02, 107.50, 106.26, 73.79, 70.71, 69.28, 52.43, 32.08, 32.07, 30.40, 29.90, 29.89, 29.88, 29.85, 29.84, 29.81, 29.79, 29.75, 29.57, 29.53, 29.53, 29.51, 26.25, 22.83, 14.23; MALDI-TOF (m/z): $[M+Na]^+$ calcd. for $C_{51}H_{86}O_7Na$, 833.63; found 834.82.

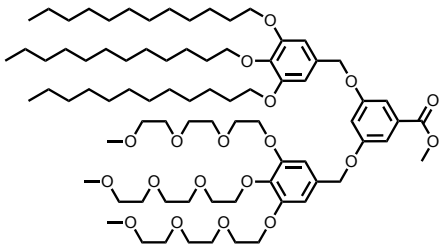

Methyl 3-((3,4,5-tris(2-(2-(2-methoxyethoxy)ethoxy)ethoxy)benzyl)oxy)-5-((3,4,5-tris(dodecyloxy)benzyl)oxy)benzoate 13. To a stirred solution of 5-(chloromethyl)-1,2,3-tris(2-(2-(2-methoxyethoxy)ethoxy)ethoxy)benzene **9** (0.83g, 1.356 mmol) and methyl 3-hydroxy-5-((3,4,5-tris(dodecyloxy)benzyl)oxy)benzoate **12** (1g, 1.232 mmol) in DMF (45 mL) was added potassium carbonate (0.56g, 4.07 mmol) and potassium iodide (0.2g, 1.2 mmol), and the resulting mixture was stirred at 90 ^{o}C for 12 hours. The reaction was cooled to room temperature, then washed with H_2O (3 x 30 mL) and 1 M HCl (3 x 30 mL). The organic layer was dried over anhydrous Na_2SO_4, filtered, and the filtrate was concentrated under reduced pressure. The product was purified using column chromatography (hexanes → 5% MeOH:EtOAc) to afford pure methyl 3-((3,4,5-tris(2-(2-(2-methoxyethoxy)ethoxy)ethoxy)benzyl)oxy)-5-((3,4,5-tris(dodecyloxy)benzyl)oxy)benzoate **13** as a pale yellow waxy solid (0.95 g, 50.5%). ^{1}H NMR ($CDCl_3$) δ 7.30 (dd, J = 2.4, 1.3 Hz, 1H), 7.27 (dd, J = 2.4, 1.3 Hz, 1H), 6.79 (t, J = 2.3 Hz, 1H), 6.66 (s, 2H), 6.62 (s, 2H), 4.95 (s, 4H), 4.16 (dt, J = 10.3, 5.1 Hz, 6H), 3.96 (dt, J = 15.3, 6.5 Hz, 6H), 3.90 (s, 3H), 3.85 (t, 4H), 3.79 (t, 2H), 3.74 – 3.71 (m, 6H), 3.67 – 3.62 (m, 12H), 3.56 – 3.52 (m, 6H), 3.37 (d, J = 5.9 Hz, 9H), 1.80 – 1.72 (m, 6H), 1.50 – 1.43 (m, 6H), 1.34 – 1.24 (m, 48H), 0.88 (td, J = 7.0, 1.9 Hz, 9H); ^{13}C NMR

($CDCl_3$) δ 166.87, 160.01, 159.87, 153.51, 153.01, 138.55, 138.31, 132.22, 131.96, 131.44, 131.03, 128.96, 108.63, 108.41, 107.51, 107.37, 106.50, 73.60, 72.51, 72.15, 72.12, 71.01, 70.92, 70.88, 70.75, 70.72, 70.71, 70.52, 69.92, 69.35, 69.13, 68.32, 59.18, 52.42, 38.93, 32.12, 32.10, 30.54, 29.94, 29.92, 29.88, 29.83, 29.62, 29.57, 29.54, 29.11, 26.33, 26.31, 23.94, 23.16, 22.87, 14.28, 14.22, 11.14; MALDI-TOF (m/z): $[M+Na]^+$ calcd. for $C_{79}H_{134}O_{19}Na$, 1409.94; found 1412.76.

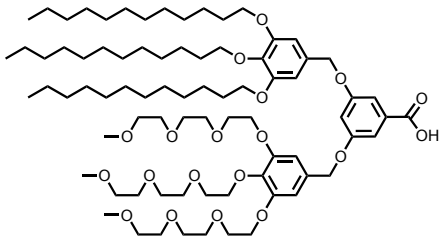

3-((3,4,5-Tris(2-(2-(2-methoxyethoxy)ethoxy)ethoxy)benzyl)oxy)-5-((3,4,5-tris(dodecyloxy)benzyl)oxy)benzoic acid 14. To a stirred solution of methyl 3-((3,4,5-tris(2-(2-(2-methoxyethoxy)ethoxy)ethoxy)benzyl)oxy)-5-((3,4,5-tris(dodecyloxy)benzyl)oxy)benzoate **13** (0.95 g, 0.684 mmol) in THF (10 mL) was added potassium hydroxide (0.115 g, 2.05 mmol), H_2O (2 mL), and MeOH (2 mL). The reaction mixture was stirred at 50 ^oC for 4 hours. The solvents were evaporated under reduced pressure, and the resulting product was acidified with 1 M HCl before being extracted with chloroform (3 x 75 mL). The organic layer was dried over anhydrous Na_2SO_4, filtered, and the filtrate was concentrated under reduced pressure to yield the pure 3-((3,4,5-tris(2-(2-(2-methoxyethoxy)ethoxy)ethoxy)benzyl)oxy)-5-((3,4,5-tris(dodecyloxy)benzyl)oxy)benzoic acid **14** as a pale yellow solid (0.815 g, 87%).^{1}H NMR ($CDCl_3$) δ 7.35 (dd, J = 2.4, 1.2 Hz, 1H), 7.31 (dd, J = 2.4, 1.3 Hz, 1H), 6.81 (t, J = 2.3 Hz, 1H), 6.66 (s, 2H), 6.62 (s, 2H), 4.96 (s, 2H), 4.94 (s, 2H), 4.18 – 4.13 (m, 6H), 3.99 – 3.93 (m, 6H), 3.83 (t, 4H), 3.78 (t, 2H), 3.73 – 3.70 (m, 6H), 3.66 – 3.62 (m, 12H), 3.55 – 3.53 (m, 6H), 3.36 (d, J = 3.6 Hz, 9H), 1.81 – 1.71 (m, 6H), 1.50 – 1.42 (m, 6H), 1.30 – 1.22 (m, 48H), 0.89 – 0.85 (m, 9H); ^{13}C NMR ($CDCl_3$) δ 169.91, 160.05, 159.81, 153.51, 152.95, 138.45, 138.32, 132.02, 131.71, 131.39, 109.10, 108.87, 108.16, 107.58, 106.55, 73.62, 72.48, 72.11, 70.94, 70.86, 70.83, 70.67, 70.66, 70.58, 69.85, 69.36, 69.05, 59.17, 59.15, 32.13, 32.10, 30.55, 29.94, 29.92, 29.89, 29.84, 29.83, 29.63, 29.58, 29.55, 26.34, 26.32, 22.87, 14.29; MALDI-TOF (m/z): $[M+Na]^+$ calcd. for $C_{78}H_{132}O_{19}Na$, 1395.93; found 1397.713.

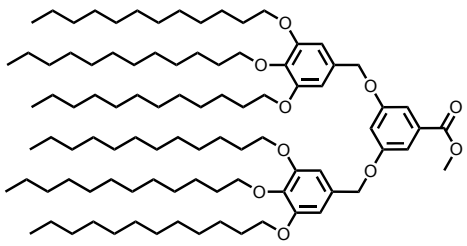

Methyl 3,5-bis((3,4,5-tris(dodecyloxy)benzyl)oxy)benzoate 15. To a stirred solution of methyl 3,5-trihydroxybenzoate **11** (0.297g, 1.77 mmol) and 5-(chloromethyl)-1,2,3-tris(dodecyloxy)benzene **4** (3g, 4.42 mmol) in DMF (45 mL) was added potassium

carbonate (0.731 g, 5.30 mmol) and potassium iodide (0.2 g, 1.2 mmol) and the resulting mixture was stirred at 90 ^{o}C for 12 hours. The reaction was cooled to room temperature, then washed with 1 M HCl (3 x 50 mL) and H_2O (3 x 50 mL). The organic layer was dried over anhydrous Na_2SO_4, filtered, and the filtrate was concentrated under reduced pressure. The product was purified using column chromatography (100:5 hexanes:ethyl acetate) to afford pure Methyl 3,5-bis((3,4,5-tris(dodecyloxy)benzyl)oxy)benzoate **15** as a white solid (2.44 g, 95%).^{1}H NMR ($CDCl_3$) δ 7.31 (d, J = 2.3 Hz, 2H), 6.81 (t, J = 2.4 Hz, 1H), 6.63 (s, 4H), 4.96 (s, 4H), 3.99 (q, J = 6.6 Hz, 12H), 3.91 (s, 3H), 1.83 – 1.75 (m, 12H), 1.52 – 1.46 (m, 12H), 1.34 – 1.27 (m, 96H), 0.92 – 0.88 (m, 18H); ^{13}C NMR ($CDCl_3$) δ 166.83, 159.96, 153.50, 138.29, 132.16, 131.49, 108.55, 107.39, 106.41, 73.56, 70.85, 69.30, 52.32, 32.14, 32.12, 30.55, 29.95, 29.93, 29.90, 29.85, 29.83, 29.81, 29.62, 29.59, 29.56, 26.34, 26.31, 22.87, 14.26; MALDI-TOF (m/z): $[M+Na]^+$ calcd. for $C_{94}H_{164}O_{10}Na$, 1476.22; found 1479.089.

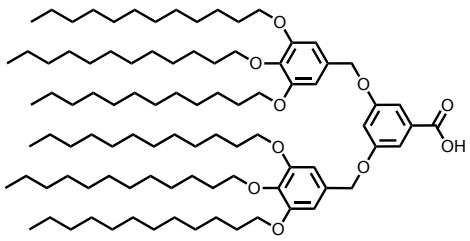

3,5-Bis((3,4,5-tris(dodecyloxy)benzyl)oxy)benzoic acid 16. To a stirred solution of methyl 3,5-bis((3,4,5-tris(dodecyloxy)benzyl)oxy)benzoate **15** (2g, 1.38 mmol) in THF (10 mL) was added potassium hydroxide (0.23g, 4.13 mmol), H_2O (2 mL), and MeOH (2 mL). The reaction mixture was stirred at 90 ^{o}C for 4 hours. The solvents were evaporated under reduced pressure, and the resulting product was acidified with 1 M HCl before being extracted with chloroform (3 x 75 mL). The organic layer was dried over anhydrous Na_2SO_4, filtered, and the filtrate was concentrated under reduced pressure to yield the pure 3,5-bis((3,4,5-tris(dodecyloxy)benzyl)oxy)benzoic acid **16** as a pale yellow solid (1.73g, 87.3%). ^{1}H NMR ($CDCl_3$) δ 7.40 (d, J = 2.4 Hz, 2H), 6.87 (t, J = 2.4 Hz, 1H), 6.65 (s, 4H), 4.98 (s, 4H), 3.99 (q, J = 6.8 Hz, 12H), 1.84 – 1.76 (m, 12H), 1.50 (t, J = 7.7 Hz, 12H), 1.33 – 1.25 (m, 96H), 0.92 – 0.88 (m, 18H); ^{13}C NMR ($CDCl_3$) δ 171.84, 160.04, 153.53, 138.33, 131.48, 131.40, 109.07, 108.22, 106.50, 77.43, 73.61, 70.93, 69.35, 32.15, 32.13, 30.56, 29.97, 29.95, 29.92, 29.91, 29.87, 29.86, 29.83, 29.78, 29.64, 29.60, 29.58, 26.36, 26.33, 22.89, 14.28; MALDI-TOF (m/z): $[M+Na]^+$ calcd. for $C_{93}H_{162}O_{10}Na$, 1462.21; found 1465.025.

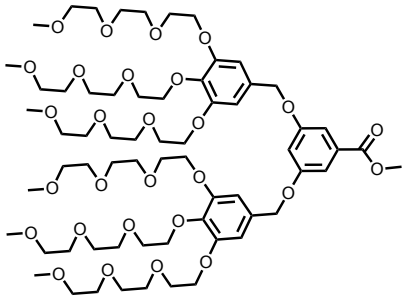

Methyl 3,5-bis((3,4,5-tris(2-(2-(2-methoxyethoxy)ethoxy)ethoxy)benzyl)oxy)benzoate 17. To a stirred solution of methyl 3,5-trihydroxybenzoate **11** (0.25g, 1.48 mmol) and 5-(chloromethyl)-1,2,3-tris(2-(2-(2-methoxyethoxy)ethoxy)ethoxy)benzene **9** (2g, 3.26 mmol) in DMF (45 mL) was added potassium carbonate (1.02 g, 7.41 mmol) and potassium iodide (200 mg, catalytic amount), and the resulting mixture was stirred at 90 ^{o}C for 12 hours. The reaction was cooled to room temperature, then washed with H_2O (3 x 50 mL) and 1 M HCl (3 x 50 mL). The organic layer was dried over anhydrous Na_2SO_4, filtered, and the filtrate was concentrated under reduced pressure. The product was purified using column chromatography (hexanes → 5% MeOH:EtOAc) to afford pure methyl 3,5-bis((3,4,5-tris(2-(2-(2-methoxyethoxy)ethoxy)ethoxy)benzyl)oxy)benzoate **17** as a golden oil (1.74 g, 89 %).^{1}H NMR ($CDCl_3$) δ 7.25 (s, 2H), 6.77 (t, J = 2.3 Hz, 1H), 6.65 (s, 4H), 4.93 (s, 4H), 4.14 (dt, J = 10.4, 5.2 Hz, 12H), 3.89 (s, 3H), 3.83 (t, J = 5.0 Hz, 8H), 3.77 (t, 4H), 3.73 – 3.69 (m, 12H), 3.65 – 3.61 (m, 24H), 3.54 – 3.50 (m, 12H), 3.35 (d, J = 6.0 Hz, 18H); ^{13}C NMR ($CDCl_3$) δ 166.86, 159.88, 152.96, 138.43, 132.24, 131.99, 108.53, 107.45, 107.34, 72.50, 72.11, 72.10, 70.97, 70.85, 70.71, 70.68, 70.67, 70.53, 69.89, 69.07, 59.18, 52.45; MALDI-TOF (m/z): $[M+Na]^+$ calcd. for $C_{64}H_{104}O_{28}Na$, 1343.66; found 1345.061.

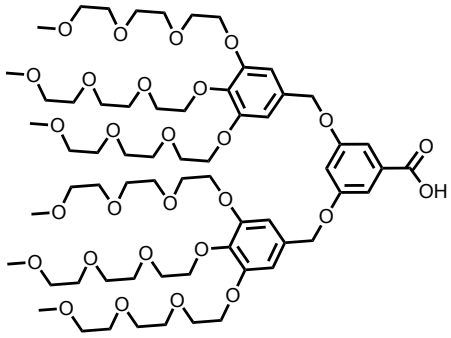

3,5-Bis((3,4,5-tris(2-(2-(2-methoxyethoxy)ethoxy)ethoxy)benzyl)oxy)benzoic acid 18. To a stirred solution of methyl 3,5-bis((3,4,5-tris(2-(2-(2-methoxyethoxy)ethoxy)ethoxy)benzyl)oxy)benzoate **17** (1.74 g, 1.32 mmol) in THF (10 mL) was added potassium hydroxide (0.22 g, 3.96 mmol), H_2O (2 mL), and MeOH (2 mL). The reaction mixture was stirred at 50 ^{o}C for 4 hours. The solvents were evaporated under reduced pressure, and the resulting product was acidified with 1 M HCl before being extracted with chloroform (3 x 75 mL). The organic layer was dried over anhydrous Na_2SO_4, filtered, and the filtrate was concentrated under reduced pressure to yield the pure 3,5-bis((3,4,5-tris(2-(2-(2-methoxyethoxy)ethoxy)ethoxy)benzyl)oxy)benzoic acid **18** as a pale yellow oil (1.52g, 88%). ^{1}H NMR ($CDCl_3$) δ 7.28 (d, J = 2.4 Hz, 2H), 6.76 (t, J = 2.3 Hz, 1H), 6.63 (s, 4H),

4.92 (s, 4H), 4.14 – 4.10 (m, 12H), 3.82 – 3.79 (m, 8H), 3.76 – 3.74 (m, 4H), 3.71 – 3.65 (m, 12H), 3.63 – 3.59 (m, 24H), 3.52 – 3.49 (m, 13H), 3.33 (d, J = 4.8 Hz, 18H); ^{13}C NMR ($CDCl_3$) δ 168.98, 159.72, 152.84, 138.34, 131.94, 131.87, 108.79, 107.84, 107.42, 77.43, 72.37, 71.99, 71.97, 70.84, 70.73, 70.58, 70.56, 70.43, 69.75, 68.96, 59.04, 59.03; MALDI-TOF (m/z): $[M+Na]^+$ calcd. for $C_{63}H_{102}O_{28}Na$, 1329.65; found 1332.078.

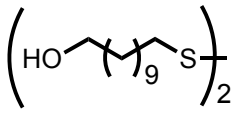

11,11'-disulfanediylbis(undecan-1-ol) 20. Compound **20** was prepared following previously reported literature.[38]

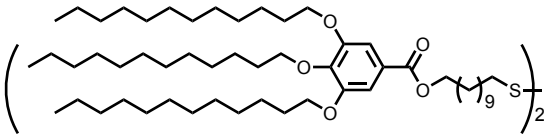

Disulfanediylbis(undecane-11,1-diyl) bis(3,4,5-tris(dodecyloxy)benzoate) 21. To an oven dried round bottom flask was added 3,4,5-tris(dodecyloxy)benzoic acid **5** (1.0 gram, 1.48 mmol) and DCM (20 mL). The solution was stirred for 10 minutes under nitrogen atmosphere before thionyl chloride (0.53 g, 4.45 mmol) was added, then the reaction mixture was stirred at room temperature for 3 hours under nitrogen. The reaction mixture was then concentrated under reduced pressure, and the crude product was dissolved in DCM (20 mL) and cooled to -10 ^{o}C. To the stirred solution was added 11,11'-disulfanediylbis(undecan-1-ol) **20** (0.26 g, 0.65 mmol), Et_3N (0.30 g, 2.97 mmol, 0.41 mL), and DMAP (0.05 g, 0.41 mmol). The reaction mixture was allowed to warm up to room temperature and stirred overnight, then was washed with 1 M HCl (2 x 50 mL). The organic layer was dried over anhydrous Na_2SO_4, filtered, and the filtrate was concentrated under reduced pressure. The crude product was purified with column chromatography (100:1 hexanes:ethyl acetate) to afford pure disulfanediylbis(undecane-11,1-diyl) bis(3,4,5-tris(dodecyloxy)benzoate) **21** as a white solid (1.09g, 96%). ^{1}H NMR ($CDCl_3$) δ 7.25 (s, 2H), 4.28 (t, J = 6.7 Hz, 2H), 4.01 (t, J = 6.5 Hz, 6H), 2.67 (t, 2H), 1.84 – 1.72 (m, 8H), 1.70 – 1.63 (m, 2H), 1.56 (s, 2H), 1.50 – 1.44 (m, 6H), 1.26 (s, 61H), 0.88 (t, J = 6.9 Hz, 9H); ^{13}C NMR ($CDCl_3$) δ 166.70, 153.00, 142.60, 125.28, 108.29, 73.71, 69.42, 65.34, 39.37, 32.16, 32.15, 30.55, 29.97, 29.95, 29.94, 29.92, 29.91, 29.88, 29.86, 29.79, 29.75, 29.75, 29.72, 29.63, 29.61, 29.59, 29.55, 29.51, 29.47, 29.44, 28.98, 28.76, 26.32, 26.28, 26.24, 22.91, 14.32; MALDI-TOF (m/z): $[M+Na]^+$ calcd. for $C_{108}H_{198}O_{10}S_2Na$, 1742.43; found 1744.684.

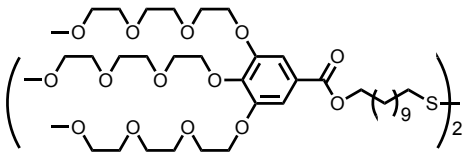

Disulfanediylbis(undecane-11,1-diyl) bis(3,4,5-tris(2-(2-(2-methoxyethoxy)ethoxy)ethoxy)benzoate) 22. To an oven dried round bottom flask was

added 3,4,5-Tris(2-(2-(2-methoxyethoxy)ethoxy)ethoxy)benzoic acid **10** (0.5 g, 0.82 mmol) and DCM (12 mL). The solution was stirred for 10 minutes under nitrogen atmosphere before thionyl chloride (0.488 g, 4.12 mmol) was added, then the reaction mixture was stirred at room temperature for 3 hours under nitrogen. The reaction mixture was then concentrated under reduced pressure, and the crude product was dissolved in DCM (20 mL) and cooled to -10 ^{o}C. To the stirred solution was added 11,11'-disulfanediylbis(undecan-1-ol) **20** (0.12 g, 0.296 mmol), Et_3N (0.358 g, 3.29 mmol, 0.50 mL), and DMAP (0.05 g, 0.41 mmol). The reaction mixture was allowed to warm up to room temperature and stirred for 24 hours, then was concentrated under reduced pressure. The crude product was purified with column chromatography (hexanes → 1:100 MeOH:EtOAc) to afford pure disulfanediylbis(undecane-11,1-diyl) bis(3,4,5-tris(2-(2-(2-methoxyethoxy)ethoxy)ethoxy)benzoate) **22** as a yellow oil (0.368 g, 78 %). ^{1}H NMR ($CDCl_3$) δ 7.22 (s, 2H), 4.20 (t, J = 6.8 Hz, 2H), 4.17 – 4.10 (m, 6H), 3.79 (t, 4H), 3.72 (t, 2H), 3.67 – 3.62 (m, 6H), 3.60 – 3.55 (m, 12H), 3.48 – 3.44 (m, 6H), 3.29 (s, 9H), 2.60 (t, J = 7.4 Hz, 2H), 1.67 (p, J = 6.9 Hz, 2H), 1.59 (p, J = 7.4 Hz, 2H), 1.37 – 1.27 (m, 5H), 1.21 (s, 9H). ^{13}C NMR (126 MHz, $CDCl_3$) δ 166.19, 152.33, 142.64, 125.42, 109.17, 72.47, 72.00, 70.88, 70.75, 70.74, 70.62, 70.61, 70.58, 69.71, 68.96, 65.29, 59.07, 59.05, 39.20, 29.58, 29.55, 29.35, 29.30, 29.28, 28.82, 28.59, 26.06; MALDI-TOF (m/z): $[M+Na]^+$ calcd. for $C_{78}H_{138}O_{28}S_2Na$, 1609.87; found 1608.389.

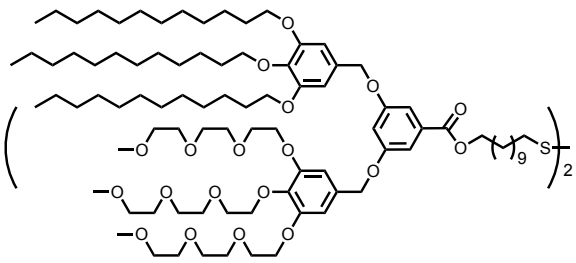

Disulfanediylbis(undecane-11,1-diyl) bis(3-((3,4,5-tris(2-(2-(2-methoxyethoxy)ethoxy)ethoxy)benzyl)oxy)-5-((3,4,5-tris(dodecyloxy)benzyl)oxy)benzoate) 23.

To an oven dried round bottom flask was added 3-((3,4,5-Tris(2-(2-(2-methoxyethoxy)ethoxy)ethoxy)benzyl)oxy)-5-((3,4,5-tris(dodecyloxy)benzyl)oxy)benzoic acid **23** (0.35 gram, 0.25 mmol) and DCM (20 mL). The solution was stirred for 10 minutes under nitrogen atmosphere before thionyl chloride (0.089 g, 0.75 mmol) was added, then the reaction mixture was stirred at room temperature for 3 hours under nitrogen. The reaction mixture was then concentrated under reduced pressure, and the crude product was dissolved in DCM (20 mL) and cooled to -10 ^{o}C. To the stirred solution was added 11,11'-disulfanediylbis(undecan-1-ol) **X** (0.047 g, 0.11 mmol), Et_3N (0.056 g, 0.51 mmol, 0.08 mL), and DMAP (0.05 g, 0.41 mmol). The reaction mixture was allowed to warm up to room temperature and stirred overnight, then was washed with 1 M HCl (2 x 50 mL). The organic layer was dried over anhydrous Na_2SO_4, filtered, and the filtrate was concentrated under reduced pressure. The crude product was purified with column chromatography (hexanes → EtOAc → 1:100 MeOH:EtOAc) to afford pure disulfanediylbis(undecane-11,1-diyl) bis(3-((3,4,5-tris(2-(2-(2-methoxyethoxy)ethoxy)ethoxy)benzyl)oxy)-5-((3,4,5-tris(dodecyloxy)benzyl)oxy)benzoate) **23** as a brown oil (0.133 grams, 36%). ^{1}H NMR

($CDCl_3$) δ 7.28 (dd, J = 2.4, 1.3 Hz, 1H), 7.26 (d, J = 3.7 Hz, 1H), 6.77 (t, J = 2.3 Hz, 1H), 6.65 (s, 2H), 6.61 (s, 2H), 4.93 (d, J = 2.0 Hz, 4H), 4.28 (t, J = 6.8 Hz, 2H), 4.14 (dt, J = 10.2, 5.1 Hz, 6H), 3.99 – 3.91 (m, 6H), 3.83 (t, 4H), 3.78 (t, 2H), 3.73 – 3.69 (m, 6H), 3.65 – 3.61 (m, 12H), 3.55 – 3.50 (m, 6H), 3.35 (d, J = 6.6 Hz, 9H), 2.65 (t, 2H), 1.81 – 1.70 (m, 8H), 1.64 (p, J = 7.3 Hz, 2H), 1.50 – 1.43 (m, 6H), 1.40 (d, J = 8.2 Hz, 1H), 1.36 – 1.23 (m, 62H), 0.88 – 0.84 (m, 9H); ^{13}C NMR ($CDCl_3$) δ 166.39, 159.92, 159.80, 153.45, 152.96, 138.51, 138.27, 132.57, 131.88, 131.37, 108.62, 108.38, 107.51, 106.92, 106.50, 73.53, 72.46, 72.09, 72.06, 70.95, 70.89, 70.82, 70.68, 70.66, 70.64, 70.49, 69.86, 69.28, 69.08, 65.45, 59.11, 39.23, 32.06, 32.04, 30.48, 29.88, 29.86, 29.82, 29.82, 29.78, 29.76, 29.75, 29.66, 29.63, 29.62, 29.56, 29.51, 29.48, 29.40, 29.38, 29.34, 28.84, 28.65, 26.27, 26.25, 26.10, 22.81, 14.23; MALDI-TOF (m/z): $[M+Na]^+$ calcd. for $C_{178}H_{306}O_{38}S_2Na$, 3139.14; found 3143.823.

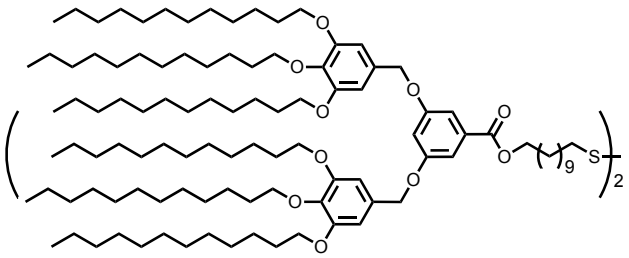

Disulfanediylbis(undecane-11,1-diyl) bis(3,5-bis((3,4,5-tris(dodecyloxy)benzyl)oxy)benzoate) 24.

To an oven dried round bottom flask was added 3,5-Bis((3,4,5-tris(dodecyloxy)benzyl)oxy)benzoic acid **16** (0.8 g, 0.56 mmol) and DCM (20 mL). The solution was cooled at 0 ^oC for 10 minutes under nitrogen atmosphere before 2,6-ditert butyl 4-methyl pyridine (0.228g, 1.11 mmol) and oxalyl chloride (0.14 g, 1.11 mmol) were added, then the reaction mixture was warmed to room temperature and stirred for 3 hours under nitrogen. The reaction mixture was then concentrated under reduced pressure, and the crude product was dissolved in DCM (20 mL) and cooled to -10 ^oC under nitrogen atmosphere. To the stirred solution was added 11,11'-disulfanediylbis(undecan-1-ol) **20** (0.102 g, 0.25 mmol), Et_3N (0.242 g, 2.22 mmol, 0.10 mL), and DMAP (0.05 g, 0.41 mmol). The reaction mixture was allowed to warm up to room temperature and stirred overnight, then was washed with 1 M HCl (2 x 50 mL). The organic layer was dried over anhydrous Na_2SO_4, filtered, and the filtrate was concentrated under reduced pressure. The crude product was purified with column chromatography (100:1 hexanes:ethyl acetate) to afford pure disulfanediylbis(undecane-11,1-diyl) bis(3,5-bis((3,4,5-tris(dodecyloxy)benzyl)oxy)benzoate) **24** as a white solid (0.213g, 26 %). ^{1}H NMR (500 MHz, Chloroform-*d*) δ 7.31 (d, J = 2.3 Hz, 2H), 6.80 (t, J = 2.3 Hz, 1H), 6.63 (s, 4H), 4.96 (s, 4H), 4.31 (t, J = 6.7 Hz, 2H), 3.98 (dt, J = 10.0, 6.5 Hz, 12H), 2.67 (t, J = 7.4 Hz, 2H), 1.83 – 1.74 (m, 14H), 1.67 (p, J = 7.3 Hz, 2H), 1.48 (p, J = 7.3 Hz, 13H), 1.37 – 1.27 (m, 110H), 0.91 – 0.88 (m, 18H); ^{13}C NMR (126 MHz, $CDCl_3$) δ 166.42, 159.94, 153.50, 138.31, 132.58, 131.46, 108.59, 107.03, 106.48, 73.56, 70.89, 69.31, 65.45, 39.29, 32.13, 32.11, 30.54, 29.94, 29.92, 29.89, 29.88, 29.84, 29.83, 29.81, 29.76, 29.71, 29.69, 29.67, 29.62, 29.58, 29.55, 29.45, 29.42, 29.39, 28.89, 28.70, 26.33, 26.30, 26.17, 22.87, 14.27; MALDI-TOF (m/z): $[M+Na]^+$ calcd. for $C_{208}H_{366}O_{20}S_2Na$, 3271.70; found 3275.524.

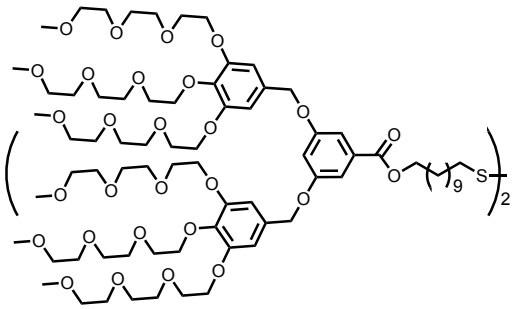

Disulfanediylbis(undecane-11,1-diyl) bis(3,5-bis((3,4,5-tris(2-(2-(2-methoxyethoxy)ethoxy)ethoxy)benzyl)oxy)benzoate) 25.

To an oven dried round bottom flask was added 3,5-Bis((3,4,5-tris(2-(2-(2-methoxyethoxy)ethoxy)ethoxy)benzyl)oxy)benzoic acid **18** (0.413 g, 0.316 mmol) and dichloromethane (12 mL). The solution was cooled at 0 ^{o}C for 10 minutes under nitrogen atmosphere before 2,6-ditert butyl 4-methyl pyridine (0.123g, 0.632 mmol) and oxalyl chloride (0.57 g, 0.632 mmol) were added, then the reaction mixture was warmed to room temperature and stirred for 3 hours under nitrogen. The reaction mixture was then concentrated under reduced pressure, and the crude product was dissolved in DCM (20 mL) and cooled to -10 ^{o}C under nitrogen atmosphere. To the stirred solution was added 11,11'-disulfanediylbis(undecan-1-ol) **20** (0.058 g, 0.142 mmol), triethylamine (0.138 g, 1.26 mmol, 0.19 mL), and DMAP (0.05 g, 0.41 mmol). The reaction mixture was allowed to warm up to room temperature and stirred overnight, then was concentrated under reduced pressure. The crude product was purified with column chromatography (hexanes → ethyl acetate → methanol) to afford pure disulfanediylbis(undecane-11,1-diyl) bis(3,5-bis((3,4,5-tris(2-(2-(2-methoxyethoxy)ethoxy)ethoxy)benzyl)oxy)benzoate) **25** as a yellow oil (0.35 g, 64 %). ^{1}H NMR ($CDCl_3$) δ 7.24 (d, J = 2.3 Hz, 2H), 6.74 (t, J = 2.3 Hz, 1H), 6.64 (s, 4H), 4.91 (s, 4H), 4.26 (t, J = 6.8 Hz, 2H), 4.15 – 4.10 (m, 12H), 3.83 – 3.79 (m, 8H), 3.79 – 3.72 (m, 4H), 3.72 – 3.66 (m, 12H), 3.66 – 3.57 (m, 24H), 3.54 – 3.48 (m, 12H), 3.33 (d, J = 6.1 Hz, 18H), 2.63 (t, J = 7.4, 2.3 Hz, 2H), 1.76 – 1.69 (m, 2H), 1.65 – 1.59 (m, 2H), 1.51 (t, J = 7.5 Hz, 1H), 1.41 – 1.20 (m, 14H); ^{13}C NMR ($CDCl_3$) δ 166.36, 159.77, 152.88, 138.36, 132.55, 131.87, 108.47, 107.42, 106.84, 72.41, 72.02, 72.00, 70.88, 70.85, 70.74, 70.61, 70.58, 70.56, 70.47, 69.80, 69.76, 68.99, 68.92, 65.46, 62.97, 59.07, 39.18, 32.86, 29.63, 29.60, 29.58, 29.36, 29.34, 29.29, 28.79, 28.58, 26.04, 25.85; MALDI-TOF (m/z): $[M+Na]^+$ calcd. for $C_{148}H_{246}O_{56}S_2Na$, 3006.57; found 3011.625.

Results and Discussion

Ligand Synthesis and Design.

To develop methods capable of creating small, yet precisely controlled patches, the dendritic ligands were designed with the surface anchoring unit (sulfur based functional group) on the apex while covalently mounting both hydrophobic and hydrophilic parts on dendron periphery. This approach gives us an efficient access to desired trifunctional Janus dendron where both hydrophobic and hydrophilic moieties are

present on the periphery allowing both of them to interact with each other as well as to surrounding media thus influencing the self-assembly and organization properties.

Scheme 1. Synthesis of hydrophobic building blocks 4 and 5.

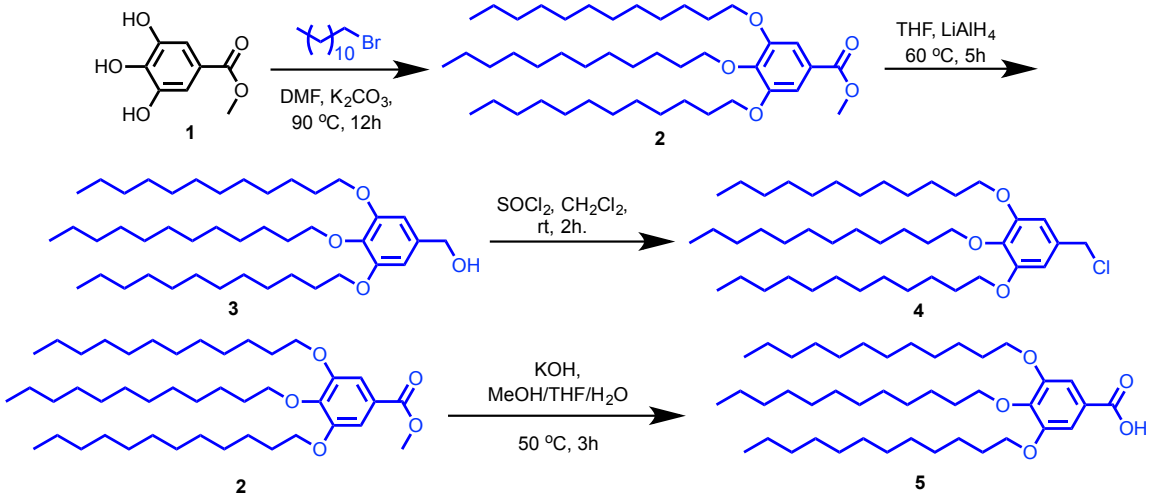

Scheme 2. Synthesis of hydrophilic building blocks 9 and 10.

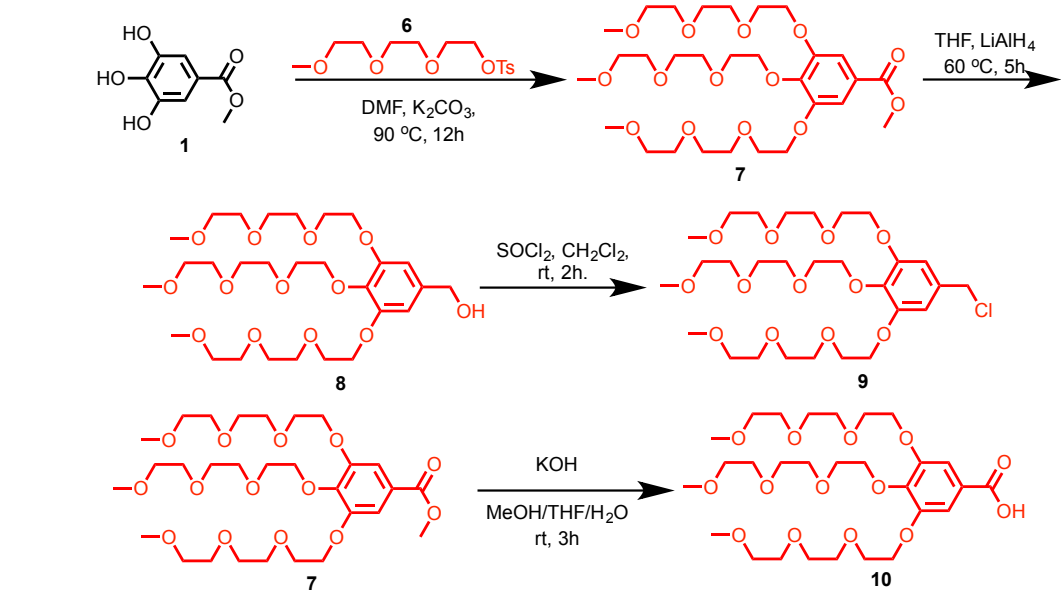

To obtain the targeted Janus ligand, the hydrophobic and hydrophilic building blocks **4** and **9** were synthesized separately through similar pathways through functional group transformation, as shown in Schemes 1 and 2.[16,17] The first step in each of the syntheses is to decorate methyl 3,4,5-trihydroxybenzoate with the hydrophobic or hydrophilic moiety through Williamson ether synthesis affording intermediates **2** and **7**. Reduction using $LiAlH_4$ yields the corresponding alcohols **3** and **8** which can be readily converted into benzyl chlorides **4** and **9** using thionyl chloride, as shown in Schemes 1

and 2. These intermediates were brought together by a strategy that involves stepwise introduction of hydrophobic and hydrophilic parts into dendritic backbone while the surface binding unit **15** was installed at the last step. The synthesis was started by Williamson etherification of methyl 3,5-dihydroxybenzoate **11** with equimolar nonpolar building block **4** giving access to monofunctionalized benzoate **12** (Scheme 3). An analogous reaction between **12** and hydrophilic building block **9** gave benzoate **13**, a Fréchet type second generation (G2) asymmetric dendron **13** where both hydrophobic and hydrophilic parts are present. Methyl ester of **13** was then hydrolyzed to the corresponding carboxylic acid **14**, which is ready to be attached to the corresponding surface binding unit. Similar to acid **14**, we have synthesized the second generation symmetric dendrons containing only hydrophobic or hydrophilic moieties as control systems. Williamson etherification of methyl 3,5-dihydroxybenzoate **11** with excess of either building block **4** or **9** gave access to corresponding second generation symmetric dendrons **15** and **17** which upon hydrolysis gave desired acids **16** and **18** (Scheme 3).

Scheme 3. Synthesis of Second Generation Dendrons 14, 16 and 18[a]

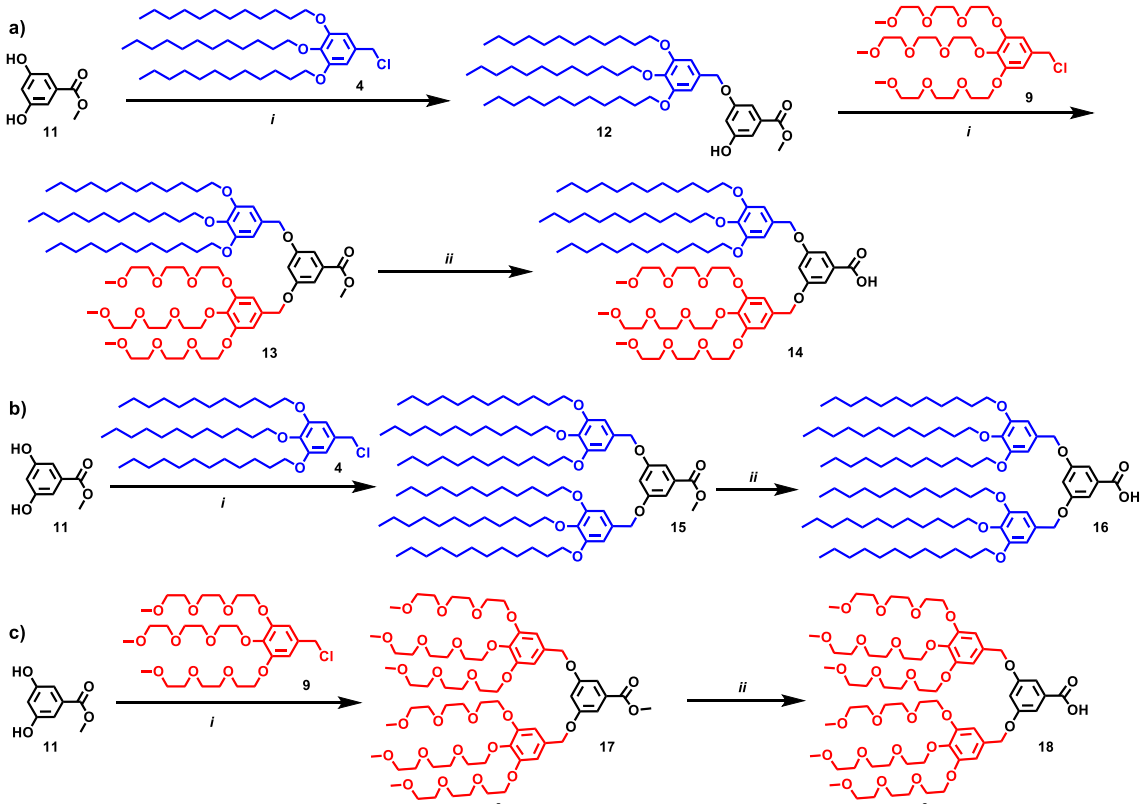

[a]Reagents and conditions: (i) K_2CO_3, KI, DMF, 80 °C, 12h; (ii) KOH, THF/H_2O/MeOH, 3h, 50 °C.

The final targets, a series of dendrons with dithiol surface anchoring units, were synthesized via an esterification reaction between dendritic acids and dithiol bearing

molecule **20**. To build a complete library of ligands, first generation hydrophobic and hydrophilic dendrons **21** and **22** were also synthesized (Scheme 4). This library will provide us with the ability to study the differences between ligands within the generation as well as the effect of different generations. Scheme 4 shows the last step for the synthesis of dendrons **21-25**. Synthesis were carried out as one pot two-step process where acid chlorides were first generated *in situ* from carboxylic acids and then reacted with alcohol **20**. For the second generation ligands, base 2,6-ditert butyl 4-methyl pyridine and oxalyl chloride were used instead of $SOCl_2$ to generate the acid chloride. When reacted with only $SOCl_2$, the second generation ligands do not proceed to the desired product, which could be due to the presence of an acidic hydrogen para to the carboxylic acid in the second generation ligands.

Scheme 4. The synthesis of dithiol dendrons 21-25[a]

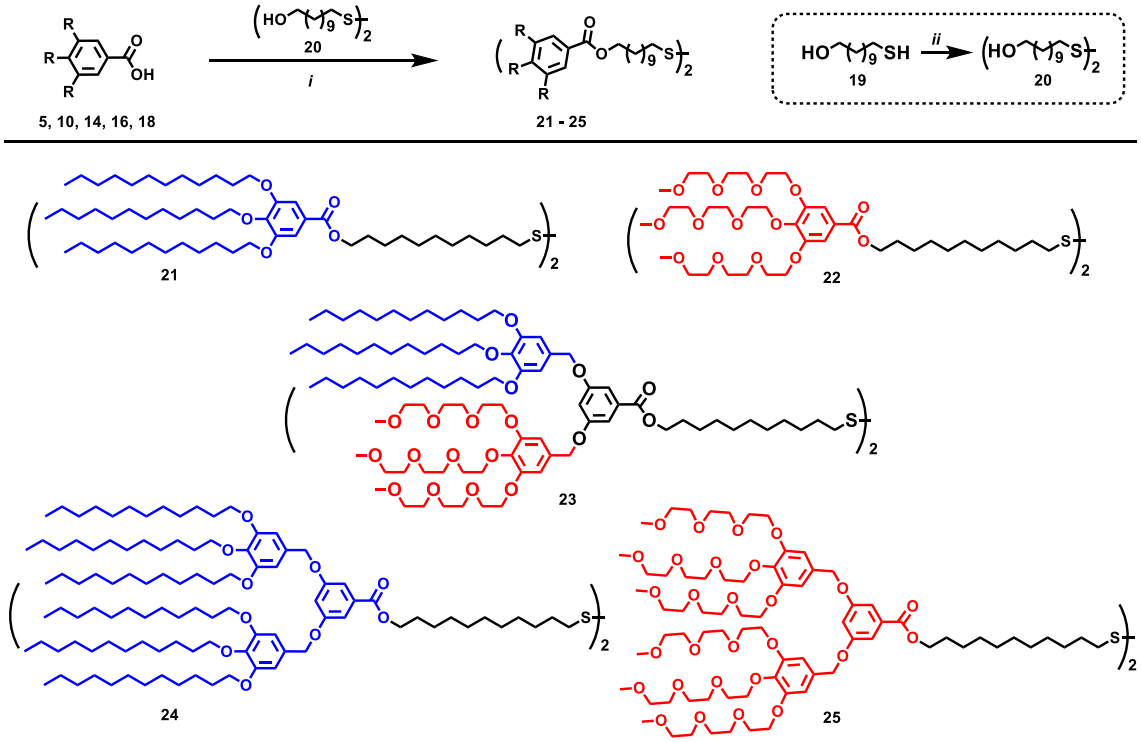

[a]Reagents and conditions: (i) $SOCl_2$, CH_2Cl_2, rt, 3h, then **20**, Et_3N, DMAP, CH_2Cl_2, -10°C→rt, 12h; (ii) I_2, CH_2Cl_2, rt, 12h.

Ligand Exchange with Gold Nanoparticles and Self-Assembly.

To study how the various dendritic ligands affect the self-assembly properties of NPs, each dendrimer was grafted onto 8 nm Au NP surfaces using solution phase ligand exchange (denoted with Au@ligand). A ligand exchange approach was chosen because it is already well known how to synthesize Au NPs with commercially available ligands to produce uniform NPs of a controlled size. The introduction of a new ligand in the NP synthesis could change the parameters of the NP synthesis, and developing the new conditions for NP synthesis is outside of the scope of this project. A ligand exchange process is quick, straightforward, and effective, particularly with a ligand containing a

sulfur group. The ligand exchange process was carried out in solution phase where oleylamine stabilized gold particles were mixed with an excess dendritic ligands and allowed to stir at room temperature. This step introduced dendritic ligands on nanoparticle surfaces without affecting the size of inorganic core, which can be seen in Figure 1.

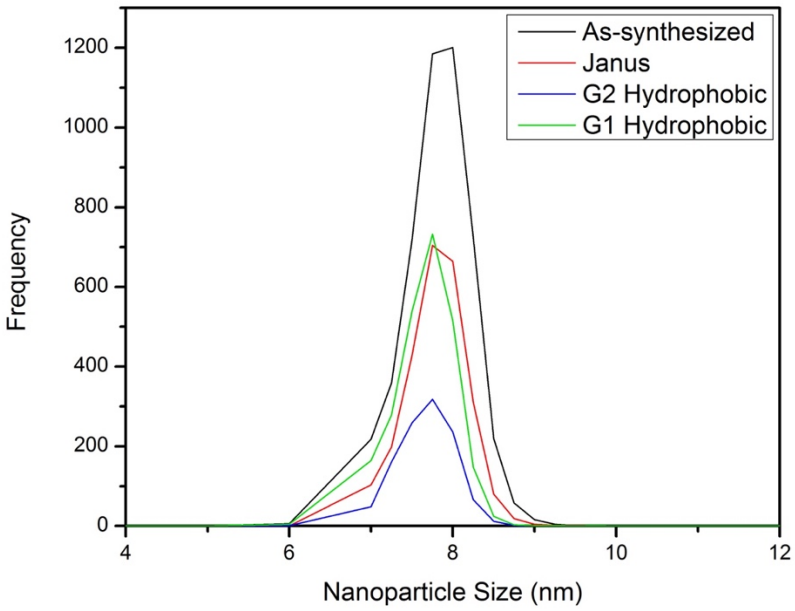

Figure 1. Size distribution of the Au nanoparticles before and after each ligand exchange.

The NPs were then allowed to self-assemble on liquid-air interface, following a previously reported procedure,[37] the results of which are shown in Figure 2. For each of the ligands tested (**21**, **23** and **24**), the NPs self-assemble into a hexagonal close packed (hcp) crystalline structures. The inter-particle spacing was analyzed for each of the self-assembly structures, the results of which are shown in Table 1. As expected, we noticed the change in inter-particle spacing during every ligand exchange step. The as synthesized oleylamine caped particles showed edge to edge inter-particle space of 2.0 nm which was gradually increased to 2.7, 3.1 and 5.2 nm for Au@**23**, Au@**21** and Au@**24**, respectively. An increase in inter-particle spacing is expected as higher generation introduces larger steric bulk. However, the case of Janus dendron **23** is somewhat special. It is a generation 2 dendron and is larger than corresponding generation 1 dendron **21** by means of molecular weight (1558 vs 860 per thiolate), but still introduces less inter-particle spacing (2.7 nm vs 3.1 nm). This is perhaps due to the presence of flexible polyethyleneglycol containing branch combined with the fact that per surface area smaller number of ligand **23** (compared to ligand **21**) would be present. Therefore, it would result in overall smaller inter-particle distance.

Ligands **22** and **25** were grafted onto NPs, but these NPs were not self-assembled. This is due to the solubility of the hydrophilic ligands, which make Au@**22** and Au@**25** soluble in solvents such as methanol. Being dispersible in only solvents such as methanol or chloroform in problematic for self-assembly investigation because of the densities and miscibility's of these solvents. For successful self-assembly, the NPs have to be dispersed

in a solvent that is less dense and not miscible with another liquid layer, which is where, upon evaporation, the assembled NPs will form. The PEG ligand is also soluble in the typical surface for a liquid-air interface self-assembly, diethylene glycol, which leads to challenges investigating self-assembly.

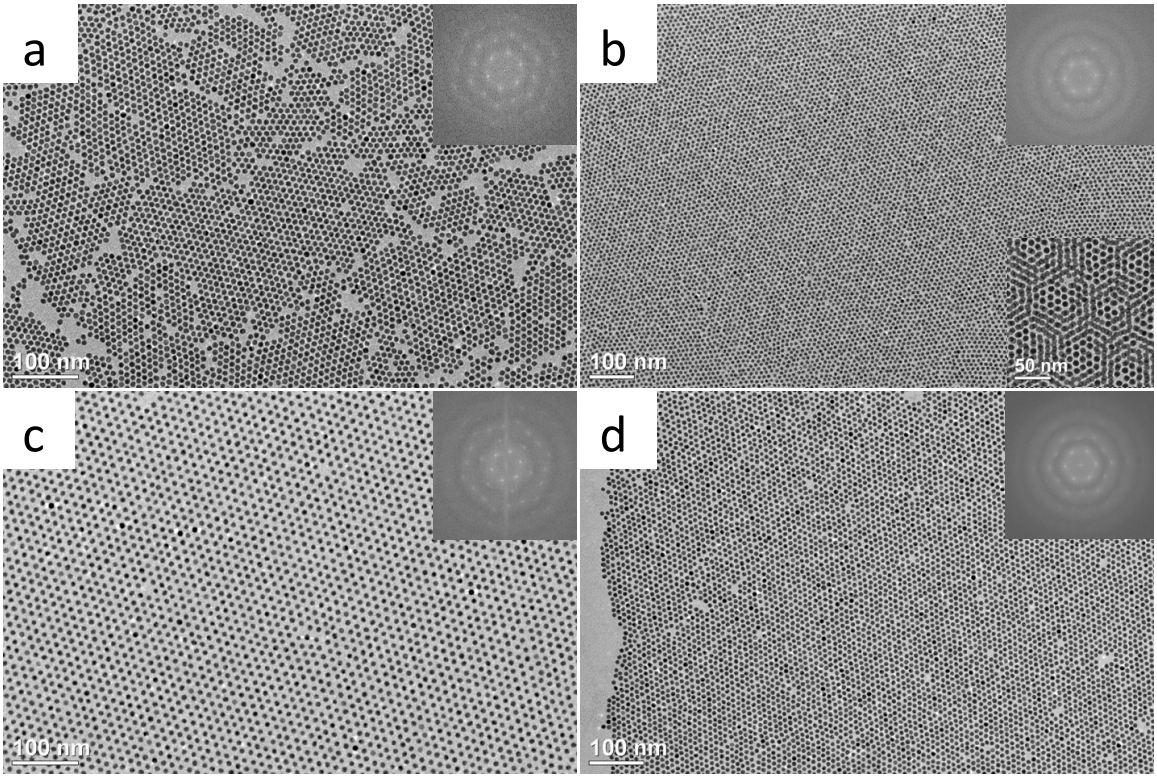

Figure 2. Self-assembly of NCs, *a*) as-synthesized NCs, *b*) G1 hydrophobic **21**, *c*) G2 hydrophobic **24**, and *d*) Janus.

To study how the different ligands interact with each other mixtures of the NPs with the various ligands on their surfaces were studied. To achieve this, the NPs with each of the respective ligands were mixed together to result in three different combinations: Au@**21** and Au@**24**, Au@**21** and Au@Janus, and Au@**24** and Au@Janus. For each of the three combinations, self-assemblies of the NPs were studied. As can be seen from Figure 3a and 3b, the mixtures of Au@**21** and Au@**24**, as well as Au@**21** and Au@Janus self-assemble into well-organized hcp crystalline structures. The inter-particle spacing analysis of these mixtures show that when NPs with G1 hydrophobic ligands **21** are mixed with NPs with **24** hydrophobic ligands self- assemble, the space in between each particle is an intermediate between single component assemblies of Au@**21** and Au@**24**. For the case when Au@**21** hydrophobic are mixed with Au@Janus self-assemble, the interparticle spacing is similar to that of Au@**21** hydrophobic. This result is consistent with the results observed for single component cases where inter-particle spacing introduced by these ligands are not very different. When Au@Janus are mixed with Au@**24** there is no ordered crystalline structure observed, which is most likely due to the fact that the difference between the two ligands is too large to allow the formation of a uniform crystalline film.

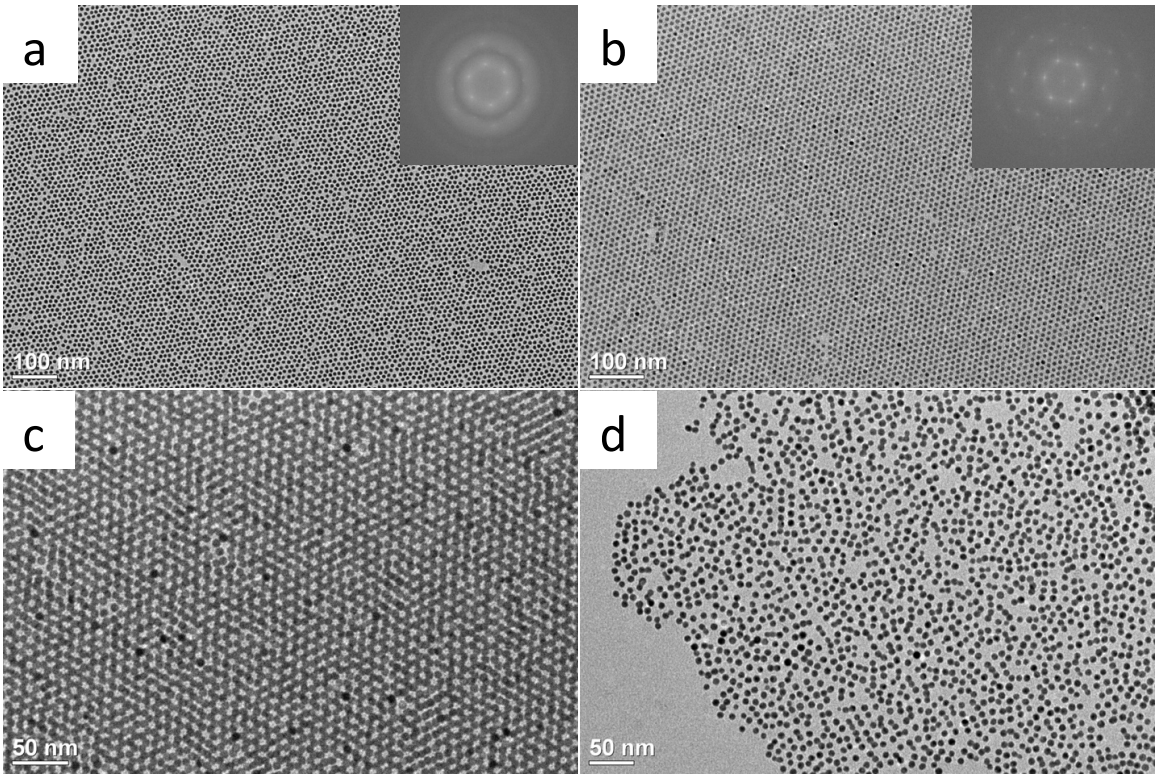

Figure 3. TEM image of self-assembled monolayers of NCs obtained with mixtures of NPs with different dendritic ligands: *a*) Au@**21** and Au@**24**, *b*) Au@**21** and Au@Janus, *c*) a multilayer of Au@**21** and Au@**24**, and *d*) Au@Janus and Au@**24**.

To confirm the crystallinity and the effects of interparticle spacing of the self-assemblies, UV-vis was performed. All of the Au NPs with different ligands have the same maximum absorption wavelength when analyzed with solution-phase UV-vis, shown in Figure 4, which is due to the NPs not being immobilized. To perform solid-state UV-vis, a solution of NPs were allowed to slowly evaporate on a glass slide, to allow for self-assembly to occur. From solid-state UV-vis, a redshift in the absorption wavelength maximum is observed, which can be seen from Figure 4. This shift is representative of the changes in interparticle spacing, which is consistent with previous research.[16,39] Contact angle measurements were also performed, as a quantitative technique to observe the change in hydrophobicity of NPs with the various ligands grafted onto their surface. As expected, the NPs with the hydrophobic ligands on their surfaces had a large contact angle, those with hydrophilic ligands had a smaller contact angle, and the Janus ligand has an intermediate contact angle. The results of the contact angle, solid-state UV-vis measurements, and interparticle spacing for each of the NPs are listed in Table 1.

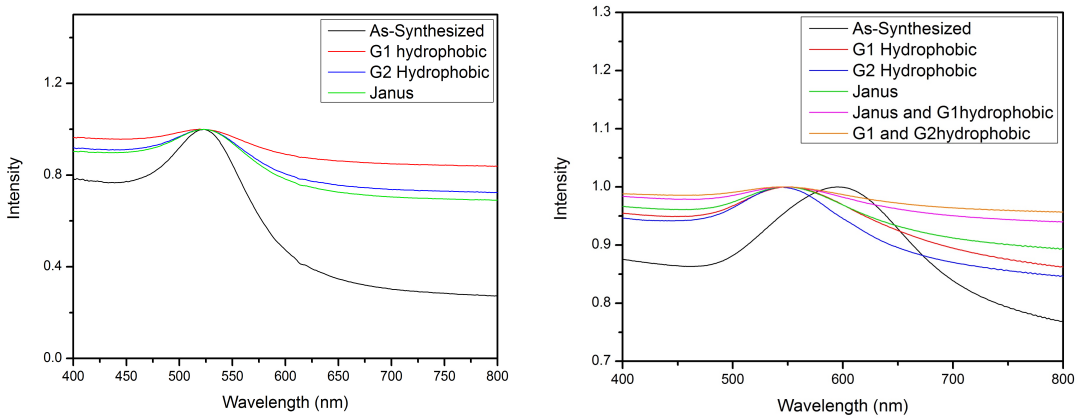

Figure 4. UV-vis measurements of nanoparticles with the various ligands grafted on their surface *a*) Solution phase and *b*) solid-state UV-vis measurements.

Table 1. Summary of interparticle spacing, absorption wavelength maximum, and contact angle measurements for each set of NPs studied.

	Center-to-Center (nm), from TEM	Edge-to-Edge (nm), from TEM	λ_{max} (nm)	Contact Angle (º)
As synthesized Au NPs	10.0	2.0	596	71.8
Au@Janus	10.7	2.7	550	65.3
Au@**21**	11.1	3.1	547	85.0
Au@**24**	13.2	5.2	544	89.2
Au@Janus and Au@**21**	11.3	3.3	547	-
Au@**21** and Au@**24**	12.0	4.0	545	-
Au@Janus and Au@**24**	-	-	-	-
Au@**22**	-	-	-	58.3
Au@**25**	-	-	-	48.8

Visualizing the Janus Dendron on Au NPs.

When considering the Janus dendron synthesized in this work, there should be a patchy surface on the Au NPs, due to the hydrophobic and hydrophilic moieties being covalently bound to each other, but still assembling with neighboring Janus dendrons. The patches that these moieties create should be less then 5nm in size. To visualize how the Janus dendrimer self assembles on the surface of the Au NPs, two different stains were employed, uranyl acetate and caesium carbonate. For both of these stains, the uranium or caesium should bind to oxygen, resulting in the oxygen rich PEG branch of the Janus dendron appearing much darker when visualizing with TEM than the oxygen

poor alkyl chain branch. As can be seen from Figure 5, for both of the stains, no change to the surface of the Au@Janus NPs can be observed. One reason for this could be due to the Au NPs already being particularly electron rich, making them very dark when visualizing with TEM, which can lead to challenges visualizing any stains. Another factor may be that a TEM with higher resolution may be required to visualize sub-5 nm patches.

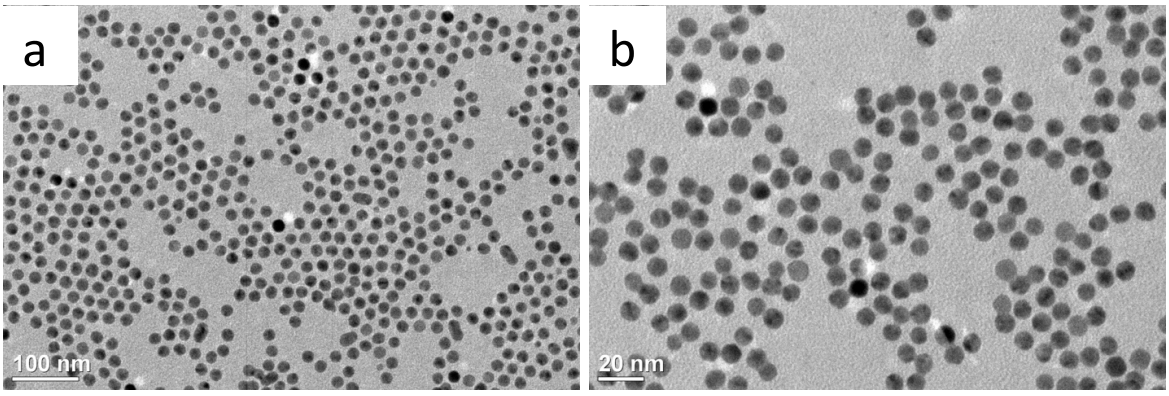

Figure 5. Au@Janus NPs stained with *a)* uranyl acetate and *b)* caesium carbonate.

In an attempt to visualize the Janus ligand, a 3 Angstrom thick layer of gold was deposited onto a TEM grid using e-beam epitaxy. The Janus ligand was then deposited onto the layer of gold, and was then stained with uranyl acetate. As can be seen in Figure 6, there are darker, patchy regions on the TEM grid that are 2-3 nm in size, which is similar to what we expected. It is difficult to determine the nature of these darker patches using only the TEM, and without confirmation from EDS or EELS, it would be inappropriate to claim that these patches are caused by the stain binding to the hydrophilic moiety of the Janus ligand, and they may be a uranyl acetate salt.

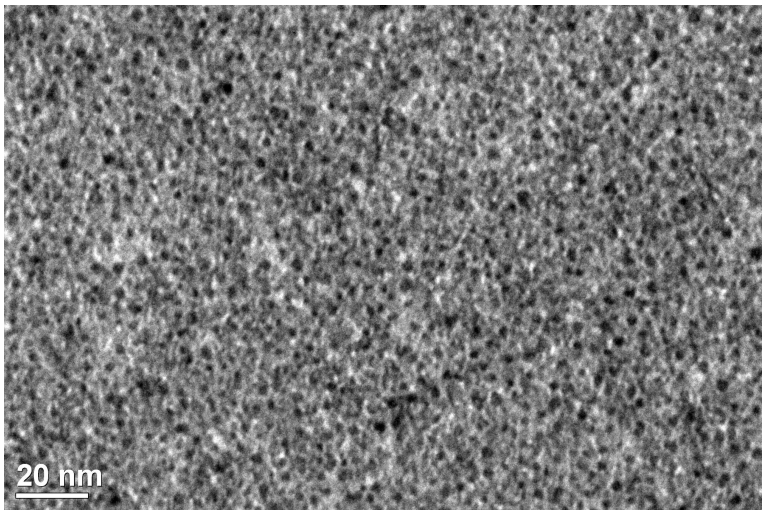

Figure 6. TEM of Au thin film with the Janus ligand that was stained with uranyl acetate.

Conclusion

I have demonstrated a flexible route to synthesize novel dendritic ligands, including the Janus ligand which includes both hydrophilic and hydrophobic moieties. The self assembly properties of the series of ligands were studied, which revealed that the NPs assemble into hcp crystalline structures, with precise interparticle spacing that increases with an increase in the dendron generation. Mixtures of NPs with different ligands were assembled, and mixtures of Au@**21** and Au@**24** as well as Au@**21** and Au@**Janus** assembled well into hcp crystalline structures. Lastly, to study the assembly properties of this Janus ligand, it was bound to a thin film of gold, then stained with a uranyl acetate solution. TEM images reveal that it may be possible to visualize the patchy surface that the Janus ligand creates, but further studies, such as high resolution TEM and EDS or the synthesis of a larger ligand, are required for definitive proof.

References

1. Kovalenko, M. V, Scheele, M. & Talapin, D. V. Colloidal nanocrystals with molecular metal chalcogenide surface ligands. *Science* **324,** 1417–20 (2009).
2. Dong, A. *et al.* A generalized ligand-exchange strategy enabling sequential surface functionalization of colloidal nanocrystals. *J. Am. Chem. Soc.* **133,** 998–1006 (2011).
3. Talapin, D. V, Lee, J.-S., Kovalenko, M. V & Shevchenko, E. V. Prospects of colloidal nanocrystals for electronic and optoelectronic applications. *Chem. Rev.* **110,** 389–458 (2010).
4. Walker, B. J., Nair, G. P., Marshall, L. F., Bulović, V. & Bawendi, M. G. Narrow-band absorption-enhanced quantum dot/J-aggregate conjugates. *J. Am. Chem. Soc.* **131,** 9624–5 (2009).
5. Giansante, C. *et al.* 'Darker-than-black' PbS quantum dots: enhancing optical absorption of colloidal semiconductor nanocrystals via short conjugated ligands. *J. Am. Chem. Soc.* **137,** 1875–86 (2015).
6. Cano, I. *et al.* Air-Stable Gold Nanoparticles Ligated by Secondary Phosphine Oxides as Catalyst for the Chemoselective Hydrogenation of Substituted Aldehydes: a Remarkable Ligand Effect. *J. Am. Chem. Soc.* **137,** 7718–27 (2015).
7. Murray, C. B., Norris, D. J. & Bawendi, M. G. Synthesis and characterization of nearly monodisperse CdE (E = sulfur, selenium, tellurium) semiconductor nanocrystallites. *J. Am. Chem. Soc.* **115,** 8706–8715 (1993).
8. Grzelczak, M., Pérez-Juste, J., Mulvaney, P. & Liz-Marzán, L. M. Shape control in gold nanoparticle synthesis. *Chem. Soc. Rev.* **37,** 1783–1791 (2008).
9. Sau, T. K. & Murphy, C. J. Room Temperature, High-Yield Synthesis of Multiple Shapes of Gold Nanoparticles in Aqueous Solution. *J. Am. Chem. Soc.* **126,** 8648–8649 (2004).
10. Sau, T. K. & Murphy, C. J. Seeded High Yield Synthesis of Short Au Nanorods in Aqueous Solution. *Langmuir* **20,** 6414–6420 (2004).
11. Reiser, B., González-García, L., Kanelidis, I., Maurer, J. H. M. & Kraus, T. Gold nanorods with conjugated polymer ligands: sintering-free conductive inks for printed electronics. *Chem. Sci.* **7,** 4190–4196 (2016).
12. Rucareanu, S., Maccarini, M., Shepherd, J. L. & Lennox, R. B. Polymer-capped gold nanoparticles by ligand-exchange reactions. *J. Mater. Chem.* **18,** 5830 (2008).
13. Kim, S., Kim, T.-H., Huh, J., Bang, J. & Choi, S.-H. Nanoscale Phase Behavior of Mixed Polymer Ligands on a Gold Nanoparticle Surface. *ACS Macro Lett.* **4,** 417–421 (2015).
14. Bronstein, L. M. & Shifrina, Z. B. Dendrimers as encapsulating, stabilizing, or directing agents for inorganic nanoparticles. *Chem. Rev.* **111,** 5301–44 (2011).
15. Daniel, M.-C. & Astruc, D. Gold nanoparticles: assembly, supramolecular chemistry, quantum-size-related properties, and applications toward biology, catalysis, and nanotechnology. *Chem. Rev.* **104,** 293–346 (2004).
16. Jishkariani, D. *et al.* Dendron-Mediated Engineering of Interparticle Separation and Self-Assembly in Dendronized Gold Nanoparticles Superlattices. *J. Am. Chem. Soc.* **137,** 10728–34 (2015).
17. Fleutot, S. *et al.* Spacing-dependent dipolar interactions in dendronized magnetic

iron oxide nanoparticle 2D arrays and powders. *Nanoscale* **5,** 1507–16 (2013).
18. Lewandowski, W., Łojewska, T., Szustakiewicz, P., Mieczkowski, J. & Pociecha, D. Reversible switching of structural and plasmonic properties of liquid-crystalline gold nanoparticle assemblies. *Nanoscale* **8,** 2656–2663 (2016).
19. Nealon, G. L. *et al.* Liquid-crystalline nanoparticles: Hybrid design and mesophase structures. *Beilstein J. Org. Chem.* **8,** 349–370 (2012).
20. Lewandowski, W., Wójcik, M. & Górecka, E. Metal nanoparticles with liquid-crystalline ligands: controlling nanoparticle superlattice structure and properties. *Chemphyschem* **15,** 1283–95 (2014).
21. Dong, A. *et al.* A Generalized Ligand-Exchange Strategy Enabling Sequential Surface Functionalization of Colloidal Nanocrystals. *J. Am. Chem. Soc.* **133,** 998–1006 (2011).
22. Fafarman, A. T. *et al.* Thiocyanate-Capped Nanocrystal Colloids: Vibrational Reporter of Surface Chemistry and Solution-Based Route to Enhanced Coupling in Nanocrystal Solids. *J. Am. Chem. Soc.* **133,** 15753–15761 (2011).
23. Walther, A. & Müller, A. H. E. Janus Particles: Synthesis, Self-Assembly, Physical Properties, and Applications. *Chem. Rev.* **113,** 5194–5261 (2013).
24. Pawar, A. B. & Kretzschmar, I. Fabrication, Assembly, and Application of Patchy Particles. *Macromol. Rapid Commun.* **31,** 150–168 (2010).
25. Poulos, T. L. The Janus nature of heme. *Nat. Prod. Rep.* **24,** 504 (2007).
26. Du, J. & O'Reilly, R. K. Anisotropic particles with patchy, multicompartment and Janus architectures: preparation and application. *Chem. Soc. Rev.* **40,** 2402 (2011).
27. Grätzel, M. Photoelectrochemical cells. *Nature* **414,** 338–344 (2001).
28. Liddell, C. M., Summers, C. J. & Gokhale, A. M. Stereological estimation of the morphology distribution of ZnS clusters for photonic crystal applications. *Mater. Charact.* **50,** 69–79 (2003).
29. Poon, Z. *et al.* Ligand-Clustered 'Patchy' Nanoparticles for Modulated Cellular Uptake and In Vivo Tumor Targeting. *Angew. Chemie Int. Ed.* **49,** 7266–7270 (2010).
30. Langer, R. & Tirrell, D. A. Designing materials for biology and medicine. *Nature* **428,** 487–492 (2004).
31. Hong, L., Jiang, S. & Granick, S. Simple Method to Produce Janus Colloidal Particles in Large Quantity. *Langmuir* **22,** 9495–9499 (2006).
32. Cho, Y.-S. *et al.* Self-Organization of Bidisperse Colloids in Water Droplets. *J. Am. Chem. Soc.* **127,** 15968–15975 (2005).
33. Pawar, A. B. & Kretzschmar, I. Multifunctional Patchy Particles by Glancing Angle Deposition. *Langmuir* **25,** 9057–9063 (2009).
34. Allison M. Yake, Charles E. Snyder & Velegol, D. Site-Specific Functionalization on Individual Colloids: Size Control, Stability, and Multilayers. *Langmuir* **23,** 9069–9075 (2007).
35. Snyder, C. E., Yake, A. M., Feick, J. D. & Velegol, D. Nanoscale Functionalization and Site-Specific Assembly of Colloids by Particle Lithography. *Langmuir* **21,** 4813–4815 (2005).
36. Gottlieb, H. E., Kotlyar, V. & Nudelman, A. NMR Chemical Shifts of Common Laboratory Solvents as Trace Impurities. *J. Org. Chem.* **62,** 7512–7515 (1997).
37. Dong, A., Chen, J., Vora, P. M., Kikkawa, J. M. & Murray, C. B. Binary

nanocrystal superlattice membranes self-assembled at the liquid–air interface. *Nature* **466,** 474–477 (2010).
38. Kell, A. J., Alizadeh, A., Yang, L. & Workentin, M. S. Monolayer-Protected Gold Nanoparticle Coalescence Induced by Photogenerated Radicals. *Langmuir* **21,** 9741–9746 (2005).
39. Jain, P. K., Wenyu Huang, A. & Mostafa A. El-Sayed. On the Universal Scaling Behavior of the Distance Decay of Plasmon Coupling in Metal Nanoparticle Pairs: A Plasmon Ruler Equation. *Nano Lett.* **7,** 2080–2088 (2007).

Appendix

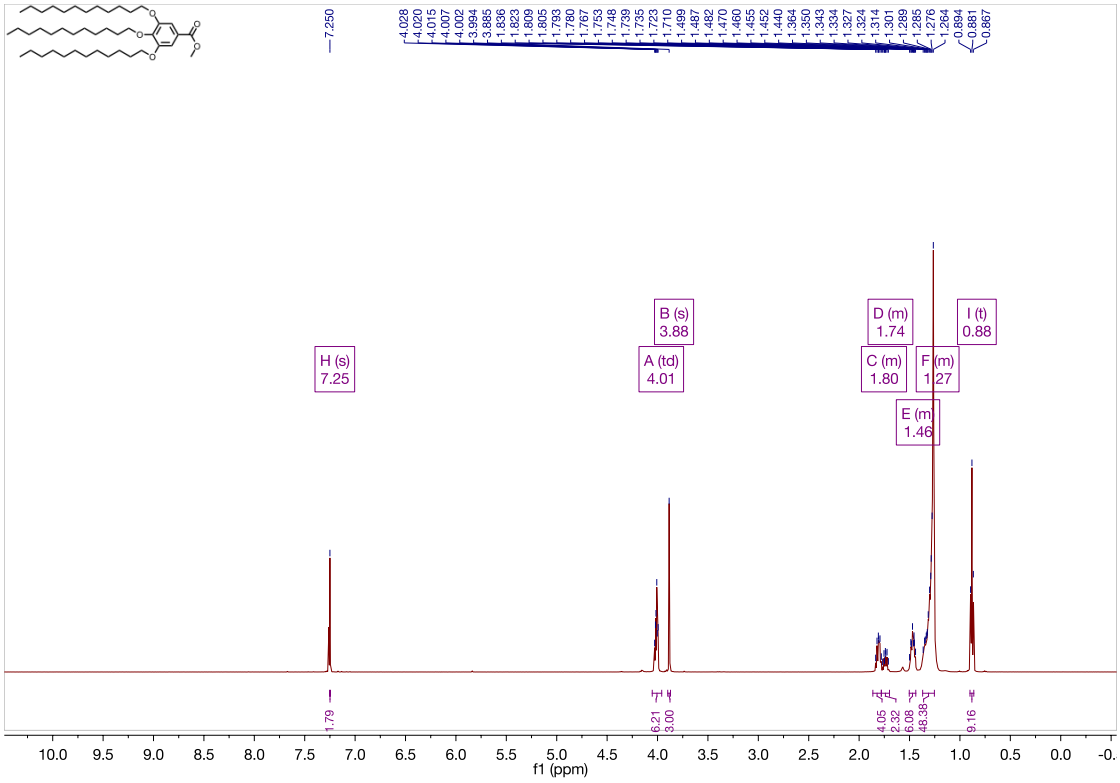
H (s)
7.25
A (td)
4.01
B (s)
3.88
C (m)
1.80
D (m)
1.74
E (m)
1.46
F (m)
1.27
I (t)
0.88
f1 (ppm)

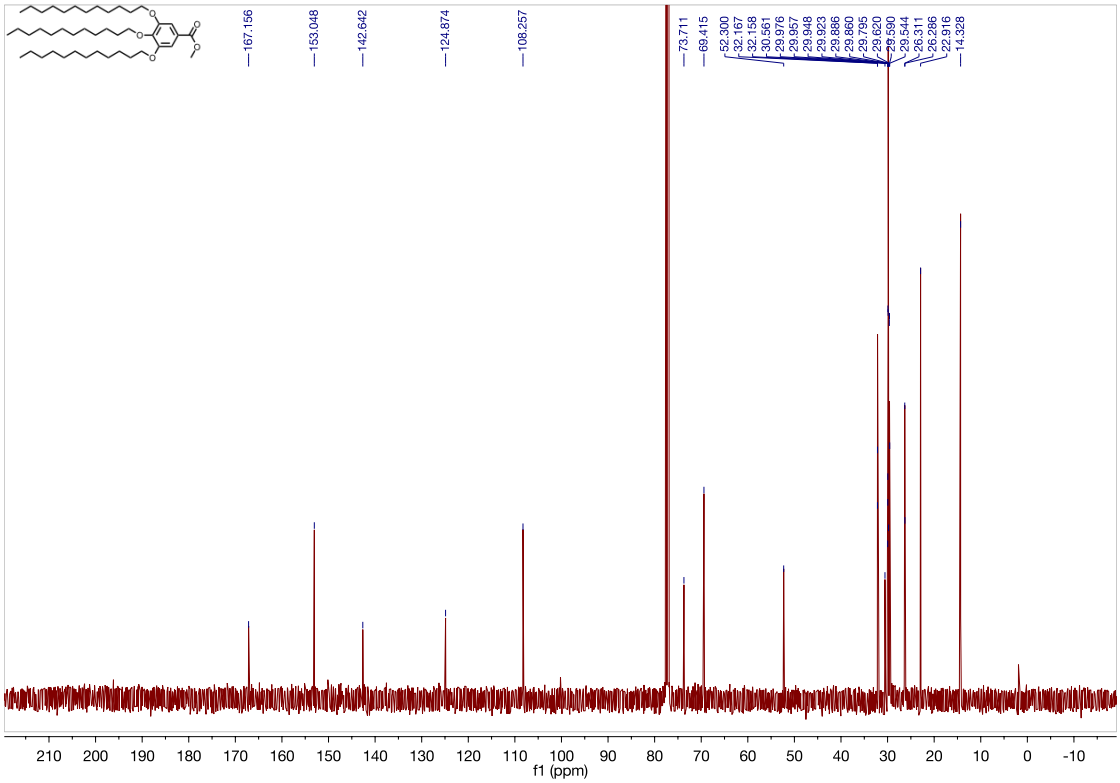
f1 (ppm)

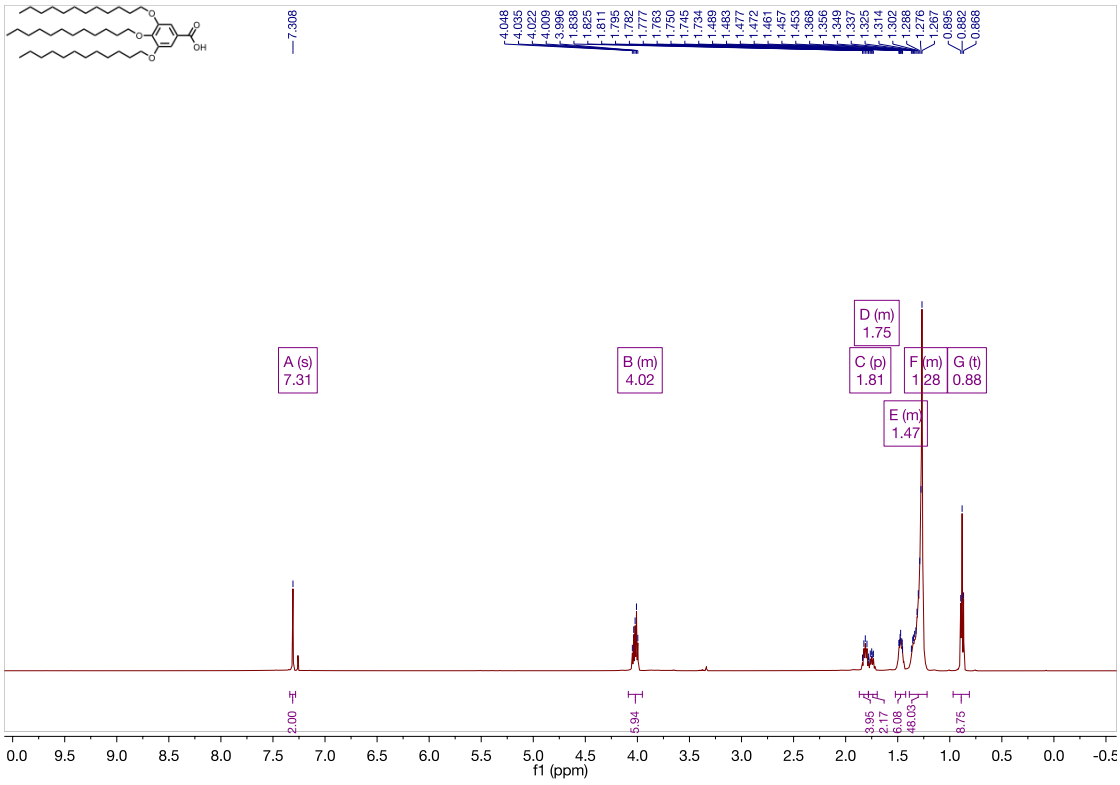
7.308
4.048
4.035
4.022
4.009
3.996
1.838
1.825
1.811
1.795
1.782
1.777
1.763
1.750
1.745
1.734
1.489
1.483
1.477
1.472
1.461
1.457
1.453
1.368
1.356
1.349
1.337
1.325
1.314
1.302
1.288
1.276
1.267
0.895
0.882
0.868
A (s) 7.31
B (m) 4.02
C (p) 1.81
D (m) 1.75
E (m) 1.47
F (m) 1.28
G (t) 0.88
2.00
5.94
3.95
2.17
6.08
48.03
8.75
f1 (ppm)

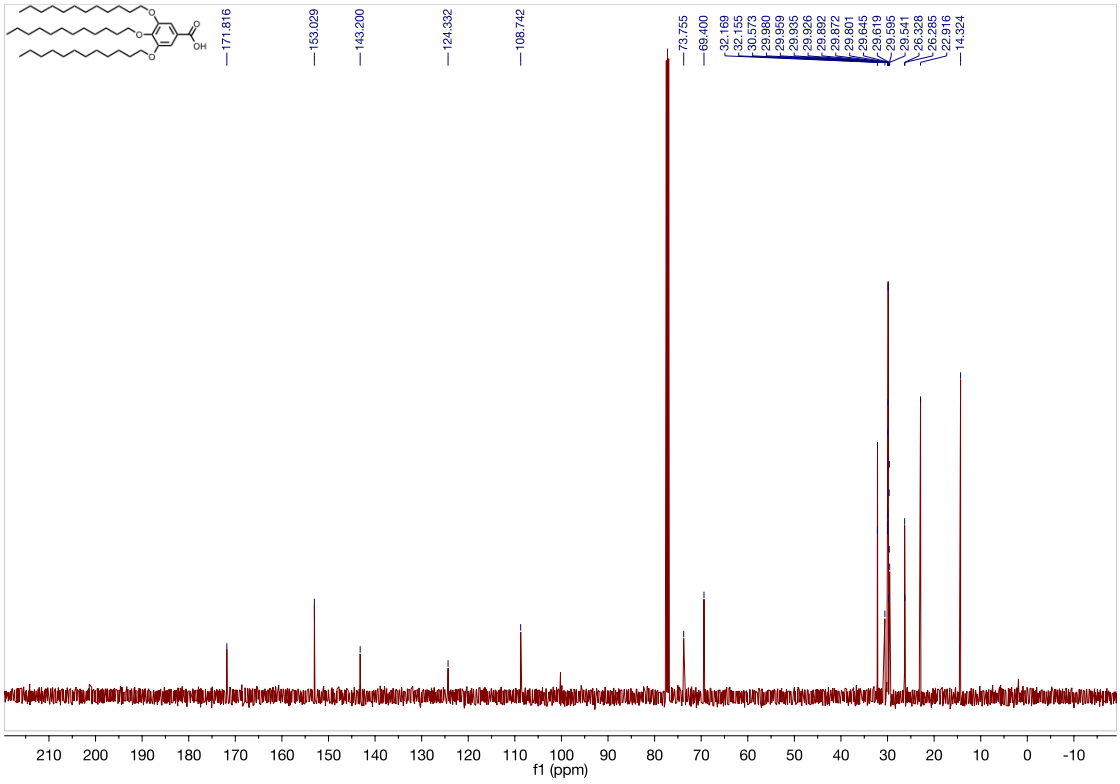
171.816
153.029
143.200
124.332
108.742
73.755
69.400
32.169
32.155
30.573
29.980
29.959
29.935
29.926
29.892
29.872
29.801
29.645
29.619
29.595
29.541
26.328
26.285
22.916
14.324
f1 (ppm)

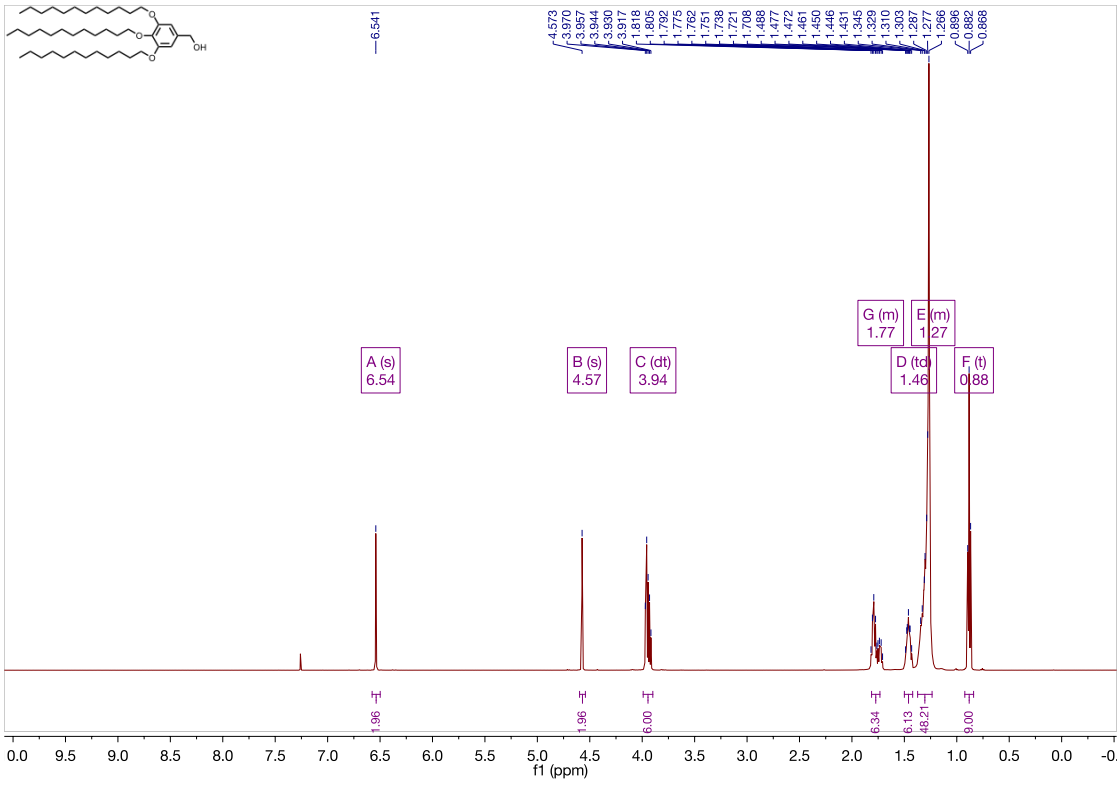
A (s)
6.54
B (s)
4.57
C (dt)
3.94
D (td)
1.46
E (m)
1.27
F (t)
0.88
G (m)
1.77
f1 (ppm)

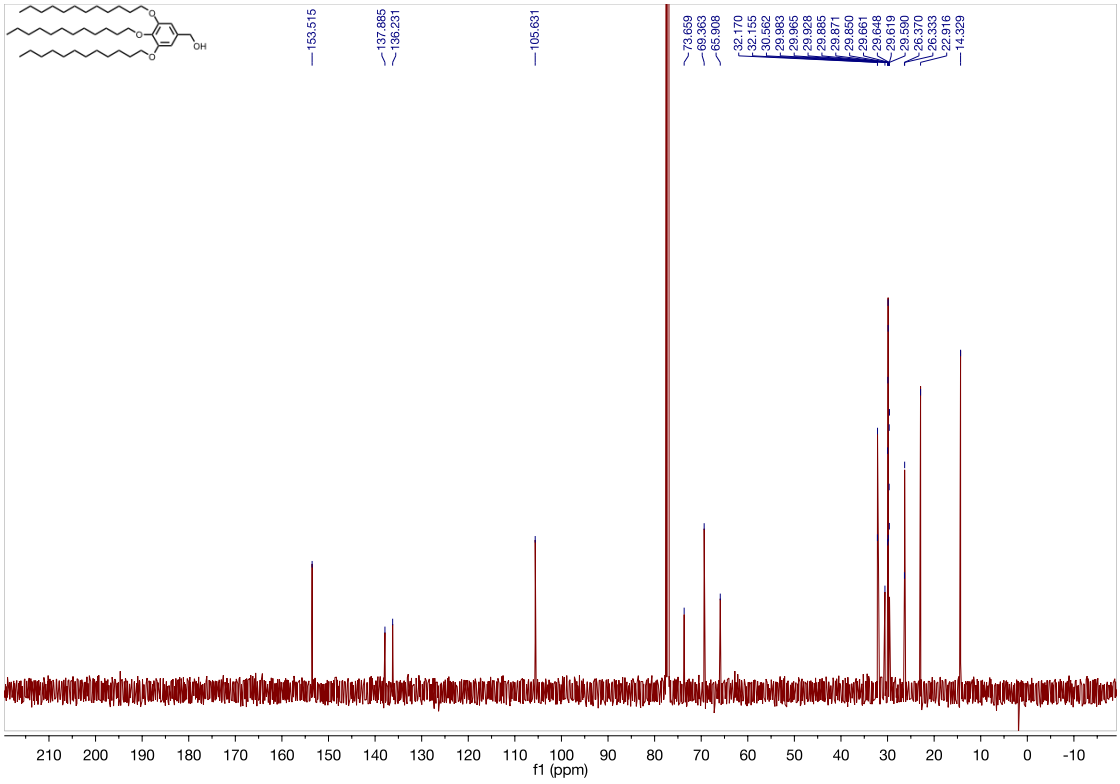
153.515
137.885
136.231
105.631
73.659
69.363
65.908
32.170
32.155
30.562
29.983
29.965
29.928
29.885
29.871
29.850
29.661
29.648
29.619
29.590
26.370
26.333
22.916
14.329
f1 (ppm)

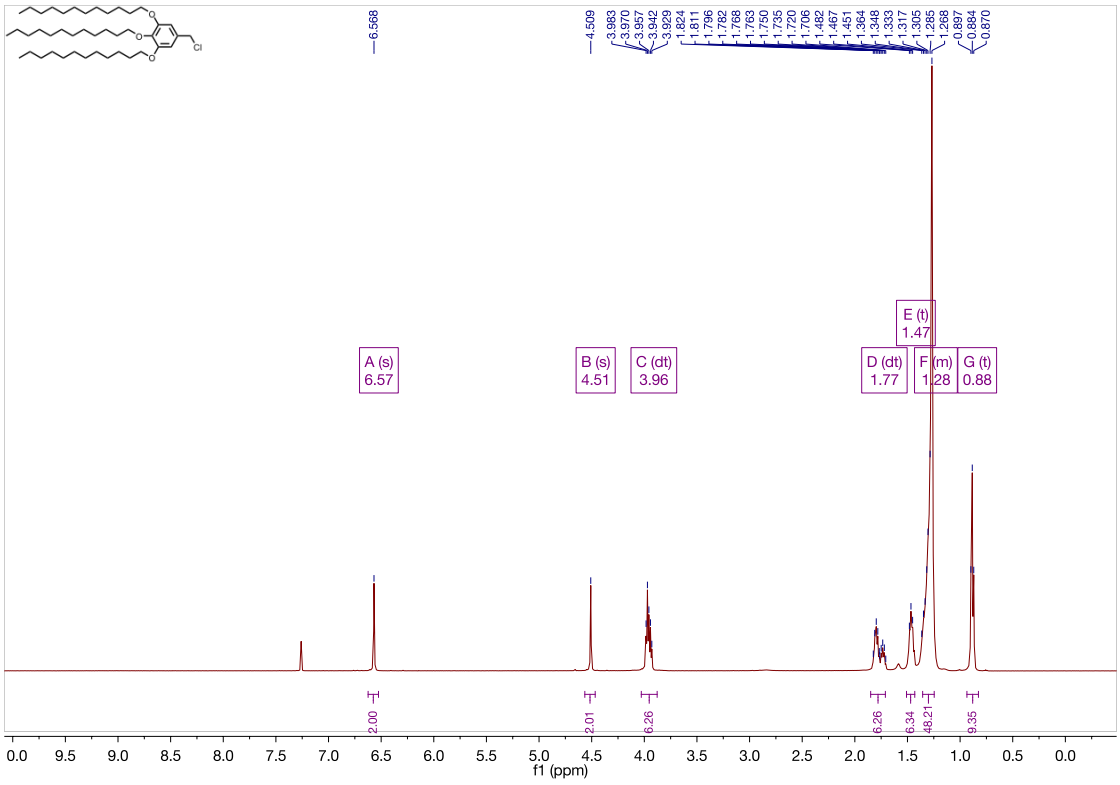
6.568
4.509
3.983
3.970
3.957
3.942
3.929
1.824
1.811
1.796
1.782
1.768
1.763
1.750
1.735
1.720
1.706
1.482
1.467
1.451
1.364
1.348
1.333
1.317
1.305
1.285
1.268
0.897
0.884
0.870
A (s) 6.57
B (s) 4.51
C (dt) 3.96
D (dt) 1.77
E (t) 1.47
F (m) 1.28
G (t) 0.88
2.00
2.01
6.26
6.26
6.34
48.21
9.35
f1 (ppm)

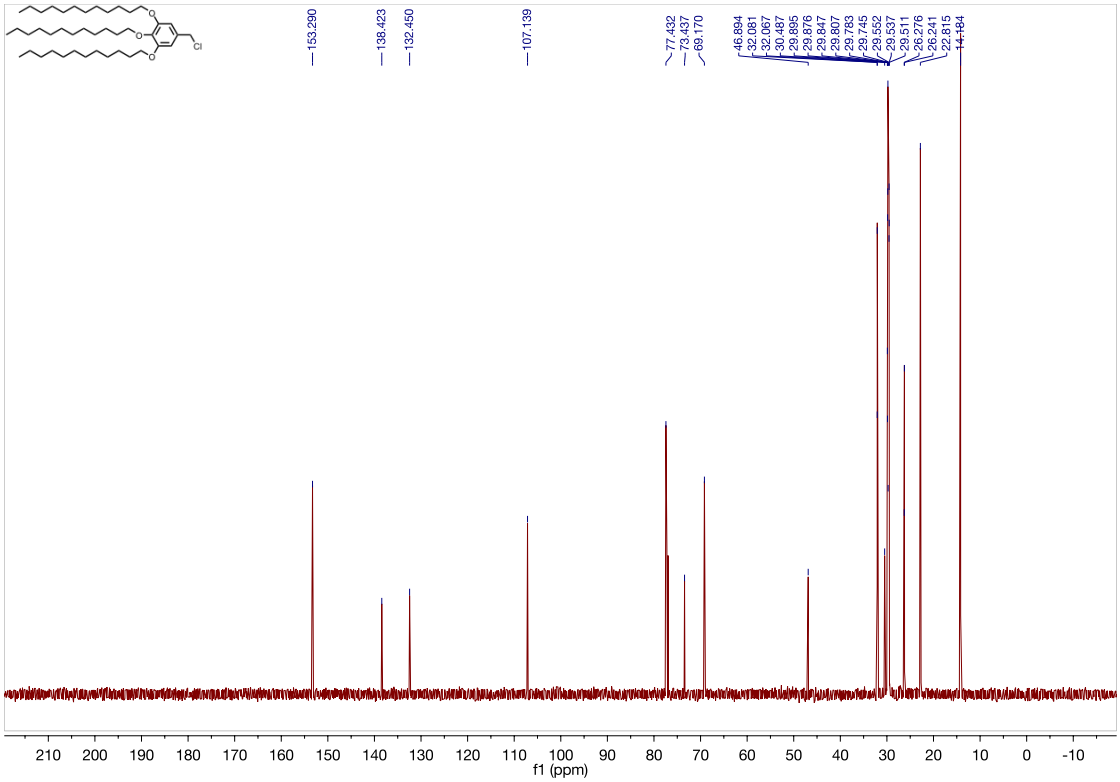
153.290
138.423
132.450
107.139
77.432
73.437
69.170
46.894
32.081
32.067
30.487
29.895
29.876
29.847
29.807
29.783
29.745
29.552
29.537
29.511
26.276
26.241
22.815
14.184
f1 (ppm)

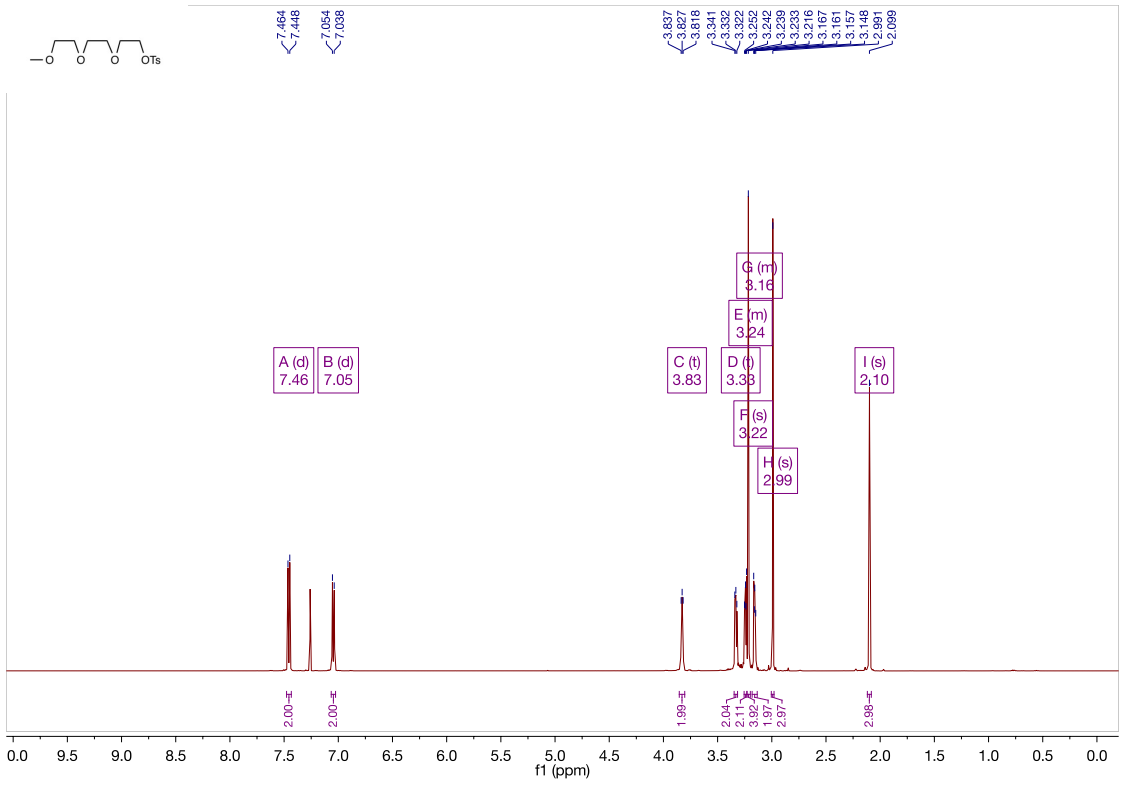
7.464
7.448
7.054
7.038
3.837
3.827
3.818
3.341
3.332
3.322
3.252
3.242
3.239
3.233
3.216
3.167
3.161
3.157
3.148
2.991
2.099
A (d) 7.46
B (d) 7.05
C (t) 3.83
D (t) 3.33
E (m) 3.24
G (m) 3.16
F (s) 3.22
H (s) 2.99
I (s) 2.10
2.00
2.00
1.99
2.04
2.11
3.92
1.97
2.97
2.98
f1 (ppm)

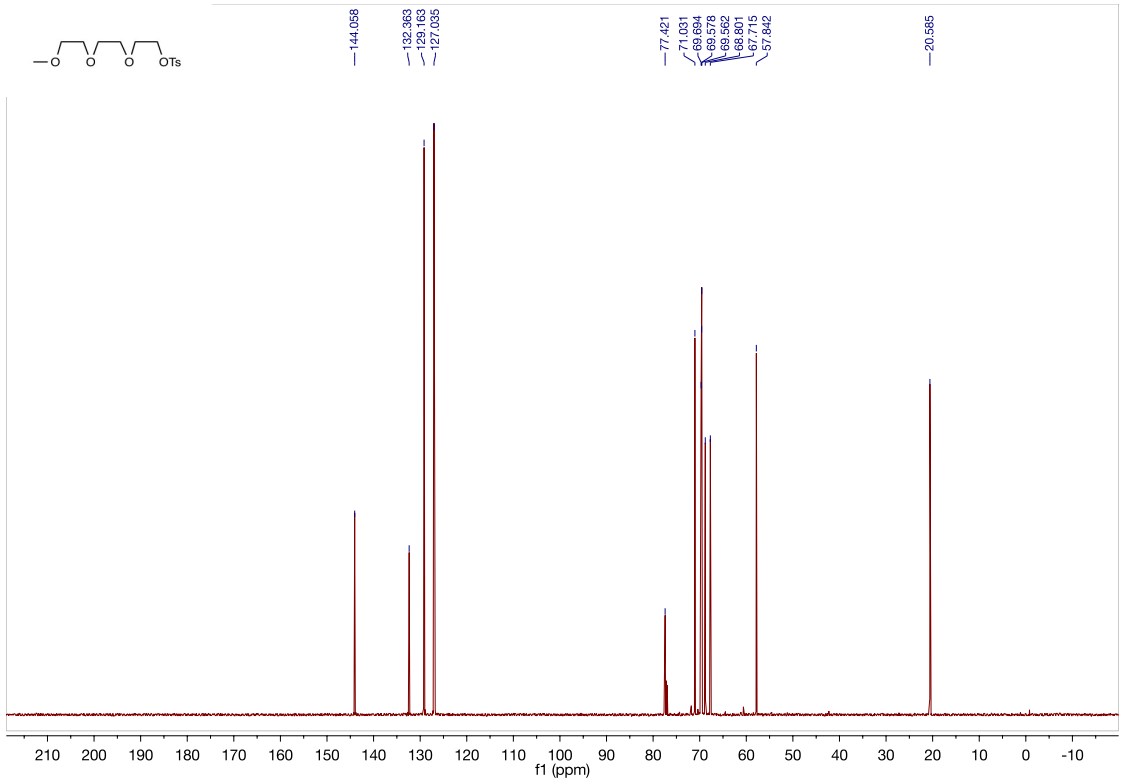
144.058
132.363
129.163
127.035
77.421
71.031
69.694
69.578
69.562
68.801
67.715
57.842
20.585
f1 (ppm)

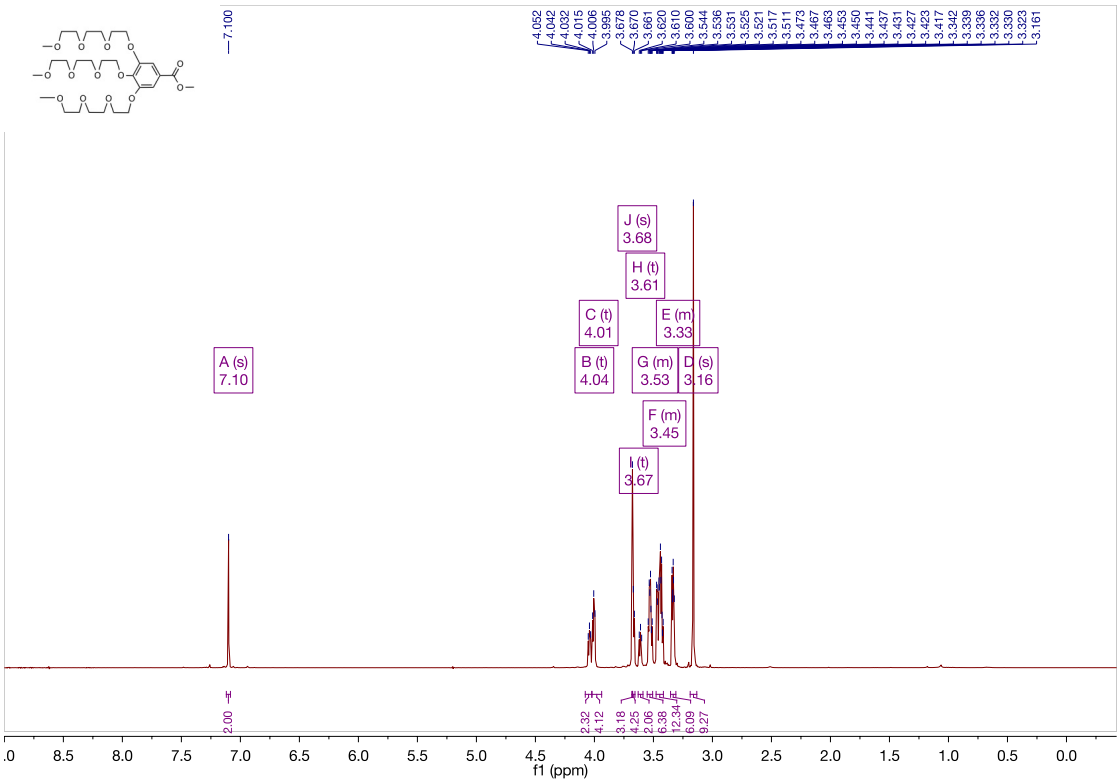
A (s)
7.10
B (t)
4.04
C (t)
4.01
D (s)
3.16
E (m)
3.33
F (m)
3.45
G (m)
3.53
H (t)
3.61
J (s)
3.68
f1 (ppm)

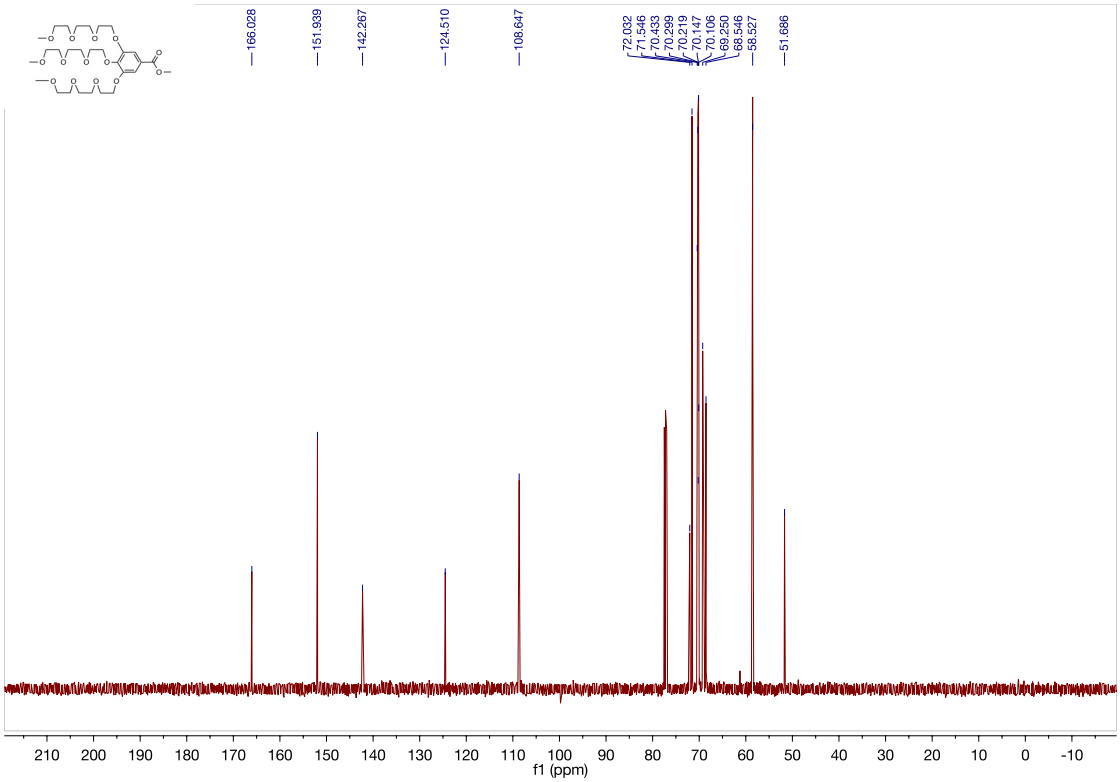
166.028
151.939
142.267
124.510
108.647
72.032
71.546
70.433
70.299
70.219
70.147
70.106
69.250
68.546
58.527
51.686
f1 (ppm)

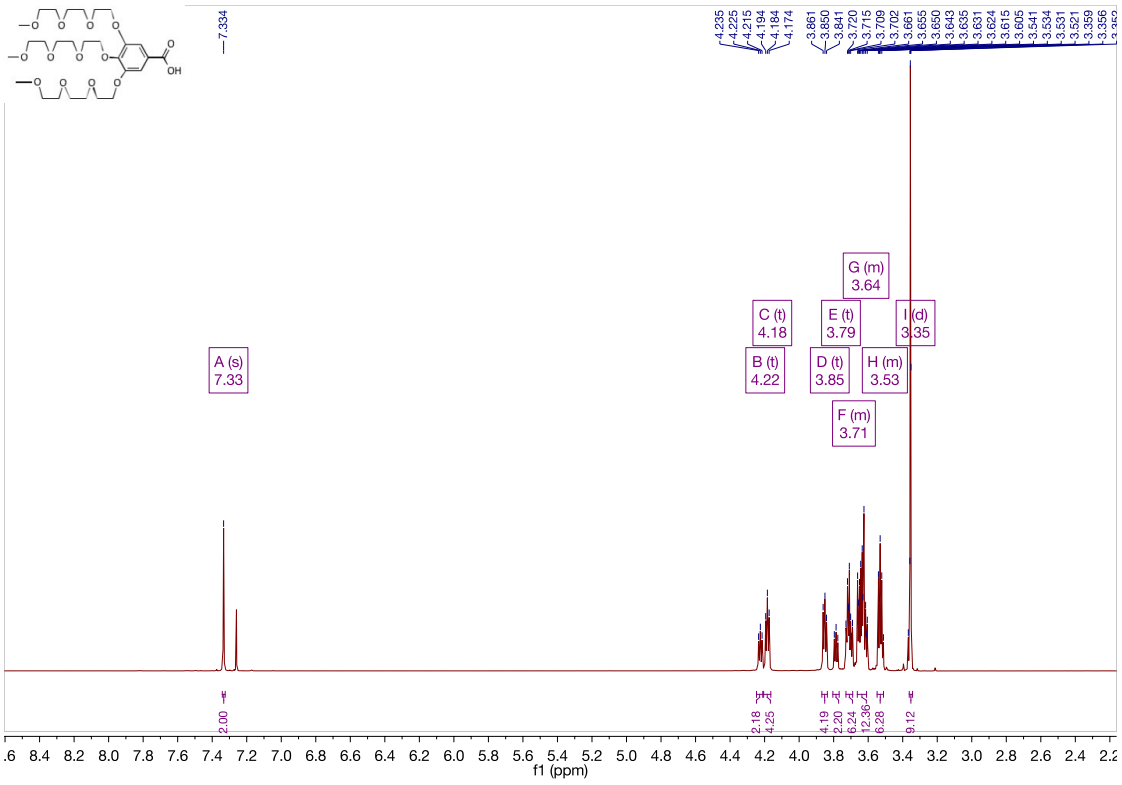
A (s)
7.33
B (t)
4.22
C (t)
4.18
D (t)
3.85
E (t)
3.79
F (m)
3.71
G (m)
3.64
H (m)
3.53
I (d)
3.35
f1 (ppm)

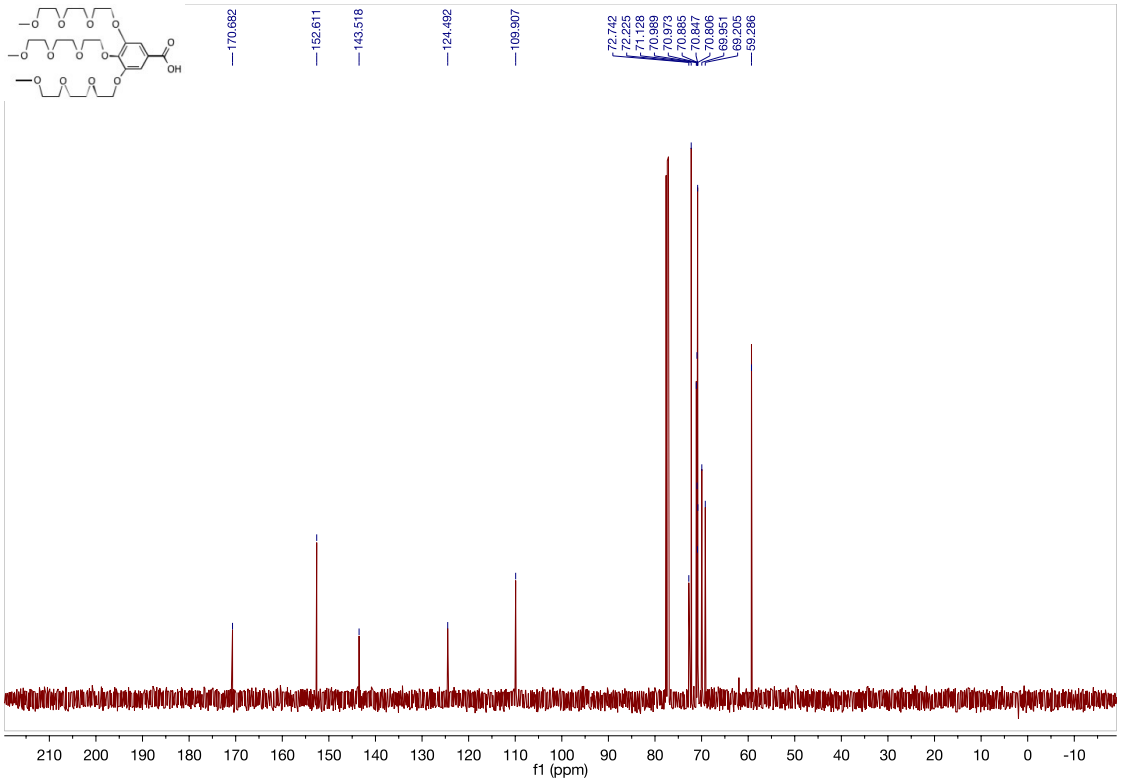
f1 (ppm)

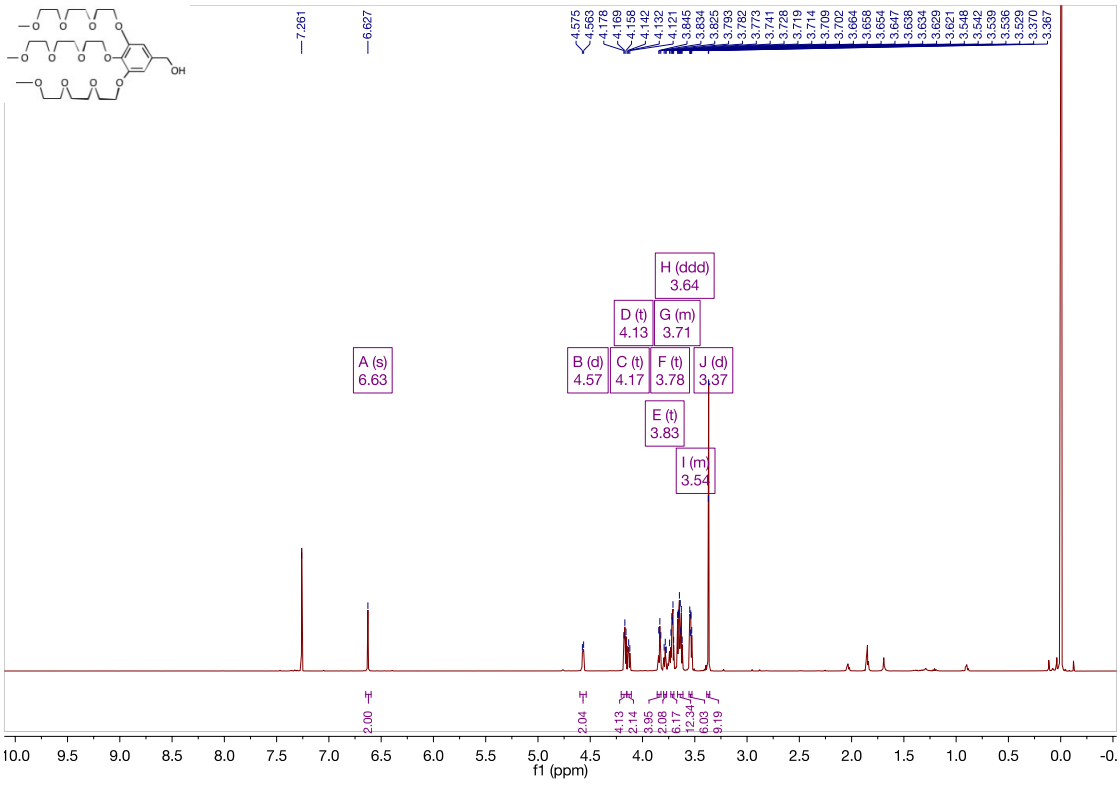
7.261
6.627
4.575
4.563
4.178
4.169
4.158
4.142
4.132
4.121
3.845
3.834
3.825
3.793
3.782
3.773
3.741
3.728
3.719
3.714
3.709
3.702
3.664
3.658
3.654
3.647
3.638
3.634
3.629
3.621
3.548
3.542
3.539
3.536
3.529
3.370
3.367
H (ddd) 3.64
D (t) 4.13
G (m) 3.71
A (s) 6.63
B (d) 4.57
C (t) 4.17
F (t) 3.78
J (d) 3.37
E (t) 3.83
I (m) 3.54
2.00
2.04
4.13
2.14
3.95
2.08
6.17
12.34
6.03
9.19
f1 (ppm)

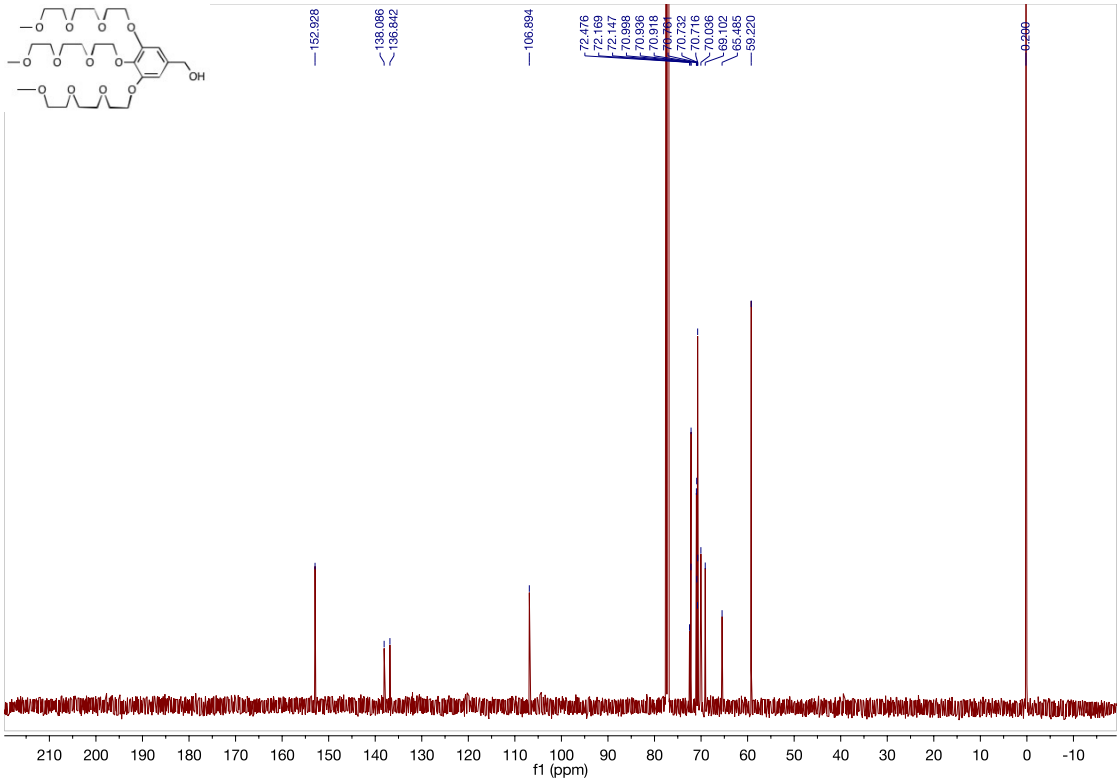
152.928
138.096
136.842
106.894
72.476
72.169
72.147
70.998
70.936
70.918
70.761
70.732
70.716
70.036
69.102
65.485
59.220
0.000
f1 (ppm)

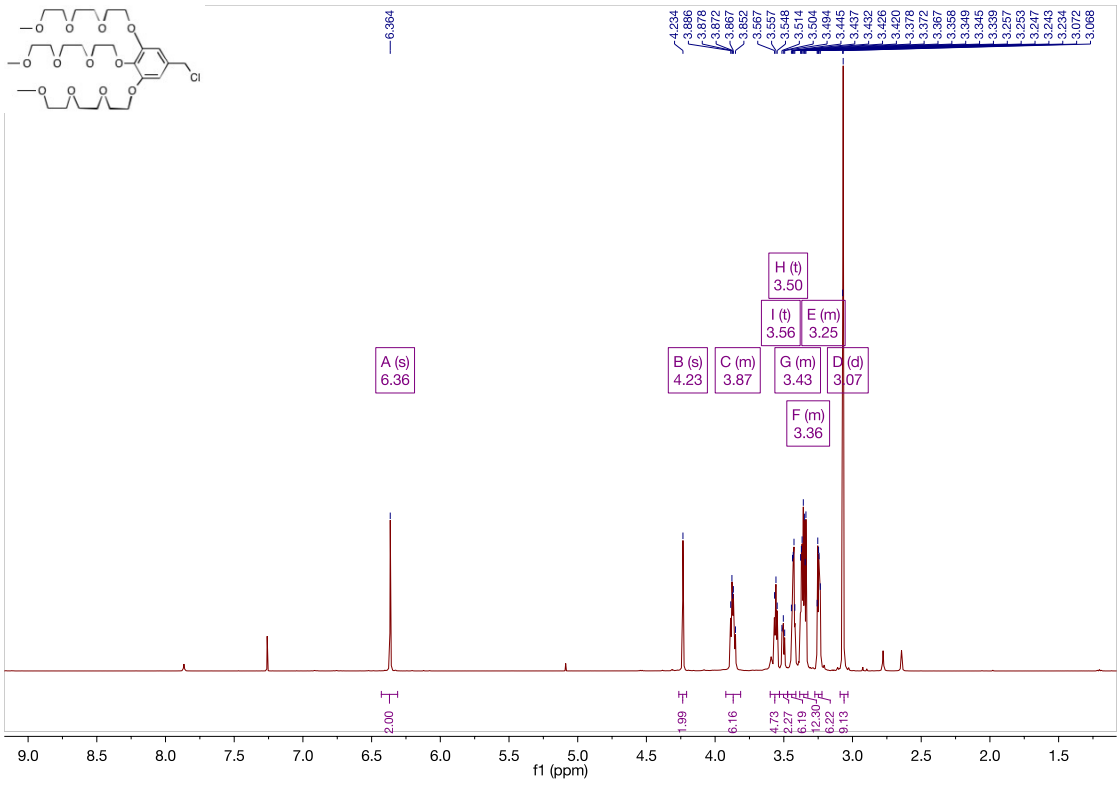
A (s)
6.36
B (s)
4.23
C (m)
3.87
D (d)
3.07
E (m)
3.25
F (m)
3.36
G (m)
3.43
H (t)
3.50
I (t)
3.56
f1 (ppm)

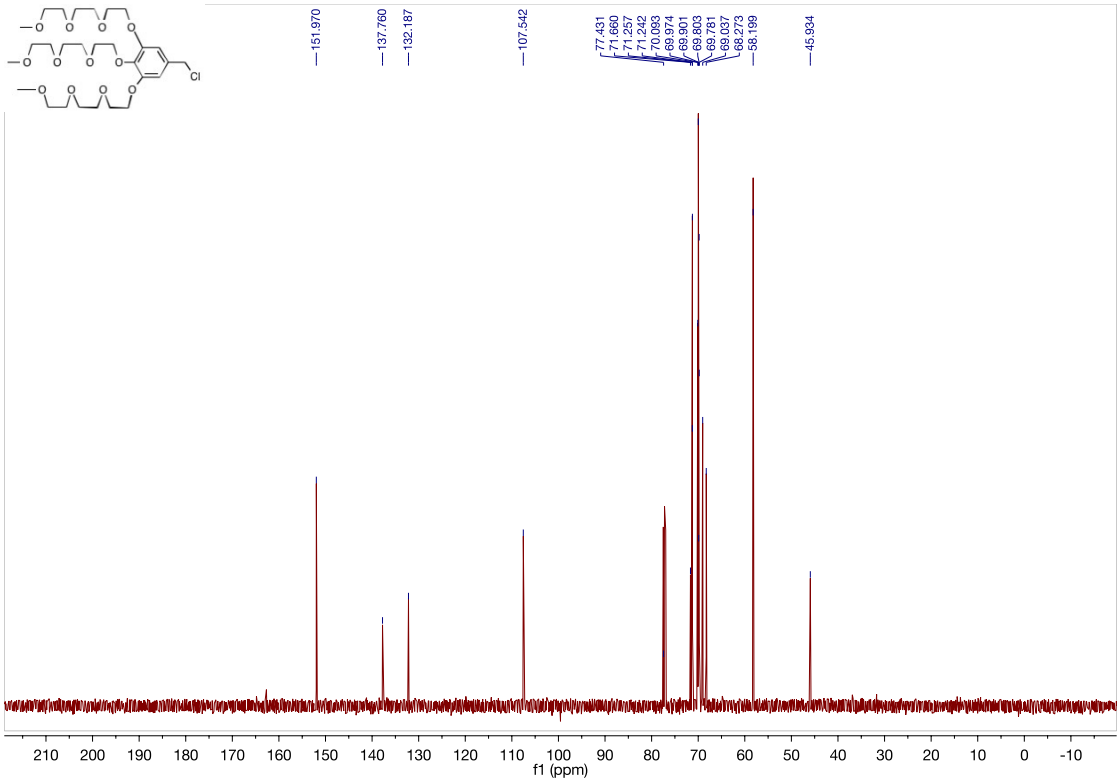
f1 (ppm)

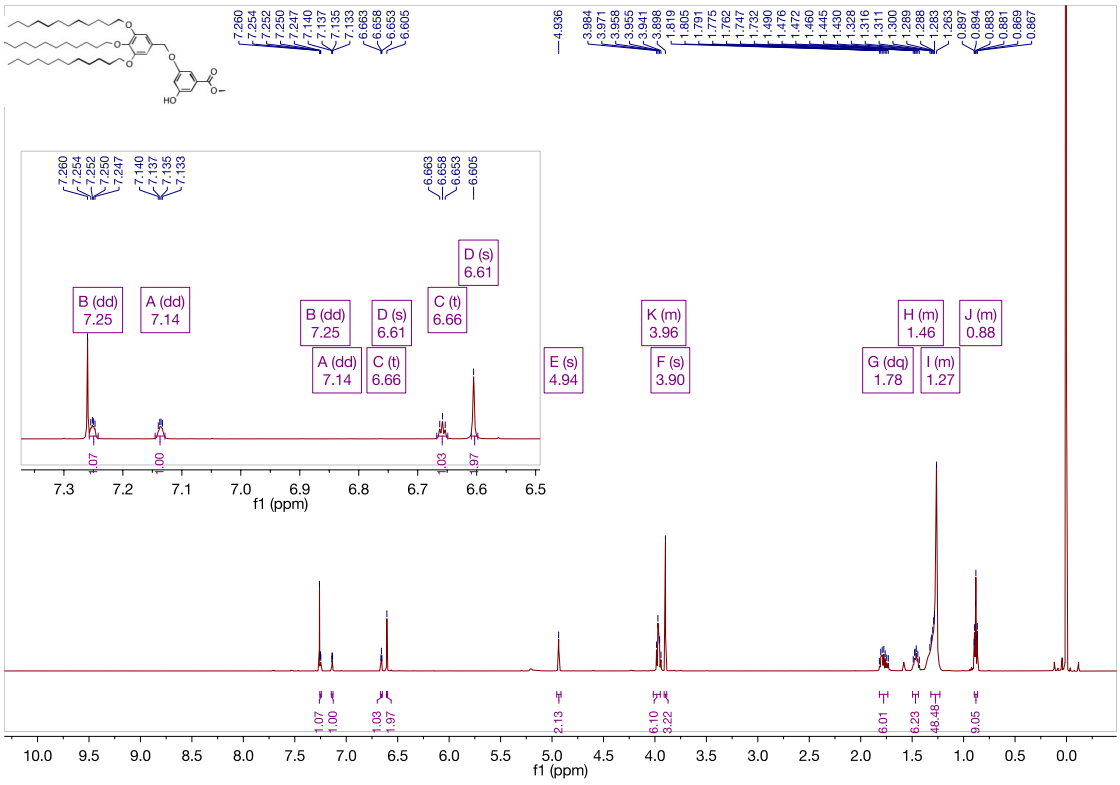
B (dd) 7.25
A (dd) 7.14
D (s) 6.61
C (t) 6.66
E (s) 4.94
K (m) 3.96
F (s) 3.90
G (dq) 1.78
H (m) 1.46
I (m) 1.27
J (m) 0.88
f1 (ppm)

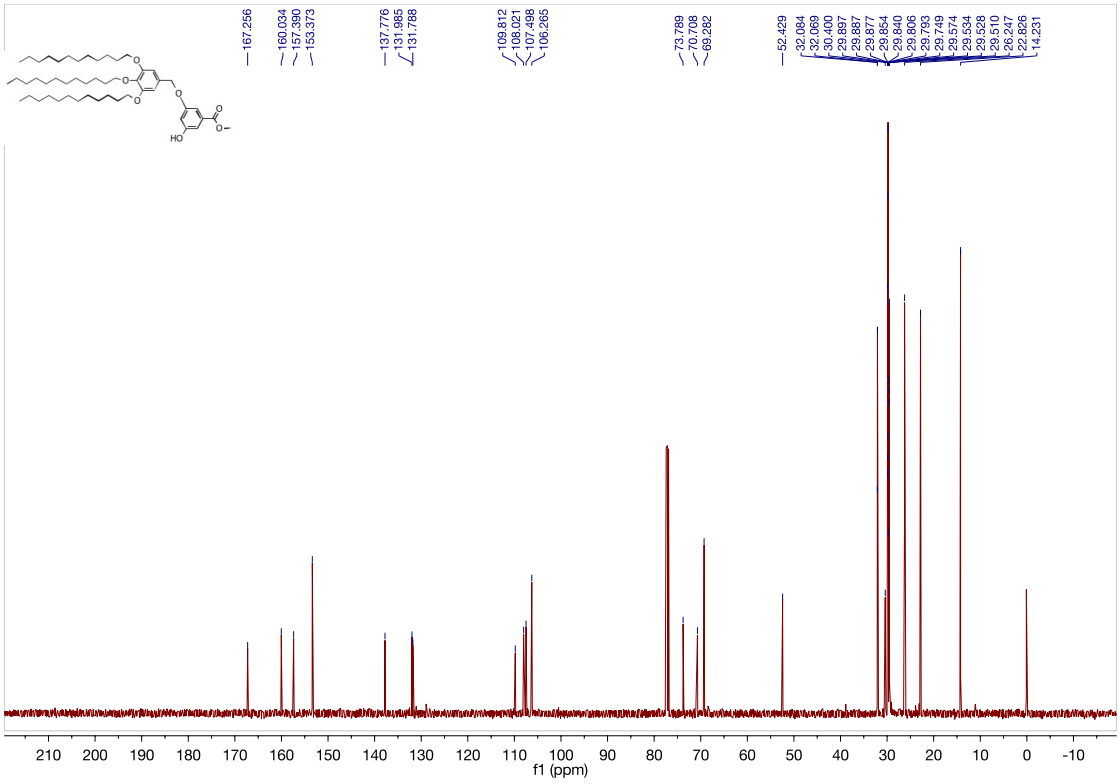
f1 (ppm)

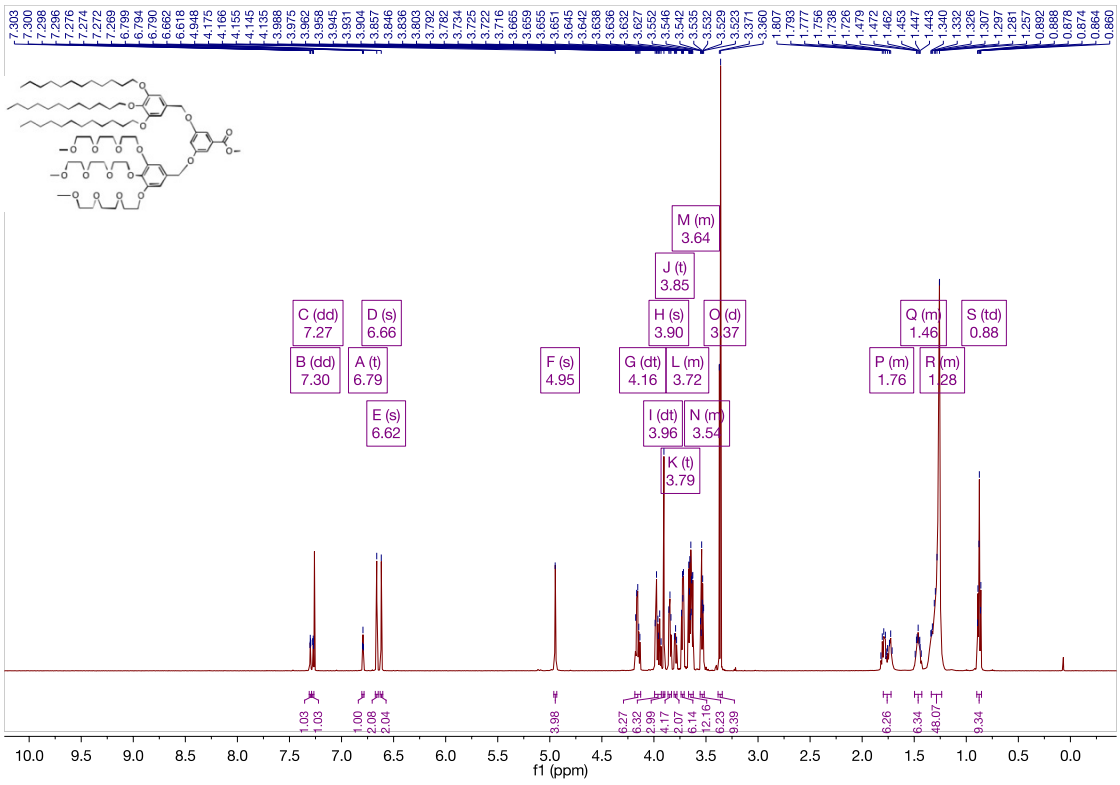
C (dd) 7.27
D (s) 6.66
B (dd) 7.30
A (t) 6.79
E (s) 6.62
F (s) 4.95
G (dt) 4.16
L (m) 3.72
I (dt) 3.96
N (m) 3.54
K (t) 3.79
M (m) 3.64
J (t) 3.85
H (s) 3.90
O (d) 3.37
P (m) 1.76
R (m) 1.28
Q (m) 1.46
S (td) 0.88
f1 (ppm)

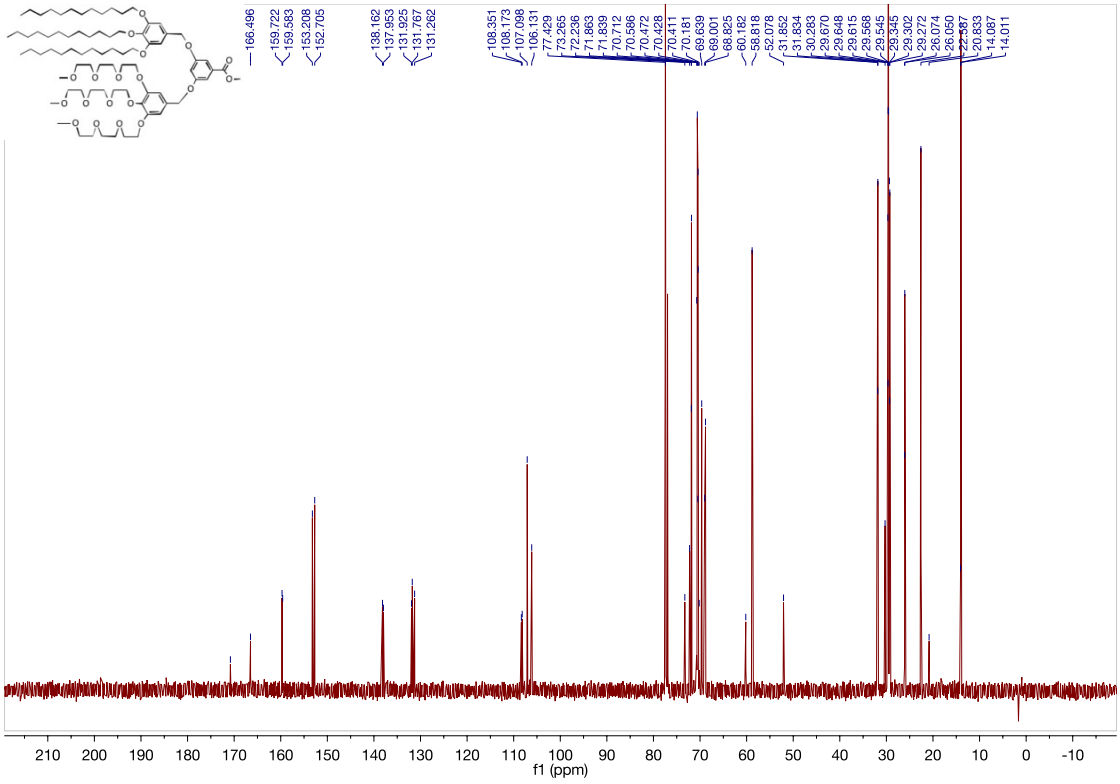
f1 (ppm)

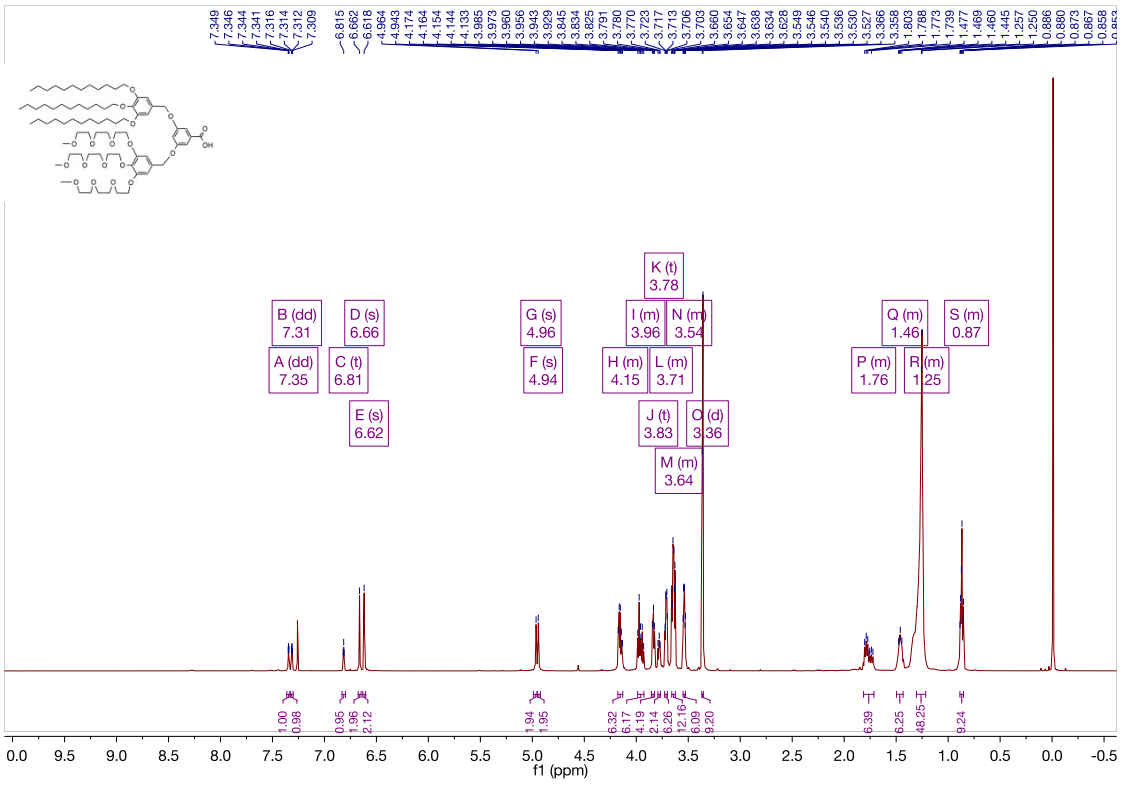
B (dd) 7.31
D (s) 6.66
A (dd) 7.35
C (t) 6.81
E (s) 6.62
G (s) 4.96
F (s) 4.94
K (t) 3.78
I (m) 3.96
N (m) 3.54
H (m) 4.15
L (m) 3.71
J (t) 3.83
O (d) 3.36
M (m) 3.64
Q (m) 1.46
S (m) 0.87
P (m) 1.76
R (m) 1.25
f1 (ppm)

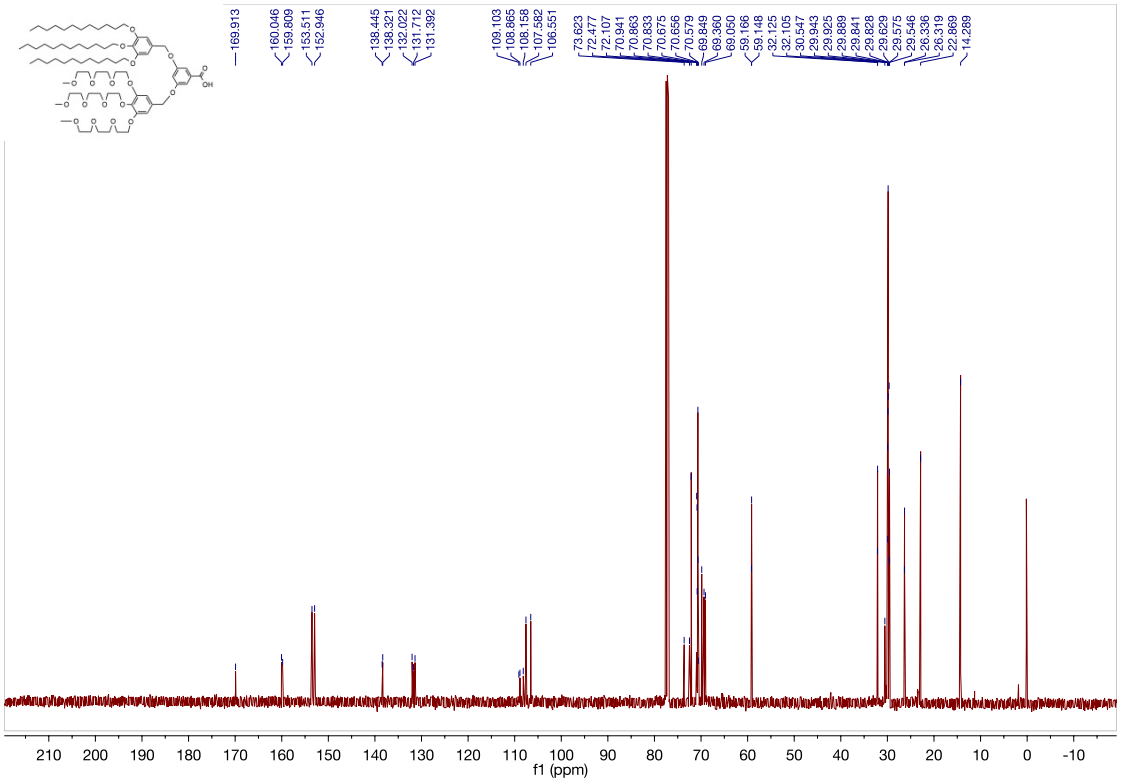
f1 (ppm)

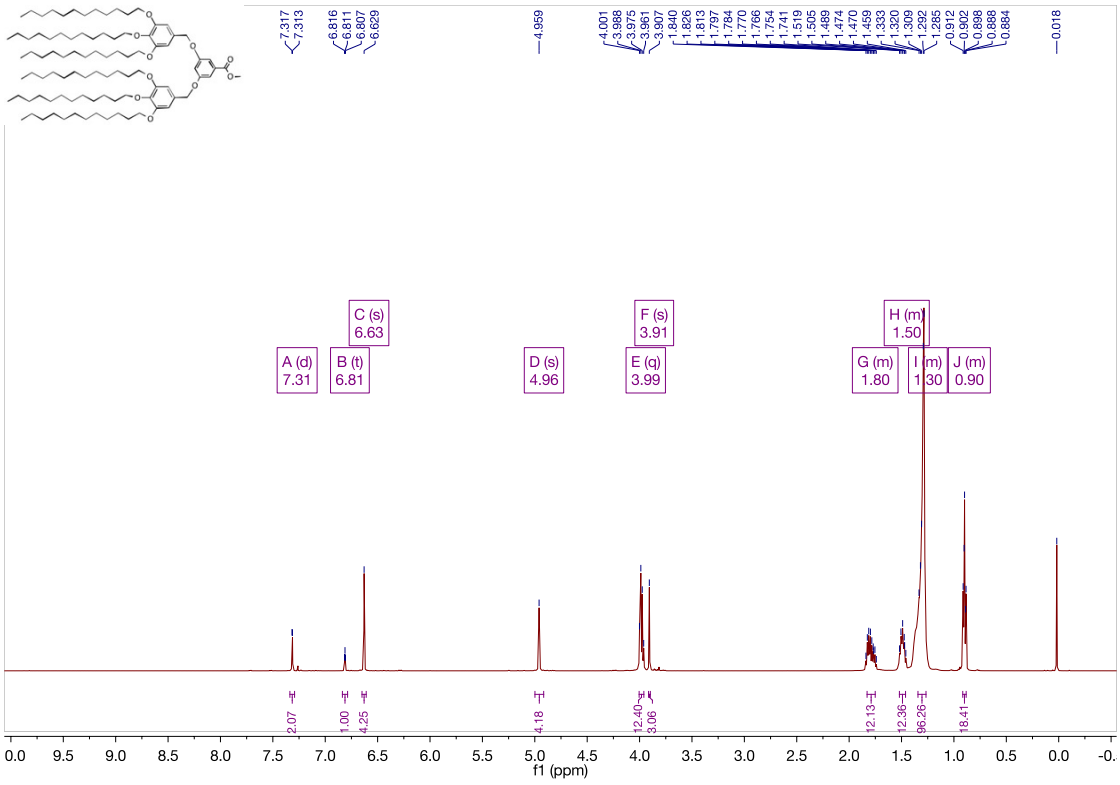
A (d) 7.31
B (t) 6.81
C (s) 6.63
D (s) 4.96
E (q) 3.99
F (s) 3.91
G (m) 1.80
H (m) 1.50
I (m) 1.30
J (m) 0.90
f1 (ppm)

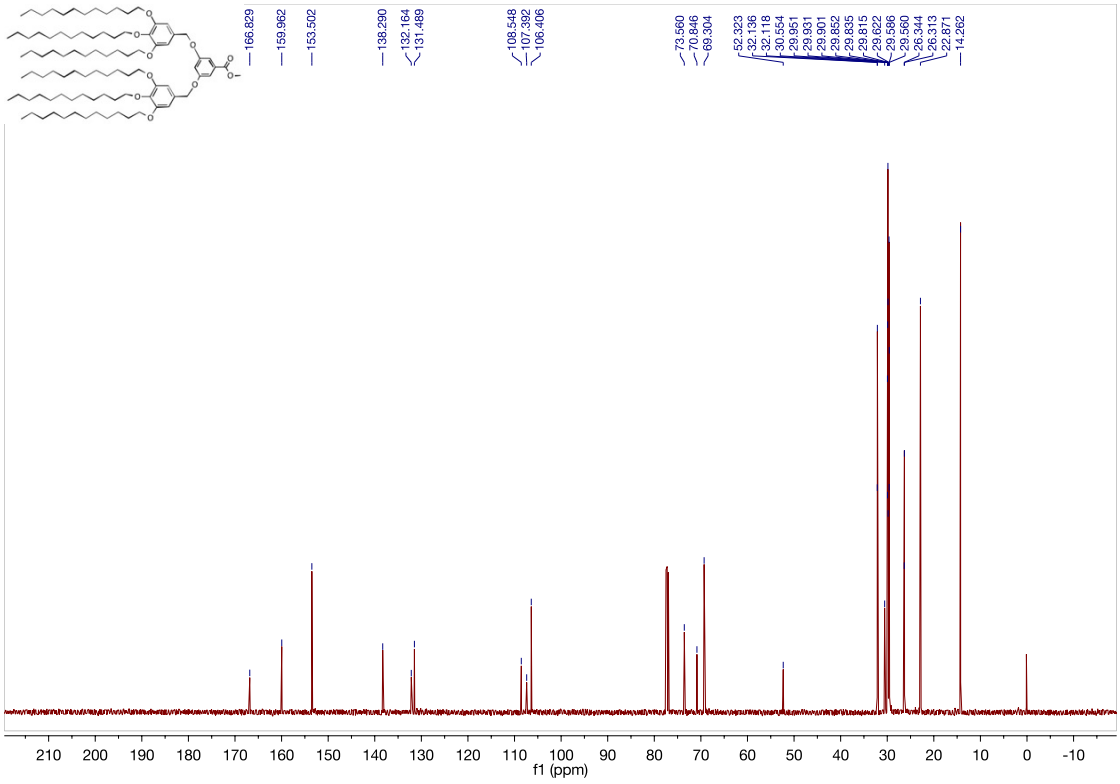
f1 (ppm)

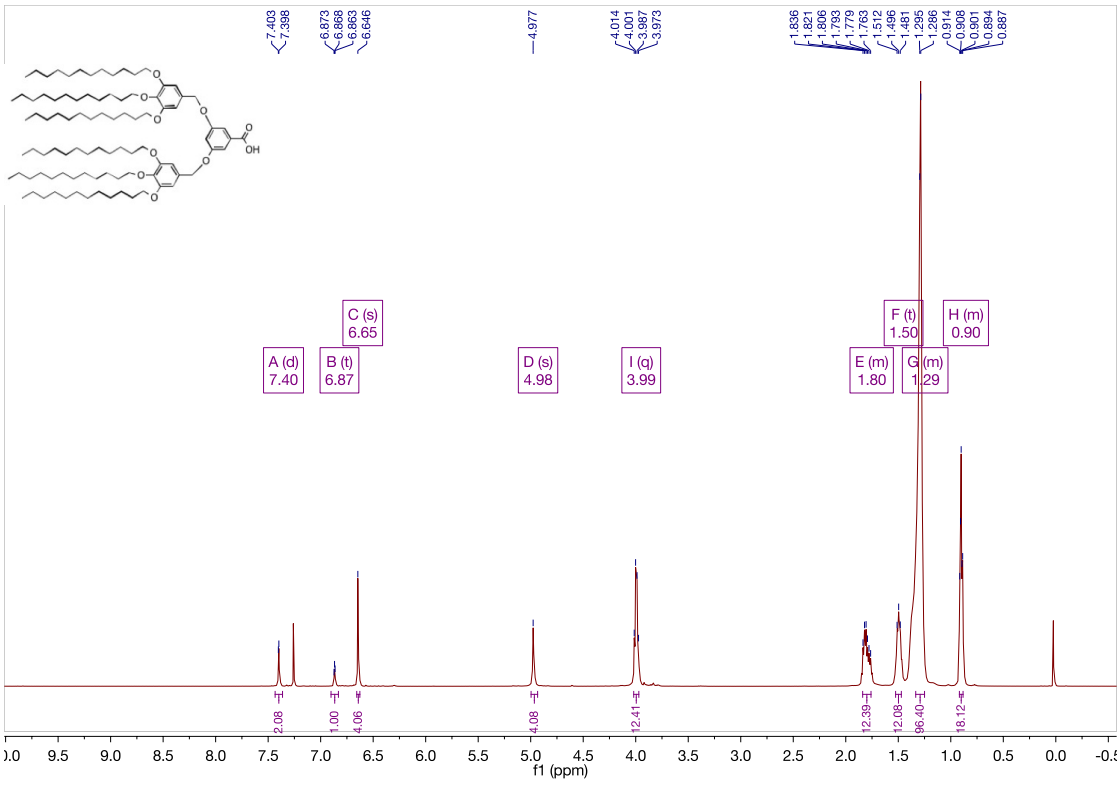
7.403
7.398
6.873
6.868
6.863
6.646
4.977
4.014
4.001
3.987
3.973
1.836
1.821
1.806
1.793
1.779
1.763
1.512
1.496
1.481
1.295
1.286
0.914
0.908
0.901
0.894
0.887
A (d) 7.40
B (t) 6.87
C (s) 6.65
D (s) 4.98
I (q) 3.99
E (m) 1.80
G (m) 1.29
F (t) 1.50
H (m) 0.90
2.08
1.00
4.06
4.08
12.41
12.39
12.08
96.40
18.12
f1 (ppm)

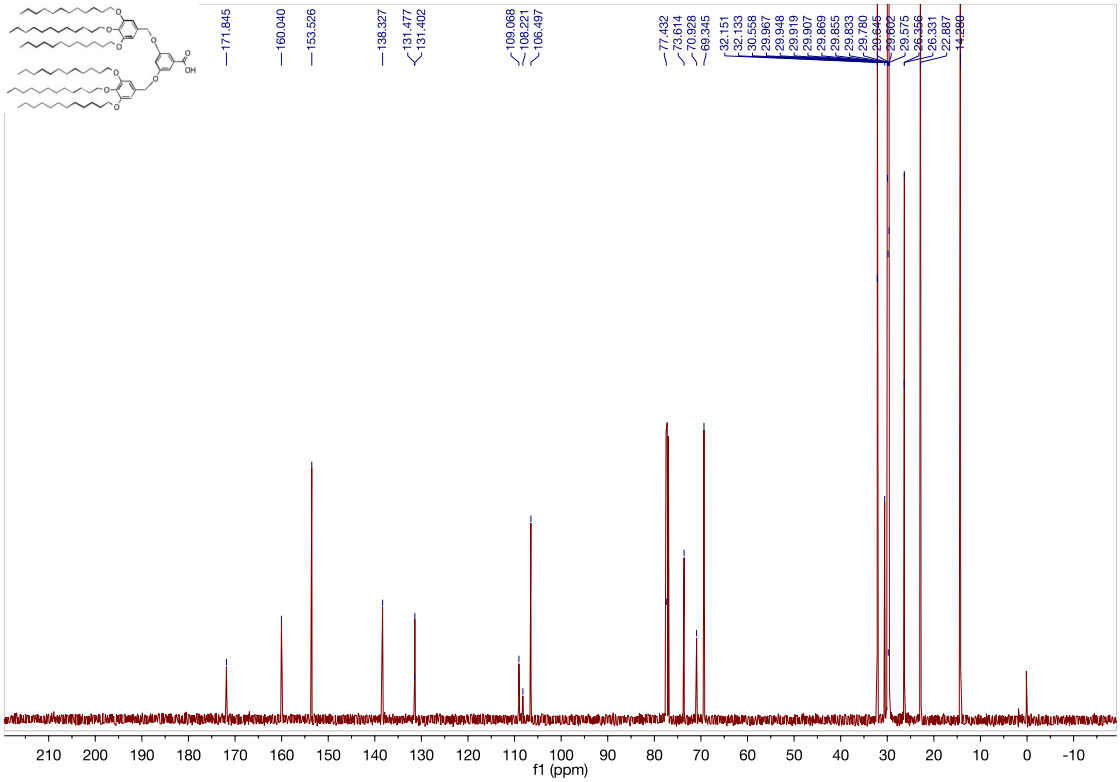
171.845
160.040
153.526
138.327
131.477
131.402
109.068
108.221
106.497
77.432
73.814
70.928
69.345
32.151
32.133
30.558
29.967
29.948
29.919
29.907
29.869
29.855
29.833
29.780
29.602
29.575
26.358
26.331
22.887
14.280
f1 (ppm)

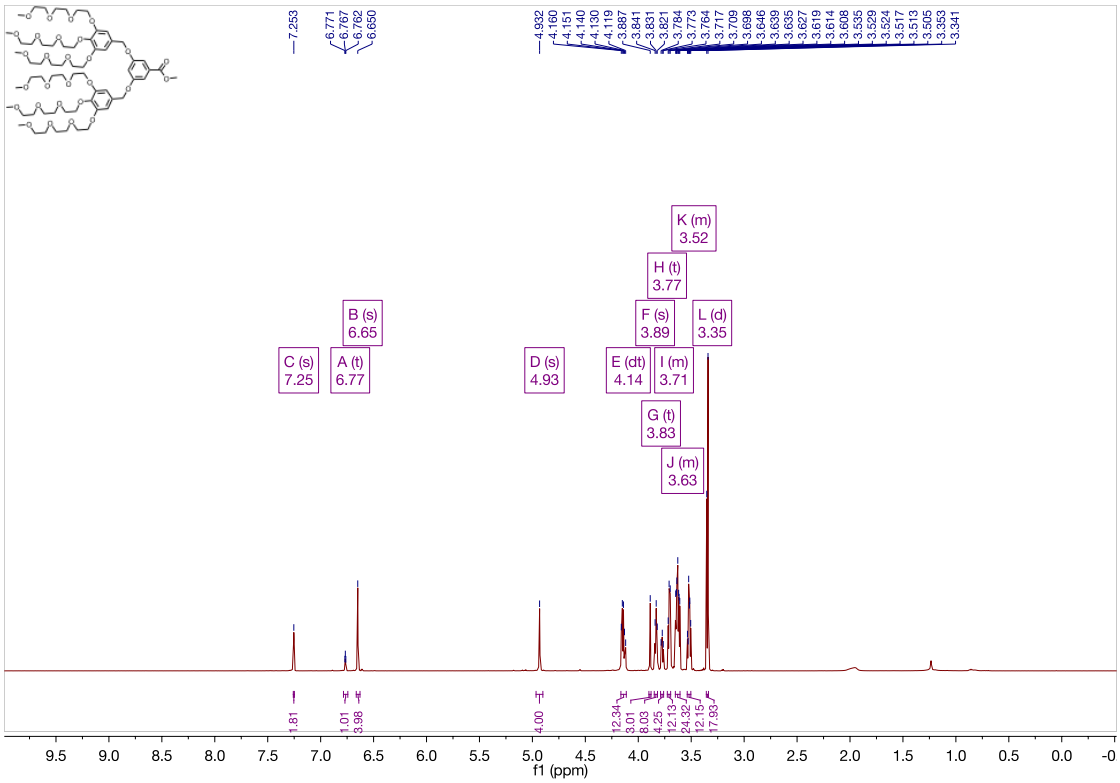
K (m)
3.52
H (t)
3.77
B (s)
6.65
F (s)
3.89
L (d)
3.35
C (s)
7.25
A (t)
6.77
D (s)
4.93
E (dt)
4.14
I (m)
3.71
G (t)
3.83
J (m)
3.63
f1 (ppm)

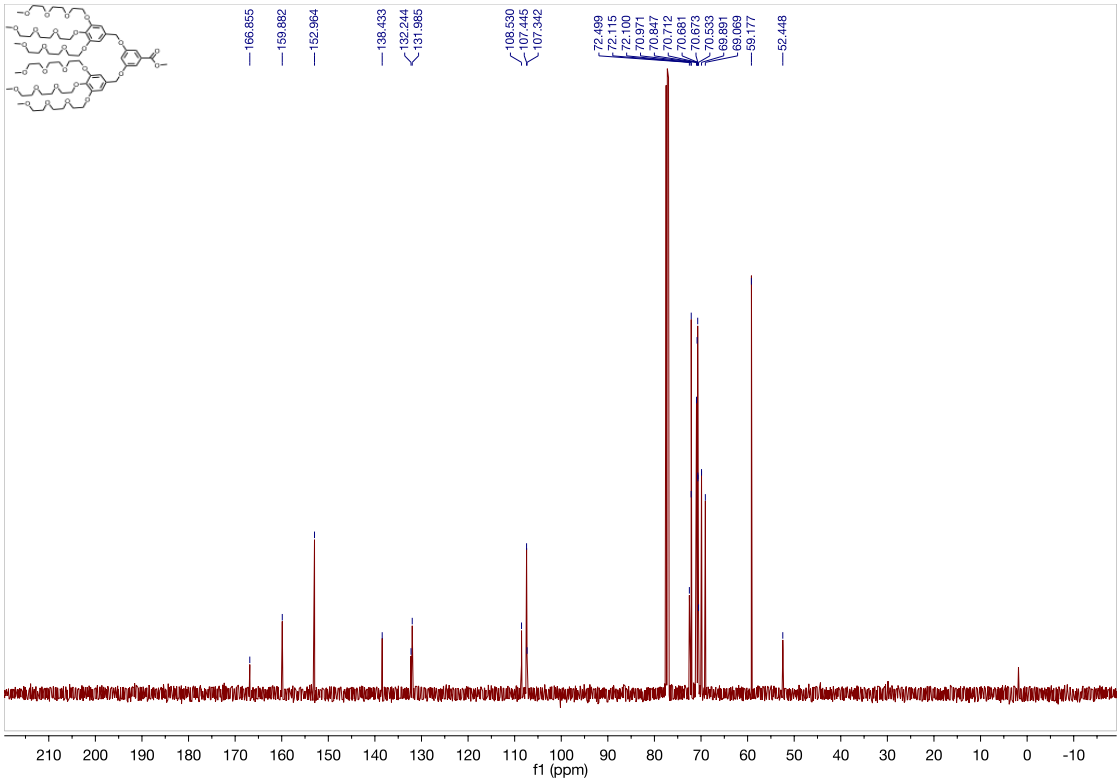
f1 (ppm)

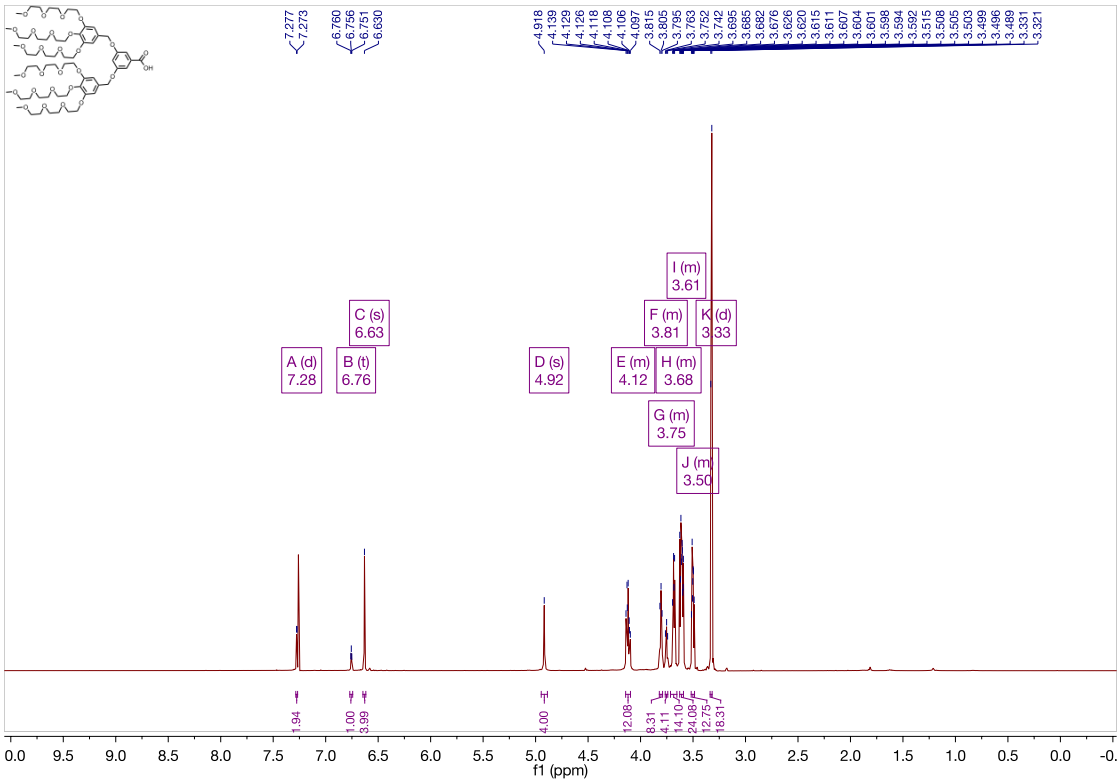
A (d) 7.28
B (t) 6.76
C (s) 6.63
D (s) 4.92
E (m) 4.12
F (m) 3.81
G (m) 3.75
H (m) 3.68
I (m) 3.61
J (m) 3.50
K (d) 3.33
f1 (ppm)

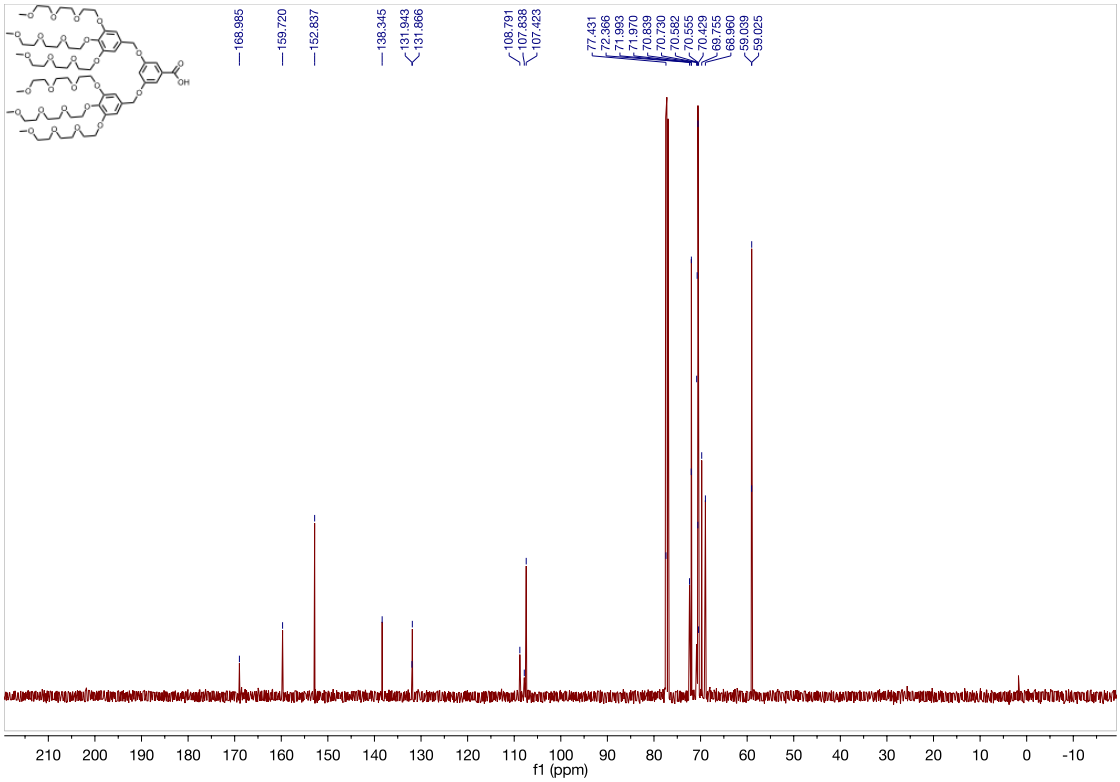
f1 (ppm)

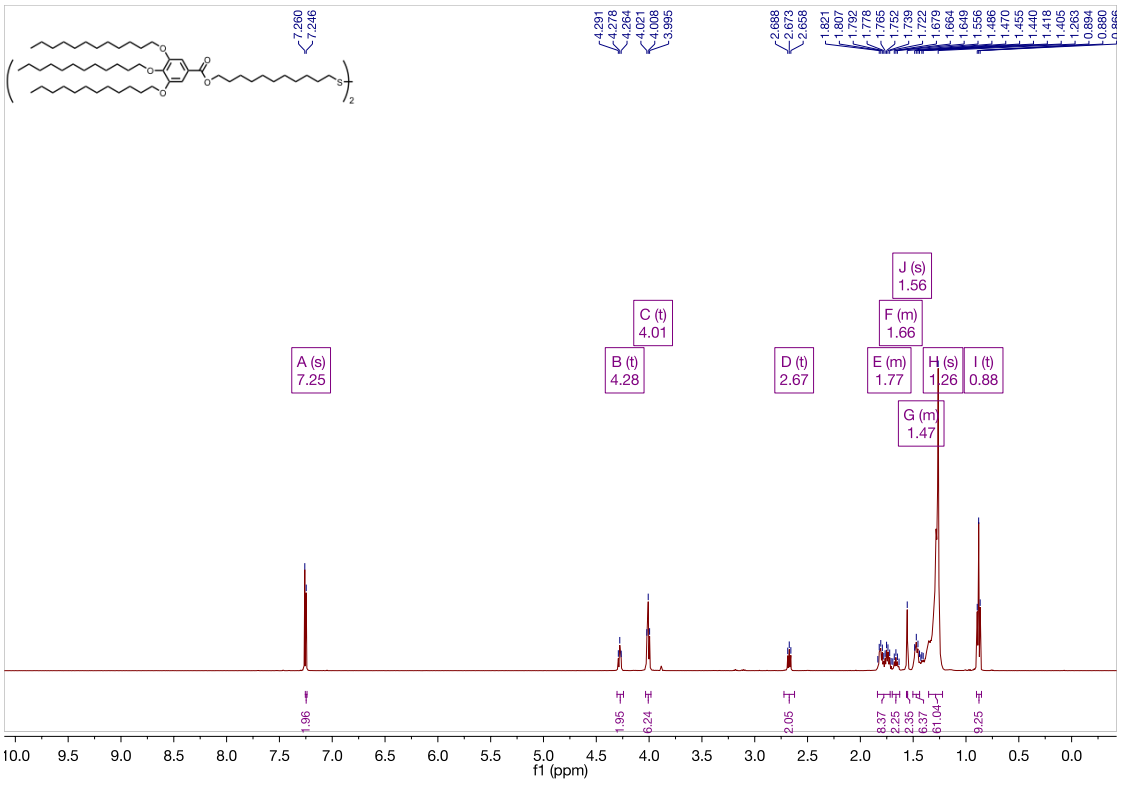
A (s)
7.25
B (t)
4.28
C (t)
4.01
D (t)
2.67
E (m)
1.77
F (m)
1.66
G (m)
1.47
H (s)
1.26
I (t)
0.88
J (s)
1.56
f1 (ppm)

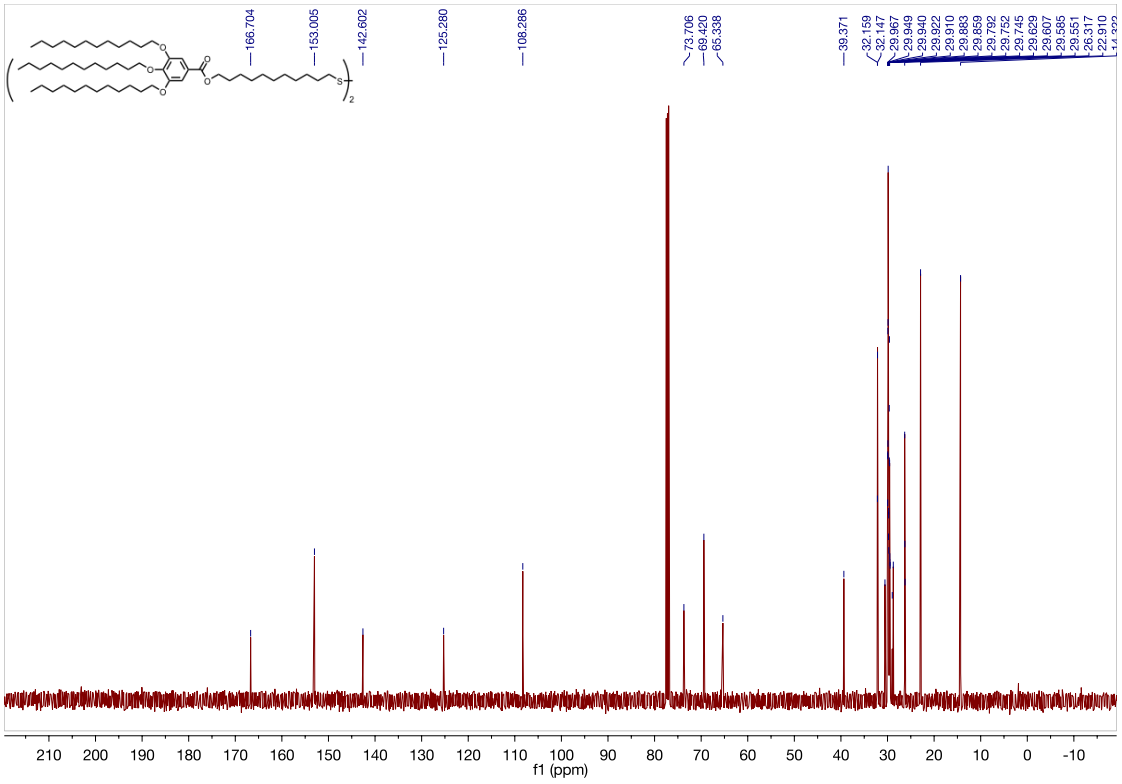
f1 (ppm)

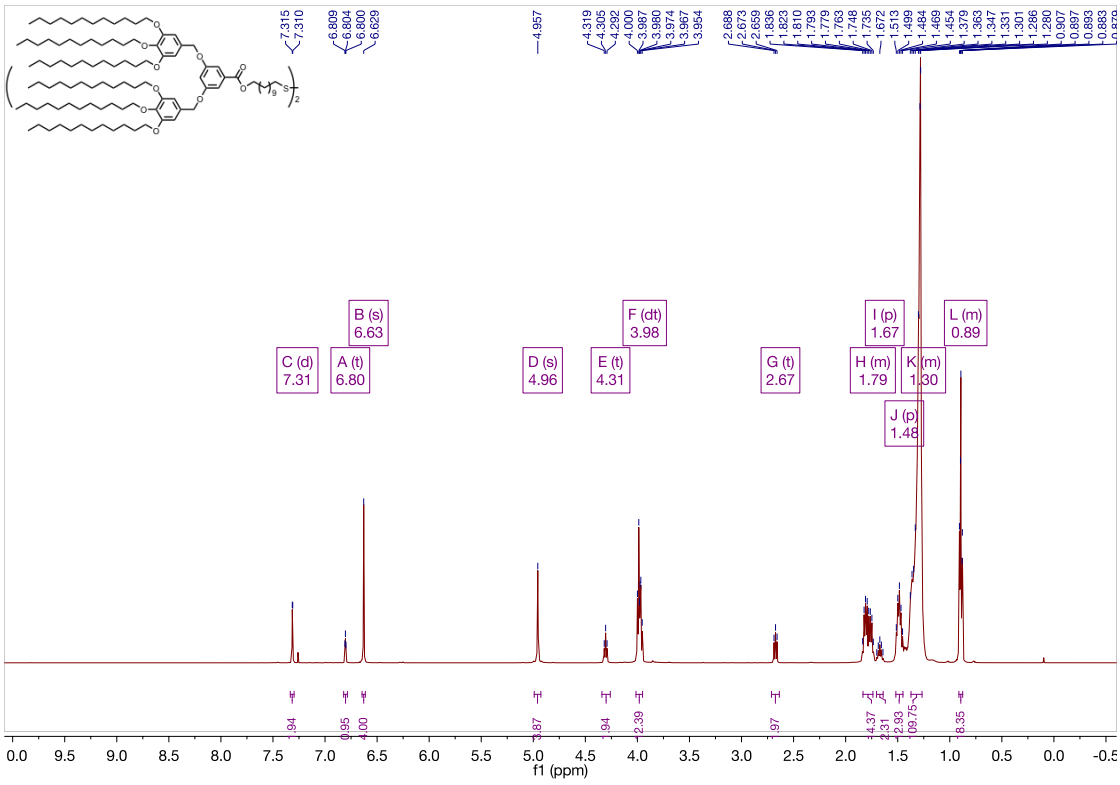
C (d) 7.31
A (t) 6.80
B (s) 6.63
D (s) 4.96
E (t) 4.31
F (dt) 3.98
G (t) 2.67
H (m) 1.79
K (m) 1.30
I (p) 1.67
L (m) 0.89
J (p) 1.48
f1 (ppm)

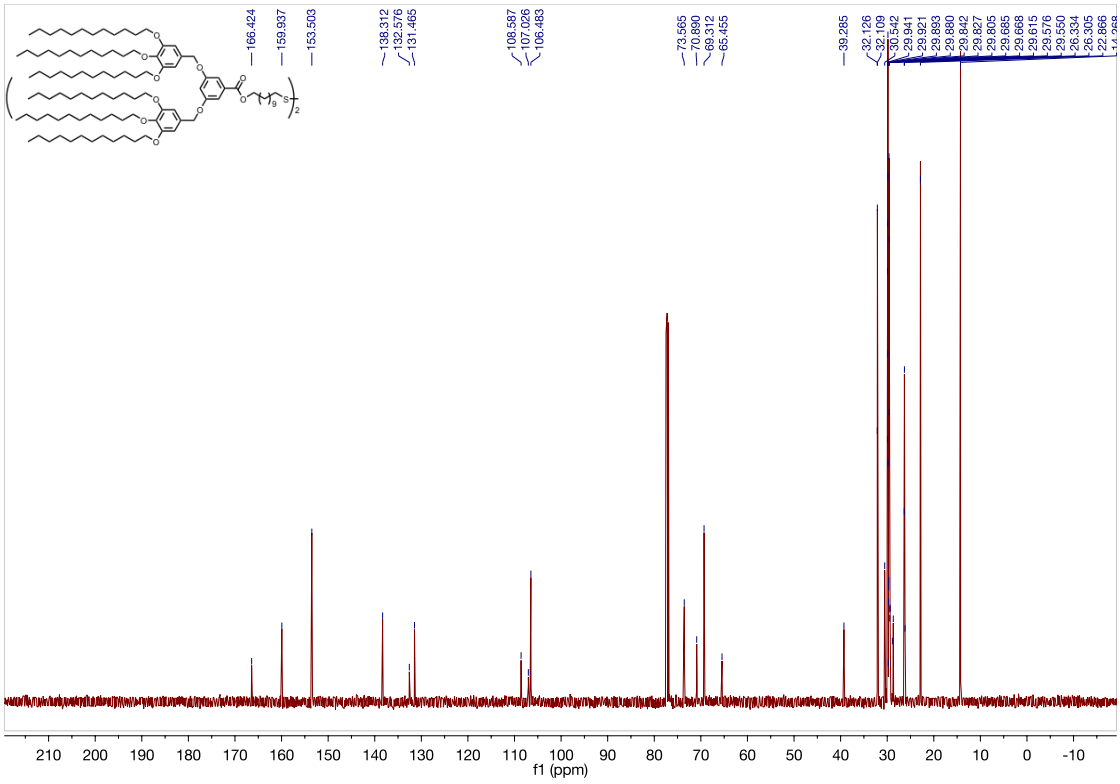
f1 (ppm)

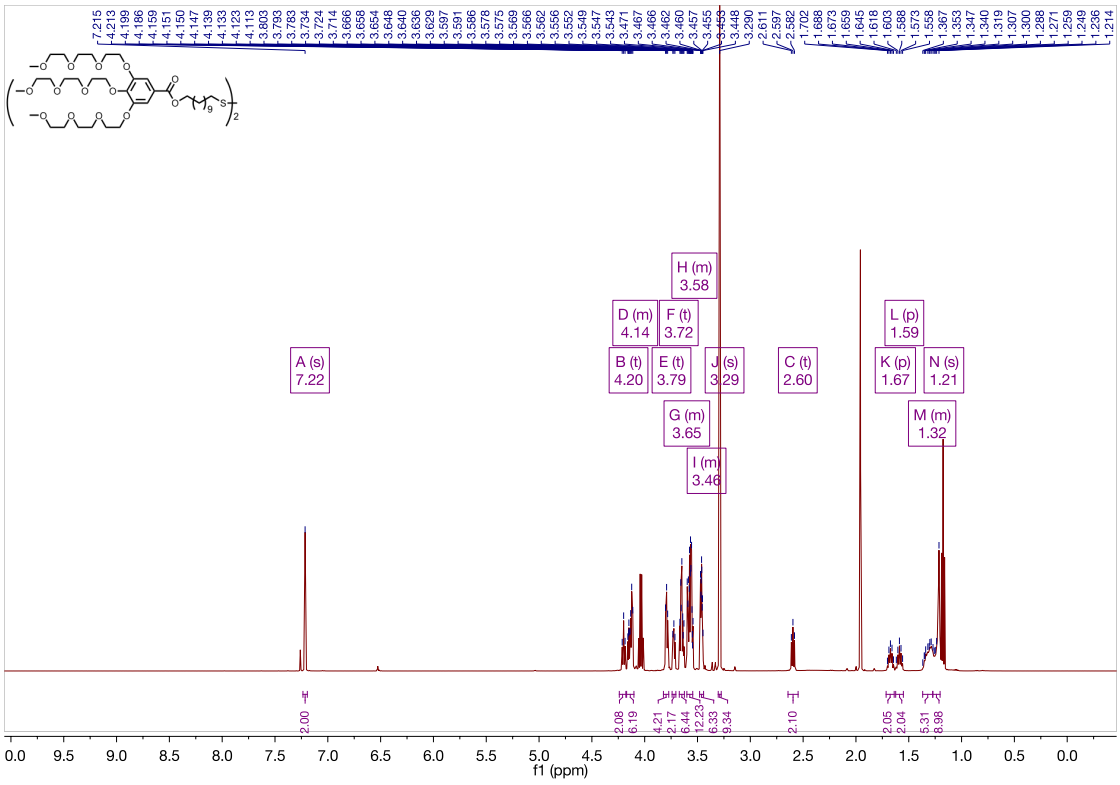
A (s) 7.22
B (t) 4.20
D (m) 4.14
E (t) 3.79
F (t) 3.72
G (m) 3.65
H (m) 3.58
I (m) 3.46
J (s) 3.29
C (t) 2.60
K (p) 1.67
L (p) 1.59
N (s) 1.21
M (m) 1.32
f1 (ppm)

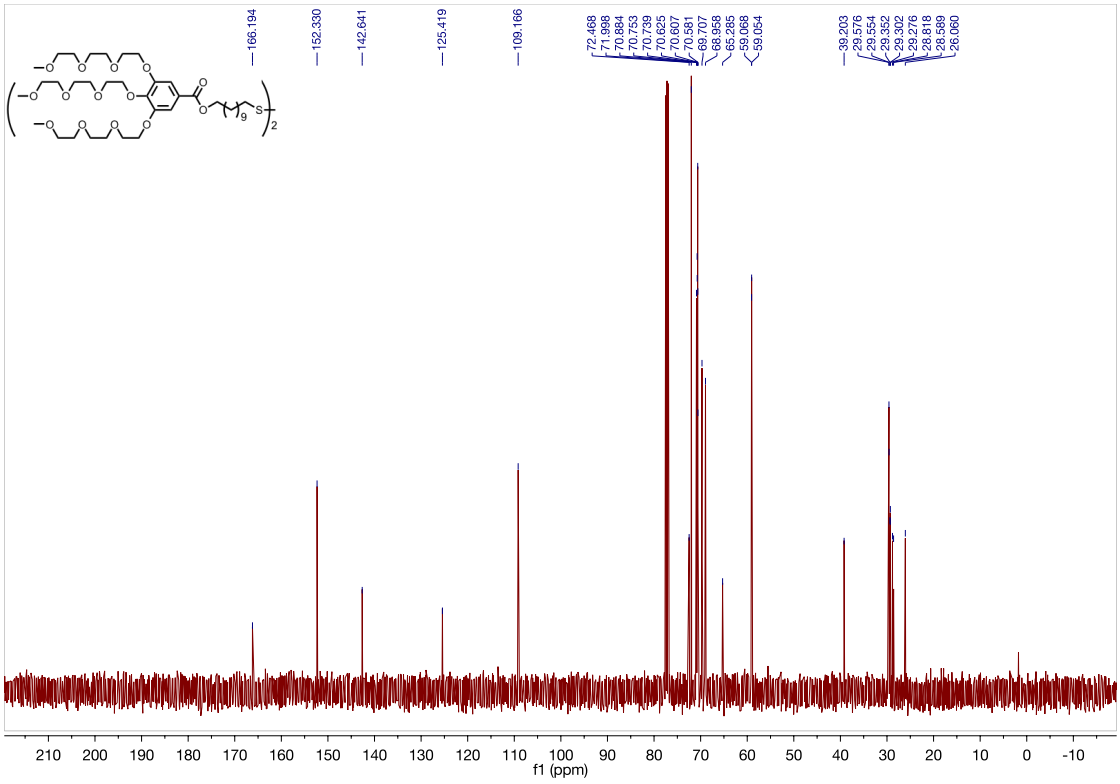
166.194
152.330
142.641
125.419
109.166
72.468
71.998
70.884
70.753
70.739
70.625
70.607
70.581
69.707
68.958
65.285
59.068
59.054
39.203
29.576
29.554
29.352
29.302
29.276
28.818
28.589
26.060
f1 (ppm)

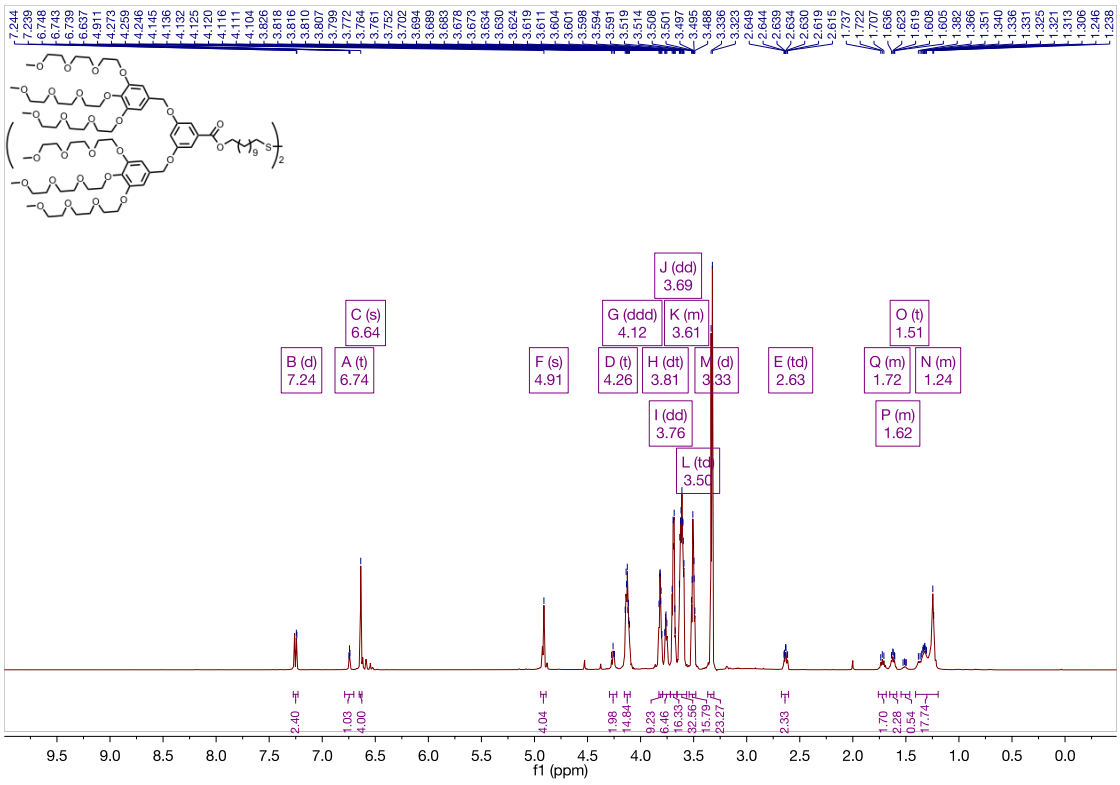
B (d) 7.24
A (t) 6.74
C (s) 6.64
F (s) 4.91
D (t) 4.26
G (ddd) 4.12
H (dt) 3.81
I (dd) 3.76
L (td) 3.50
K (m) 3.61
J (dd) 3.69
M (d) 3.33
E (td) 2.63
Q (m) 1.72
P (m) 1.62
N (m) 1.24
O (t) 1.51
f1 (ppm)

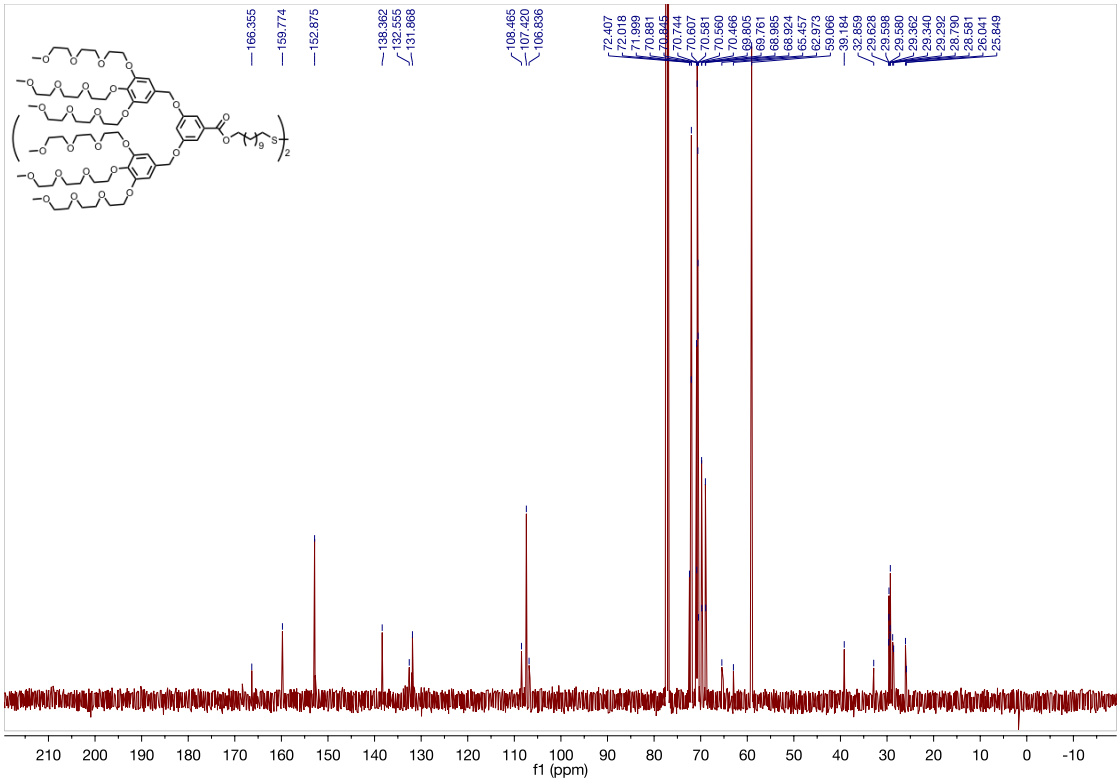
f1 (ppm)

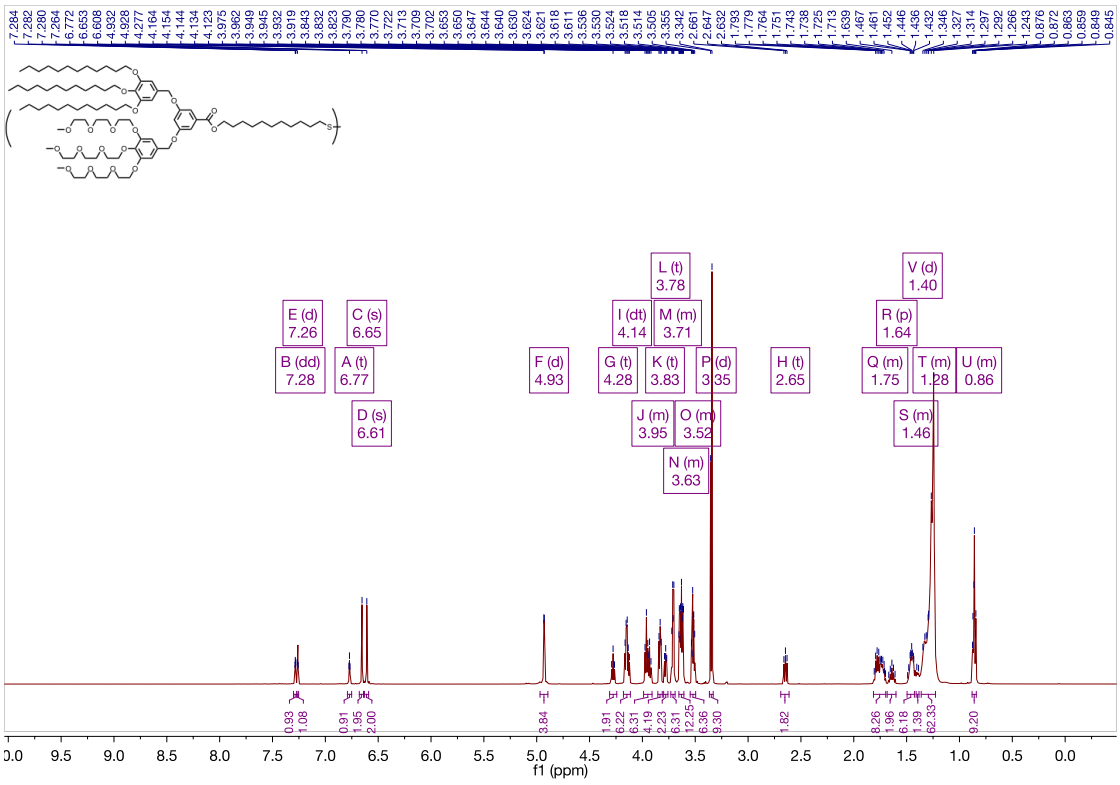
E (d) 7.26
C (s) 6.65
B (dd) 7.28
A (t) 6.77
D (s) 6.61
F (d) 4.93
L (t) 3.78
I (dt) 4.14
M (m) 3.71
G (t) 4.28
K (t) 3.83
P (d) 3.35
J (m) 3.95
O (m) 3.52
N (m) 3.63
H (t) 2.65
V (d) 1.40
R (p) 1.64
Q (m) 1.75
T (m) 1.28
U (m) 0.86
S (m) 1.46
f1 (ppm)

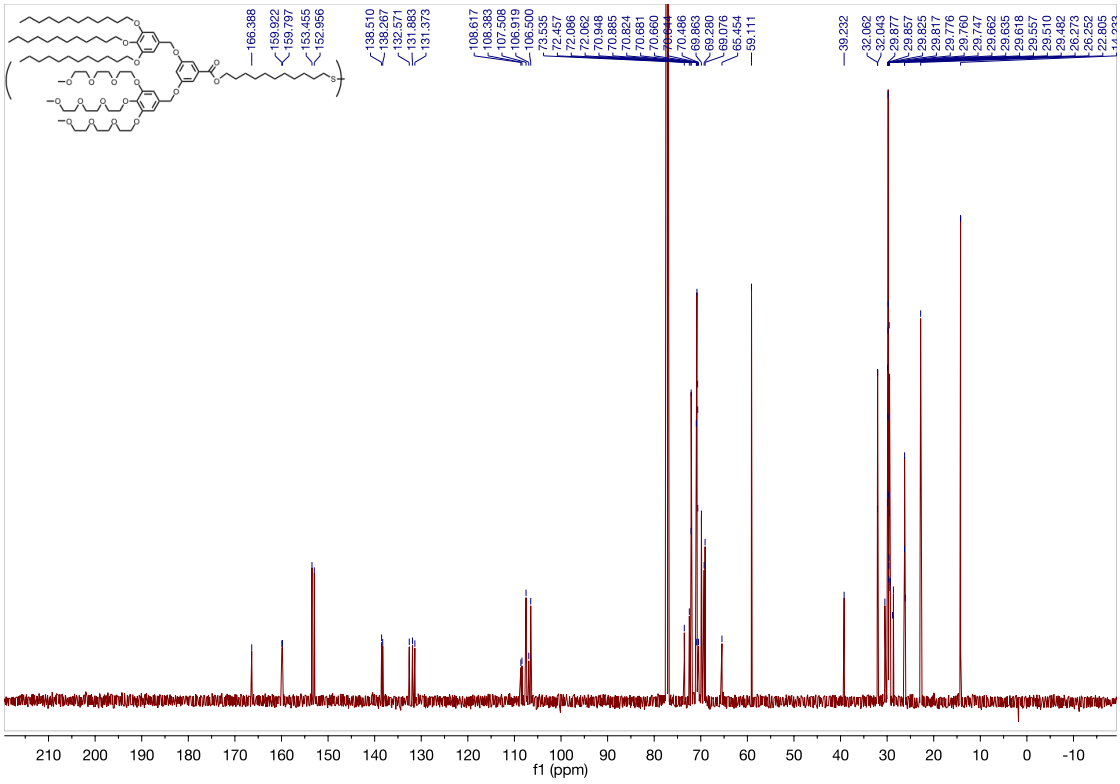
f1 (ppm)